Investigation of activity dependent Arl5b mediated signaling in synaptic plasticity

Dissertation

Zur Erlangung der Würde des Doktors der Naturwissenschaften

des Fachbereichs Biologie, der Fakultät für Mathematik, Informatik und

Naturwissenschaften, der Universität Hamburg

vorgelegt von

Daniel Mensching

aus Stadthagen

Hamburg, 2014

1st reviewer: Prof. Dr. Dietmar Kuhl

2nd reviewer: Prof. Dr. Christian Lohr

Date of Disputation

Genehmigt vom Fachbereich Biologie
der Fakultät für Mathematik, Informatik und Naturwissenschaften
an der Universität Hamburg
auf Antrag von Professor Dr. D. KUHL
Weiterer Gutachter der Dissertation:
Professor Dr. C. LOHR
Tag der Disputation: 04. April 2014

Professor Dr. C. Lohr
Vorsitzender des
Fach-Promotionsausschusses Biologie

Table of contents

Acknowledgement / Danksagung

I would like to thank Prof. Dietmar Kuhl, who entrusted me with the project of my doctoral research and for the good possibilities to deepen my knowledge and skills in his laboratory and by advice during my thesis. Additionally I would like to thank him for the scholarship of the State Excellence Initiative (LEXI) which allowed me to pursue my scientific goals during the last four years.

Further, I would like to thank Prof. Christian Lohr for agreeing to be one of the reviewers of this thesis.

For his thoughtful and close supervision during my project in the laboratory I thank PD Dr. Guido Hermey. His critical suggestions as well as his way to question and address issues and interesting scientific advice were a great support and guidance for my scientific development.

My time at the ZMNH would not have been half as enjoyable without the fellow PhD students in the last years. Especially I would like to mention Lars, Jerome (oh look, it doubled in value), Laura (thanks for the weekend-coffee-breakes), Jakob (great job setting up the lab), Sandra, Sergio ("do you have a minute?" – "Sure!"), Xiaoyan, Francesca, Florian, Kay and Daniel (it was a wonderful January, wasn't it?).

For their open ears, helping hands, critical suggestions and ideas I would like to thank all members of the Institute for Molecular and Cellular Cognition.

Special catering-thanks go to Kirat for his Gäng Massaman Gai and Sushi.

Abstract

Synaptic plasticity, the ability of synapses to undergo experience-dependent changes in synaptic strength, is thought to underlie long-term adaptive responses of the central nervous system, including learning and memory. All forms of long-term plasticity rely on the expression of activity-dependent genes. Although a number of these plasticity related genes have been identified information on how their cellular functions alter synaptic strength is elusive and scarce.

Hermey and colleagues identified a novel, so far uncharacterized, activity-dependent protein, a member of the ADP-ribosylation factor (Arf) like proteins (Arl) family, the small GTPase Arl5b. Its expression is strongly induced and rapidly reduced in the hippocampus by plasticity producing stimulation. Since related proteins have been demonstrated to play roles in intracellular trafficking and signaling, I hypothesized that Arl5b may regulate such processes in plasticity related events. I found that the small GTPase Arl5b shares many characteristics with proto-typical Arf proteins. By analyzing the subcellular localization of mutant recombinant Arl5b variants I showed that N-terminal myristoylation of Arl5b is required for GTP-dependent attachment to membranes of the Golgi apparatus and endosomes. The recruitment of Arl5b to vesicles can be induced by Brain-Derived-Neurotrophic-Factor (BDNF). Moreover, Arl5b co-localizes with the BDNF receptor TrkB in late endosomes. Further, investigations revealed an Arl5b function in long-range axonal retrograde endosomal transport. A dominant-negative Arl5b variant deficient in GTP-mediated activation impaired fast retrograde trafficking of late endosomes in cultured hippocampal neurons. In addition, Arl5b interacts with signaling and cytoskeleton associated proteins. Biochemical assays and immunocytochemistry verified the interaction with one of these proteins, Casein kinase 1 alpha (CK1α). The results suggest that this interaction may be part of a signaling cascade initiated by BDNF. I generated a conditional Arl5b knock-out mouse model. First results show that the loss of Arl5b reduced the activation of ribosomal protein S6, a regulator of translation required for synaptic plasticity. This indicates an impairment of the BDNF induced protein kinase B / mammalian target of rapamycin (AKT/mTOR) signaling pathway. In behavioral experiments Arl5b-deficient mice show a weak impairment in learning.

In conclusion, I characterized Arl5b as a canonical Arf-like protein which conveys targeting of late endosomes. In addition, the results suggest a role in BDNF-dependent signaling which underlies synaptic plasticity related events. In agreement with such a possible role in neuronal plasticity Arl5b Knockout mice show a tendency for reduced long-term memory formation.

Zusammenfassung

Es wird angenommen, dass langfristigen adaptiven Antworten des Zentralnervensystems, einschließlich Lernen und Gedächtnis, synaptische Plastizität zugrunde liegt. Dies ist die Fähigkeit der Synapsen erfahrungsabhängig die Stärke der synaptischen Übertragung zu verändern. Alle Formen von Langzeit-Plastizität beruhen auf der Expression von Aktivitäts-abhängigen Genen. Obwohl eine Vielzahl dieser Plastizität-assoziierten Gene identifiziert wurde sind Informationen darüber, wie ihre zellulären Funktionen zur Veränderung der synaptischen Stärke führen schwer zu erlangen und knapp.

Hermey und Kollegen identifizierten ein neues, bisher nicht charakterisiertes, aktivitätsabhängiges Protein, ein Mitglied der Familie der ADP-Ribosylierungs Faktor (Arf) ähnlichen Proteine (ARL), die kleine GTPase Arl5b. Im Hippocampus wird dessen Expression von Plastizität auslösenden Stimuli stark induziert, aber im Anschluss auch schnell wieder reduziert. Da für homologe Proteine nachgewiesen wurde, dass sie Aufgaben im intrazellulären Transport und in Signalkaskaden übernehmen, habe ich die Hypothese aufgestellt, dass Arl5b solche Prozesse in Plastizität zugehörigen Mechanismen reguliert. Ich habe herausgefunden, dass viele Eigenschaften der kleinen GTPase Arl5b denen von proto-typischen Arf –Proteinen entsprechen. Durch die Analyse der subzellulären Lokalisierung von mutierten, rekombinanten Arl5b Varianten konnte ich zeigen, dass die N-terminale Myristoylierung von Arl5b für seine, GTP-abhängige Bindung, an Membranen des Golgi-Apparat und Endosomen erforderlich ist. Die Rekrutierung von Arl5b an Vesikel kann durch Stimulation mit *Brain-Derived-Neurotrophic-Factor* (BDNF) induziert werden. Darüber hinaus ko-lokalisiert Arl5b mit dem BDNF-Rezeptors TrkB in späten Endosomen. Es zeigte sich eine Funktion von Arl5b im retrograden, axonalen Endosomen-Transport über lange Strecken. Eine dominant-negative Variante von Arl5b, gestört in der GTP-vermittelten Aktivierung, beeinträchtigt den schnellen retrograden Transport später Endosomen in kultivierten hippocampalen Neuronen. Darüber hinaus interagiert Arl5b mit Signalübertragungs- und Zytoskelett-assoziierten Proteinen. Biochemischen Analysen und Immunzytochemie-Versuche bewiesen die Interaktion mit einem dieser Proteine, der Casein Kinase 1 alpha (CK1α). Diese Ergebnisse legen nahe, dass diese Interaktion ein Teil einer von BDNF initiierten Signalkaskade ist. Ich generierte ein konditionales Arl5b Knockout Mausmodell. Erste Ergebnisse zeigen, dass der Verlust von Arl5b die Aktivierung des ribosomalen Proteins S6 reduziert. S6 ist ein Regulator der für synaptische Plastizität essentiellen Translation. Dies deutet auf eine Beeinträchtigung des BDNF- induzierten Proteinkinase B / *mammalian target of Rapamycin* (AKT/mTOR)-Signalweges hin. In Verhaltensexperimenten zeigten Arl5b Knockout-Mäuse Lern-Defizite.

Schlussfolgernd konnte ich Arl5b als kanonisches Arf -ähnliches Protein charakterisieren, welches

das den Ziel-gerichteten Transport von späten Endosomen vermittelt. Darüber hinaus deuten die Ergebnisse auf eine Funktion für die BDNF-abhängige Signalweiterleitung hin, welche synaptischer Plastizität zugrunde liegt. In Übereinstimmung mit dieser möglichen Funktion für die neuronale Plastizität zeigen Arl5b Knockout-Mäuse eine Tendenz zur reduzierten, langfristigen Gedächtnisbildung.

1. Introduction

1.1 Learning and memory

Basic research in the field of learning and memory is driven to understand how the nervous system of animals is capable to perceive, process, store and recall information. The capability to learn and to reactivate previously formed memories is of major importance for animals to successfully adapt to their ever changing environment and to survive. One of the main questions of modern neuroscience is where and how the brain stores memories. The approximately 86 billion cells of the brain are subdivided into two major classes, neurons and glia cells. A neuron forms around 1000 to 10000 connections with other neurons (Herculano-Houzel 2012). The dynamic modification of these connections is thought to be a key factor for memory formation.

The connections between neurons are formed by highly specialized regions of two neurons and are called synapses. While the morphology, size and type of synapses are variable the underlying principle is common among all. Neurons are highly polarized cells usually divided into the soma, where the nucleus resides, an axon and dendrites. One neuron sends information, usually by releasing chemical neurotransmitter such as glutamate or gamma-Aminobutyric acid (GABA) from its axonal presynaptic regions into the synaptic cleft. A second neuron (or alternatively a muscle cell) perceives the signal at a postsynaptic site which is located in the dendrite or soma.

Upon reception of the signal in the postsynapse it can be converted into an electrical signal. This signal is propagated along the membrane of the neuron towards the axon hillock, located at the transition between soma and axon. A signal send by a neuron can be excitatory or inhibitory. The structure and protein composition determine excitatory and inhibitory synapses. Only if multiple excitatory signals arrive at the axon hillock simultaneously a certain threshold is overcome and a so-called action potential is send along the axon. Here the signal is responsible for neurotransmitters to be released into the synaptic cleft. By this mechanism the signal can be passed along a network of neurons.

A possible deviation from this dogma has been proposed. Glia cells may affect neuronal activity (Newman, 2003) and modulate synaptic strength (Kang et al., 1998). More recently, it was shown that neurons are not the only cells in the brain that generate action potentials. Oligodendrocyte precursor cells are capable to fire action potentials themselves *in vivo* (Karadottir et al., 2008).

The synaptic cleft is in many cases isolated from the environment by astrocytic glia cells. The glia cells contribute to the synaptic submission and therefore the term tripartite synapse was established in the last decade (Araque et al., 1999; Dityatex and Rusakov, 2011).

In the last years Gundelfinger and Frischknecht published results about a fourth factor of major importance in addition to the pre-, postsynaptic neuron and surrounding glia cells. The proper function of the ECM (extracellular matrix) is as well a prerequisite for the synaptic transmission (Gundelfinger et al., 2010; Frischknecht and Gundelfinger, 2012).

One of the most interesting and yet unsolved questions in neuroscience is the mechanism by which the brain is able to form and store memories over a period as long as a lifetime. In the contrary to early assumptions studies in the past decades suggest that the complex neuronal network is not inflexible but connectivity between the cells in the brain is highly modifiable.

While electrical signals are relatively inflexible the possibility to regulate the chemical transmission of the signal between neurons are multifarious. Many factors involved in synaptic transmission are variable and regulated by various cellular mechanisms. To name only a few of the variables: The strength of neurotransmitter release depends on the structure of the presynapse. The residence time of the neurotransmitters is influenced inter alia by the astrocytic glia. The composition of the postsynaptic receptors defines the postsynaptic signal reception. The number of functional connections between two neurons or in a neuronal circuit is modifiable. This dynamically adjusted connectivity between the neurons in the brain is known as synaptic plasticity. Even though it is not entirely proven the mechanism of synaptic plasticity is so far the best candidate to be the physiological concept that underlies learning and memory formation (Bliss and Collingridge, 1993; Hyman and Malenka, 2001; Malenka and Bear, 2004; Johnston, 2004; Whitlock et al., 2006; Mayford et al., 2012).

1.2 Synaptic plasticity

An early hypothesis about the long-term storage of memory was postulated by Donald O. Hebb. He claimed that the correlated activity of a pre- and postsynapse leads to a long-lasting strengthening of the synapse. A specific circuit of neurons would undergo strengthening upon a learning input leading to storage of information (Hebb, 1949). This theory was later confirmed in physiological studies. It was shown that strong and long lasting forms of synaptic plasticity are present in hippocampal neurons (Bliss and Lomo, 1973). This process involves changes in the physiology and morphology of the synapse, is well established today and known as long-term potentiation (LTP). Its counterpart is the uncorrelated pre- and postsynaptic activity. Factors involved in LTP can be regulated in the opposite direction, e.g. the internalization of receptors in the postsynapse, leading to weakening of synaptic transmission. Early studies proved existing of this process (Stent, 1973). Weakening of a synapse over a long period of time is called long-term depression (LTD).

During the last decades a variety of different mechanisms of plasticity were described. Strikingly

long as well as short lasting forms of synaptic plasticity were described in various brain regions including the hippocampus, cerebral cortex, amygdala and cerebellum. The broadest studied form of LTP is the NMDA-receptor dependent form at the synapses of the Schaffer collaterals and commissural neurons in the CA1 region of the hippocampus.

The hippocampus of the mammalian brain is anatomically highly structured and is found in the temporal lobe. The hippocampal formation is subdivided into the perirhinal and entorhinal cortices, subiculum (SB), dentate gyrus (DG) and cornu ammonis regions 1-3 (CA1-3). In the modern literature the term "hippocampus" is used to describe the structure that consists of the last three mentioned regions. Due to the fact that it is connected with many sensory systems as well as with parts of the neocortex, the hippocampus was very early a candidate to be an important region for learning and long-term memory formation (Eichenbaum, 2000; van Strien et al., 2009). A trisynaptic loop is thought to be the main pathway for information processing. The axons from layer II of the entorhinal cortex, invading the dentate gyrus (termed the perforant path), form synapses with dendrites of granule cell neurons. Their axons form mossy fiber axon bundles and connect to pyramidal neurons in the CA3 region. Via the Schaffer collaterals the pathway is carried on to pyramidal neurons in the CA1. The loop is completed by projecting back from the CA1 into the entorhinal cortex (Amaral and Witter, 1989; Yeckel and Berger, 1990) (Figure 1.1).

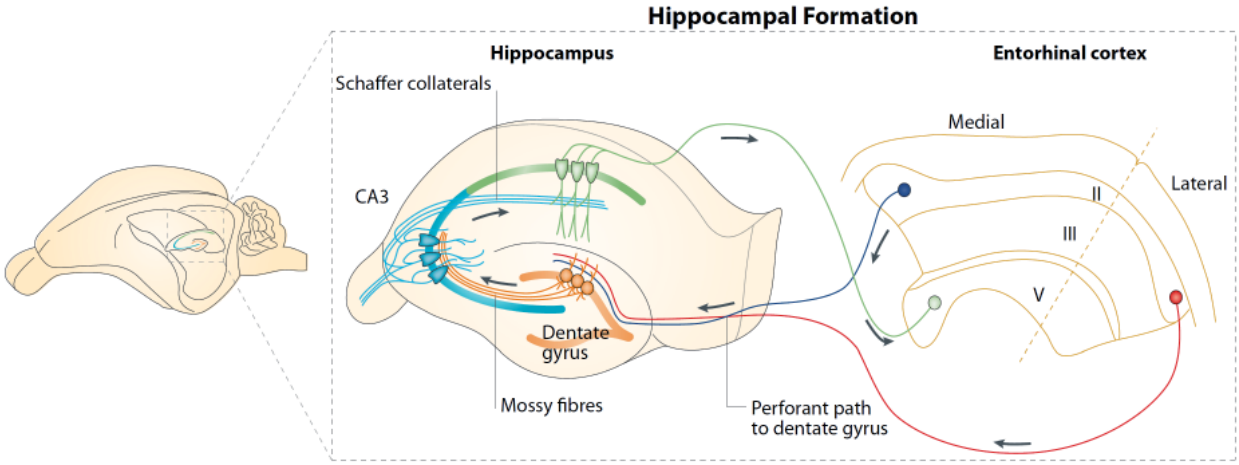

Figure 1.1. Schematic representation of the hippocampal formation. Shown are the main connections within the hippocampus and from or to the entorhinal cortex. The route of the informational flow of the most investigated trisynaptic loop is depicted by black arrows. From layer II in the entorhinal cortex the information is passed to the dentate gyrus, is forwarded to CA3 region and from here to the CA1 region before it leaves the hippocampus and is received in layer V of the entorhinal cortex (modified from Neves et al., 2008).

A result of the extensive research on the hippocampal synaptic connections is the finding that the hippocampus is necessary for declarative memory formation (Levy and Steward, 1979). This further strengthens the speculation that memory processes rely on the computations made possible by plasticity (Bliss and Collingridge, 1993; Malenka and Bear, 2004; Fusi et al., 2005; Neves et al., 2008).

Many studies of the past decades focused on the molecular and cellular mechanisms of synaptic

plasticity aiming to understand the phenomenon of memory storage and retrieval. One of the crucial excitatory neurotransmitters is glutamate which is released of synaptic vesicles stored in the presynapse. At the postsynaptic membrane it can bind to and activate different receptors. Two major receptor classes were defined by their selective agonists AMPA (α-amnio-3-hydroxy-5-methyl-4-isoxazole-propionic acid) and NMDA (N-methyl D-aspartate). Both receptors consist of four variable transmembrane spanning subunits. Together these subunits form ion selective pores in the membrane of the postsynapse (Wisden and Seeburg, 1993; Hollmann and Heinemann, 1994). Even though AMPA- and NMDA-receptors are activated by the same transmitter they have distinct functions in the synapse. Upon glutamate binding AMPA-receptors immediately open their core pore and mediate the main ionic conductance of the postynaptic cell. In contrast the NMDA-receptor remains in its locked form at resting potential due to an Mg^{2+} block after glutamate binding. To release the block the postynaptic membrane needs to be depolarized (Mayer et al., 1984; Nowak et al., 1984). This depolarization is mediated by the repetitive stimulation of AMPA-receptors. Due to these two properties the NMDA-receptor acts as a coincidence detector. Both, presynaptic glutamate release and postsynaptic membrane polarization must occur jointly to elucidate a reaction downstream of the receptor.

The NMDA-receptor mediated influx of Ca^{2+} ions into the cell is essential for the induction of LTP (Lynch et al., 1983; Malenka et al., 1992). One effect of increased Ca^{2+} levels is the auto-phosphorylation and the constitutive activation of the Ca^{2+}/Calmodulin-dependent protein kinase II (CaMKII) resulting in the phosphorylation of the protein kinase A (PKA) via cAMP and activation of protein kinase C (PKC) (Malinow et al., 1989; Frey et al., 1993; Huang et al., 1994; Abel et al., 1997). Different studies identified the targets of these signaling cascades. Their activation after Ca^{2+} influx lead to gene transcription under the control of several well investigated transcription factors such as serum response factor (SRF) (Treisman, 1987), cAMP response-element binding protein (CREB) (Sheng et al., 1991; Arthur et al., 2004) and Myocyte enhancer factor 2 (MEF2) (McKinsey et al., 2002). These are only a few examples for the manifold signaling cascades involved in various forms of plasticity.

Like memory formation, it is well established that LTP can be divided at least into two phases. The early phase (E-LTP), which is independent of protein translation, and the late phase (L-LTP) that requires the synthesis of new protein during induction. Distinction between the early and late phase is not as easy because the two phases vary based on the protocol of induction as well as on the experimental specimen, e.g. acute hippocampal slices or *in vivo* recordings. However, L-LTP can last for hours up to weeks in living animals, while E-LTP is stable up to three hours under protein synthesis inhibition and relies on post-translational modifications. Consistent with the impairment of LTP by inhibition of translation, long-term memory formation relies on translation. (Squire and Barondes, 1972, Krug et al., 1984; Stanton and Sarvey,

1984; Deadwyler et al., 1987; Frey et al., 1988; Huber et al., 2001; Karachot et al., 2001).

Various cellular mechanisms are associated with LTP and LTD. The relocation of AMPA receptors by trafficking from extra synaptic locations and/or additional intracellular storages to or from the post-synaptic density is thought to be a modulator of synaptic strength in terms of LTP and LTD (Isaac et al., 1995; Liao et al., 1995; Carroll et al., 1999; Heynen et al., 2000; Malinow and Malenka 2002). Another mechanism shown to be implicated in the induction of LTP is the growth of synapses. A repetitive, high frequency stimulation of the Schaffer collateral-commissural projections from CA3 to CA1 *in vivo* results in the formation of stubby spine synapses of CA1 neurons (Lee et al., 1980; Chang and Greenough, 1984). In slices the persistent change of synapses were linked to long-lasting LTP stimulations (8 hours) (Chang and Greenough, 1984). LTD on the other hand can be mediated by the loss of synaptic connections. Pharmacological induction of LTD in hippocampal slices was shown to be sufficient to reduce the number of functional synapses (Shinoda et al., 2005; Kamikubo, 2006). Additionally in a recent study it was shown that LTD is at least in part caused by pruning of a percentage of synaptic contacts between two neurons while others remain stable in terms of size of the pre- and postsynapse over a period of time as long as one week (Wiegert and Oertner, 2013).

The observation that LTP requires protein and RNA synthesis (Squire and Barondes, 1972; Krug et al., 1984; Frey et al., 1996) and that induction of LTP regulates gene expression led to the conclusion that genes which are upregulated play important roles for learning and memory processes.

1.3 Activity regulated genes

In early studies unbiased differential screening techniques were used to identify genes that are transcriptionally induced by seizure activity in the hippocampus (Qian et al., 1993; Nedivi et al., 1993; Yamagata et al., 1994). Although long-term potentiation (LTP) is considered to be more physiological than experimentally induced seizures, both lead to a long lasting enhancement of synaptic activity. In fact, almost all genes that are known to be induced during long-term potentiation (LTP) were initially identified in such screens and several activity-dependent genes were shown to play important roles in the structural and functional changes underlying long-term plastic events in the nervous system. A few example for extensively studied activity regulated genes are zif/268, c-fos, c-jun (Cole et al., 1989; Wisden et al., 1990), rgs2 (Ingi et al., 1998), arg3.1/arc (Link et al., 1995; Lyford et al., 1995), homer1a (Brakeman et al., 1997), snk (Kauselmann et al., 1999), tPA (Qian et al., 1993), arcadlin (Yamagata, 1999), narp (Tsui et al., 1996) and bdnf (Patterson et al., 1992). An example for an activity-regulated small GTPase is rheb, which is additionally growth factor regulated and plays a role in the mTOR signaling cascade (Yamagata et al., 1994).

Understanding the roles of activity-dependent proteins was and is of great importance to gain insight of the cellular mechanisms underlying learning and memory. Therefore the comprehensive analysis of genes regulated in response to neuronal activity is of general interest. The development of large scale genome wide analysis made it possible to identify global changes in expression and lead to the identification to large sets of genes induced at certain time points after neuronal activity provoked by different paradigms.

In a screen from Greenberg and colleagues KCl was used to induce transcription by membrane depolarization and subsequent calcium influx in dissociated hippocampal neurons after 10 days of cultivation. At this age manipulation of MEF2 has influence on synapse development. Besides known activity regulated genes such as c-fos, arg3.1/arc and bdnf, 643 genes were upregulated after 1 or 6 hours after membrane depolarization. In additional experiments they assessed which genes were upregulated by artificial activation of MEF2 (251 genes in total) or downregulated by inhibition of MEF2 (1365 genes in total). Surprisingly few genes (45 in total) overlapped between the upregulated genes after KCl treatment or MEF2 activation (Flavell et al., 2008).

Another study deciphered the genetic response to NMDA receptor signaling by whole-genome expression profiling also using dissociated hippocampal neurons cultured for 10-12 days *in vitro*. Induction of synaptic NMDA receptors using an action potential bursting protocol, inducing long-lasting, transcription-dependent synaptic plasticity, led to upregulation of 478 genes. Some of these genes are associated with neuroprotection. In contrast mRNA levels of pro-death genes were decreased. A second approach, bath application of glutamate and simultaneous blocking of synaptic NMDA receptors, initiated cell-death pathways downstream of extrasynaptic NMDA receptor stimulation. This protocol led to activation of transcription of 106 genes, only partly overlapping with the genes upregulated in the first assay (Zhang et al., 2007).

In vivo genome-wide profiling identified about 1000 activity-regulated genes in the hippocampus. Genes were classified to five groups based on their expression kinetics. The genes were identified by kainic acid induced seizures and scarification of the mice to obtain hippocampal tissue after 1, 4, 8 or 24 hours and subsequent microarray analysis. The upregulation of 24 of those genes was validated by *in situ* hybridization (Hermey et al., 2013). One of the validated genes is the GTPase Arl5b which will be described later in more detail and the role of Arl5b in synaptic plasticity is subject of this thesis.

Most screens confirm the regulation of already well studied genes. Many of these belong to a particular class of genes that were classified as immediate early genes (IEGs). These genes show a strong upregulation within 60 minutes after activity induction independent of translation. The regulation of these genes is highly regulated in the neuronal system (Sheng and Greenberg, 1990). Most of those genes were originally identified as transcription factors (e.g. npas4, zif/268 or c-fos) (Morgan et al., 1987; Cole et al.,

1989; Lin et al., 2008) or were found to be responsive to different growth-factors in non-neuronal cells (Hayward et al., 1981; Kelly et al., 1983; Sheng and Greenberg, 1990). Other IEGs such as Homer1A, tPA or Arg3.1/Arc are known as effector proteins. Among those Arg3.1/Arc stands out as its mRNA was shown to be selectively targeted to dendritic regions of dentate gyrus granule cells after receiving synaptic stimulation (Link et al., 1995; Lyford et al., 1995; Wallace et al., 1998). Upon genetic deletion of Arg3.1/Arc mice fail to stabilize plasticity such as LTP or LTD. This results in the lack of long-term memory formation on a behavioral level (Plath et al., 2006).

1.4 BDNF and TrKB in synaptic plasticity

One of the most well studied activity regulated genes is the brain derived neurotrophic factor (BDNF). One variant of bdnf mRNA was found to be upregulated after kainic acid induced seizures (Zafra et al., 1990). As a pleiotropic effector BDNF is known to be a major regulator of various developmental processes. Beside its ability to modulate synaptic plasticity it has an impact upon axon growth, pathfinding and regeneration, dendrite aborization and spine morphology (McAllister, 1995; Cohen-Cory, 1999, Cohen-Cory, 2010). For the scope of this work its structural effects are less important than its role in synaptic plasticity. It is known that BDNF acts on synaptic transmission in excitatory as well as inhibitory synapes (Kang and Schuman, 1995; Carmignoto et al., 1997; Rutherford et al., 1998). BDNF fulfills important functions for the induction and maintenance of LTP. Removing BDNF from the genome of mice results in impairment of hippocampal LTP. However supplementation of exogenous BDNF is sufficient to rescue this phenotype (Korte, 1995). BDNF itself influences transcription and translation. Its multifaceted mechanism of action also enables it to regulate other activity-regulated genes. Among others it can induce transcription of arg3.1/arc, narp, cpg15 and tPA (Wibrand et al., 2006, Fiumelli, 1999; Waltereit et al., 2001).

Modification of plasticity by BDNF can be explained by its ability to activate several signaling cascades upon binding to the receptor TrkB (Tyrosine receptor kinase B). The main intercellular signaling cascades activated by BDNF will be described briefly (also depicted in more detail in figure 1.2). All three signaling cascade are activated by binding of BDNF to TrkB. Upon binding different tyrosine sites in the cytoplasmic domain of TrkB are phosphorylated. Dependent on the phosphorylation site different cascades are activated.

The Ras-mitogen-activated protein kinase (MAPK) pathway is activated by binding growth factor receptor-bound protein 2 (GRB2) and son of sevenless (SOS) after recruitment and phosphorylation of Shc adaptors (Kouhara et al., 1997; Wright et al., 1997; Hadari et al., 1998). Additionally, other signaling proteins are recruited further strengthening the sustained activation of the MAPK pathway.

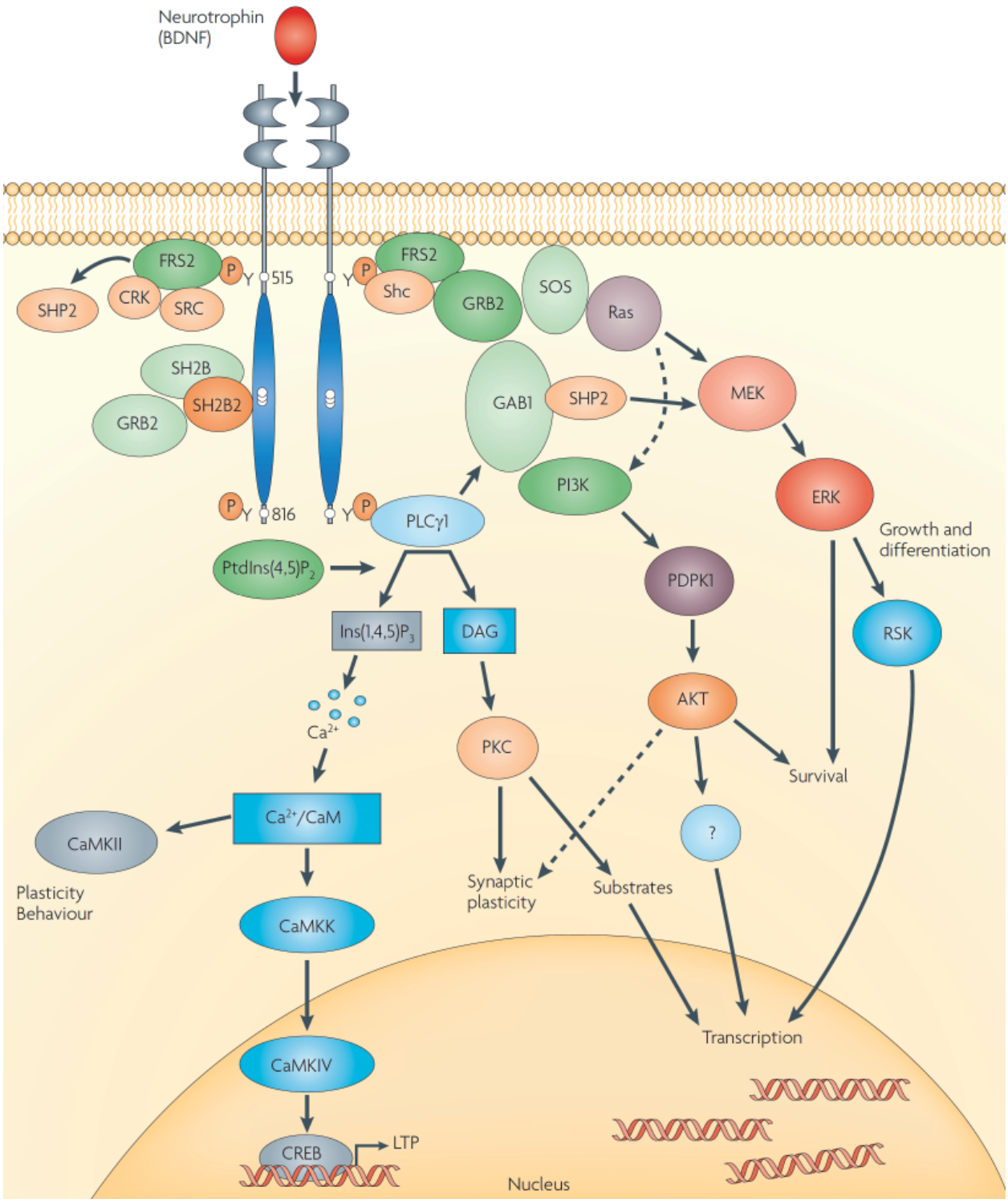

Figure 1.2 Major signaling pathways downstream of BDNF/TrkB. Three main pathways are influenced by the activation of TrkB by BDNF. i) The Ras-mitogen-activated protein kinase (MAPK) pathway is activated through recruitment and phosphorylation of adaptor proteins. Subsequent MEK (MAPK/ERK) kinase, ERK (extracellular signal-regulated kinase) result in neuronal differentiation/growth. ii) Recruitment of the phospholipase Cγ1 (PLCγ1) activates Ins(1,4,5)P3 and DAG generation. The first causes activation of a CaMKII/CaMKK/CaMKIV cascade through Ca^{2+} release mediating synaptic plasticity by activation of CREB. DAG influences synaptic plasticity by activation of PKC. iii) Recruitment of GAB1 allows Ras to activate PI3K which leads to AKT activation and subsequent signaling through the mTOR pathway resulting in synaptic plasticity, survival and growth. (modified from Minichiello, 2009)

Phosphorylation of TrkB at the tyrosine 816 leads to recruitment and activation by phosphorylation of PLCγ1 (Kaplan and Miller, 2000). This activation of PLCγ1 enables hydrolysis of phosphatidylinositol-4,5-bisphosphate (PtdIns(4,5)P2) to generate inositol-1,4,5-trisphosphate (Ins(1,4,5)P3) and diacylglycerol (DAG). These two molecules both possess signaling abilities. DAG stimulated specific PKC isoforms and Ins(1,4,5)P3 triggers CA^{2+} release from internal stores. In turn Ca^{2+}/Calmodulin-dependent protein kinases are activated (Reichardt, 2006).

The third activated pathway is the phosphatidylinositol 3-kinase (PI3K)-Akt pathway. As in the MAPK pathway activated TrkB binds to GRB2 which recruits adaptor proteins. In this case these are GRB-associated binder-1 (GAB1) and Insulin-receptor substrate 1 and 2 (IRS1/2). Subsequently PI3K is associated with the receptor and generates 3-phosphoinositides due to its activation which activate 3-phosphoinsositide-dependent protein kinase 1 (PDPK1). Substrate of PDPK1 is the protein kinase AKT, a key player in multiple signaling pathways (Holgado-Madruga et al., 1997; Yamada et al., 1997; Franke et al., 1997; Crowder and Freeman, 1998). Additionally these signaling pathways cannot be viewed isolated from each other. Cross-talk exists between the AKT/mTOR and MAPK pathways. For example the GAB activation has the power to enhance MAPK signaling (Liu and Rohrschneider, 2002).

One example how BDNF can act on synaptic plasticity by translation is its influence on the mammalian target of rapamycin (mTOR) pathway through this activation of AKT. The signaling pathway is depicted in more detail in figure 1.3. AKT inactivates hamartin (TSC1) and tuberin (TSC2) which form the tuberous sclerosis complex by phosphorylation. This inhibition blocks their function as GAP of Rheb (Ras homolog enriched in brain). Higher levels of active (GTP-bound) Rheb induce activation of mTOR (Manning et al., 2002; Garami et al., 2003; Tee et al., 2003). If present in the TORC1 complex (mTOR/Raptor complex) mTOR regulates a variety of cellular processes such as protein translation, transcription, protein degradation, glycolysis and microtubule dynamics.

Certain forms of LTP rely on synthesis of new protein (Kelleher et al., 2004; Squire and Davis, 1981). Therefore increased translational capacity after BDNF signaling through the mTOR pathway is a reasonable mechanism to facilitate these synaptic changes. The TORC1 complex is best known for its ability to positively regulate translation by phosphorylation of p70S6K and 4E-BP (Burnett et al., 1998; Hara et al., 1997). Due to this phosphorylation 4E-BP dissociates from eIF-4E, which is now capable to initiate cap-dependent translation by binding to eIF-4G (Beretta et al., 1998). TORC1 mediated phosphorylation of p70S6 kinase in turn phosphorylates the ribosomal protein S6. This activation stimulates translation of mRNAs containing a 5’ oligopyrimidine tract (TOP-RNAs). Members of this subgroup of mRNAs code for other ribosomal proteins and elongation factors. Therefore their enhanced translation increases translation in general (Jefferies et al., 1997; Meyuhas, 2000).

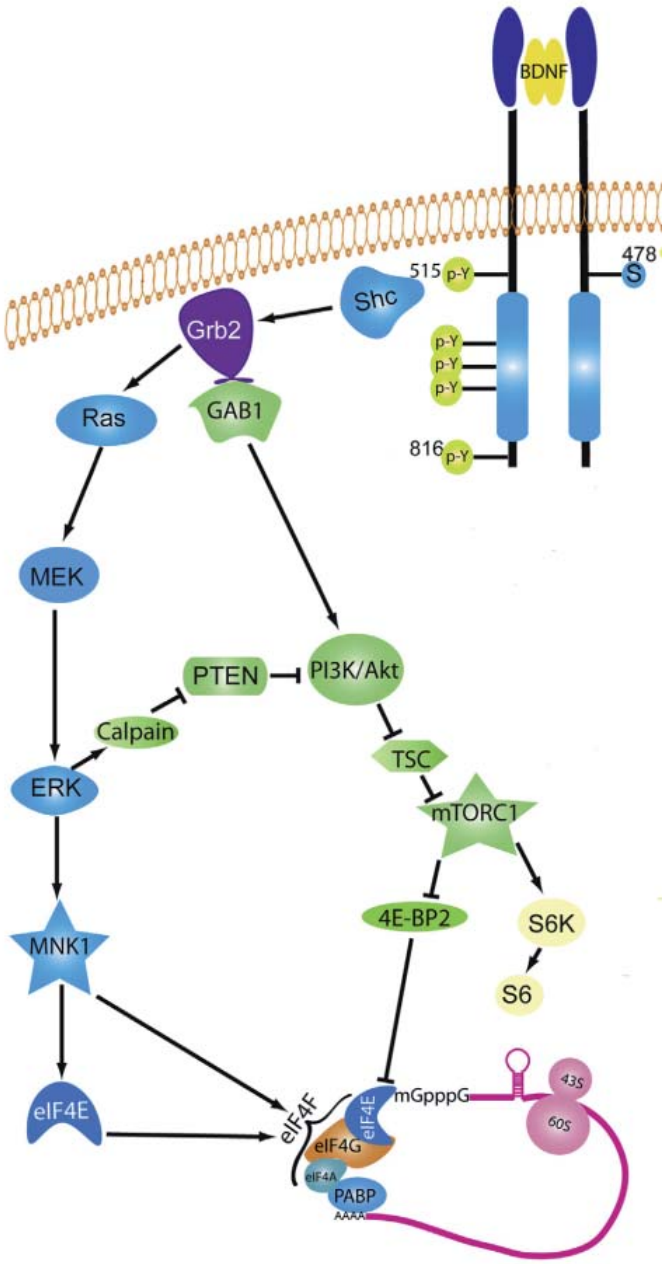

Figure 1.3 Activation of Translation by BDNF mediated signaling. Phosphorylation of Y515 of TrkB by BDNF binding activates the PI3K/AKT pathway. AKT deactivates the TSC1 and TSC2. In turn rheb (not shown) is activated leading to activation of the TORC1 complex which phospohorylates two proteins involved in regulation of translational. The phosphorylation of 4E-BP shuts down its negative regulation on eIF-4E stimulating translation. The phosphorylation of p70S6K (S6K) activates ribosomal protein S6 (S6) and therefore also enhances translation. Also shown are parts of the MAPK pathway which has an influence on the PI3K/AKT pathway for example over regulating PTEN (phosphatase and tensin homolog) (modified from Panja and Bramham, 2013).

In addition, the mTOR pathway controls mRNAs of which several are known to have a function in synapse formation and synaptic plasticity in response to BDNF. Prominent examples are CamKIIα, LIMK1, NR1 (Schratt et al., 2004; Schratt et al., 2006). Another protein, PSD95, an important scaffold protein in the post synaptic density of excitatory synapses, is upregulated upon activation of the mTOR pathway by the hormones insulin or estrogen (Lee et al., 2005; Akama and McEwen, 2003). Related to BDNF signaling is the finding that activation of TrkB by CDK5 mediated phosphorylation at serine 478 is required to induce AKT dependent activation of ribosomal protein S6 and therefore induction of PSD95 translation after bicuculline/glycine treatment of cultured cortical neurons. Knock-in mice in which this serine is replaced by alanine fail to facilitate TBS-induced LTP (Lai et al., 2012).

1.5 Arl5b, a member of the Arf family of G proteins, is an activity regulated small GTPase

Another activity regulated gene is the currently poorly understood arl5b. The protein Arl5b is a member of the ADP-ribosylation factor (Arf) like proteins (Arl) family. Members of this family share a few features that distinguish them from other classes of small GTPases.

The large family of small GTPases is known for the ability to bind GTP. They usually act as low molecular weight “on/off” switches in intracellular signaling cascades. Among the best described GTPases are Rac, Ras and CDC42. A good example for the implication of GTPases in synaptic plasticity is the above mentioned Rheb. Commonly small GTPases are activated upon GTP binding and inactivated by hydrolysis of the GTP to GDP. They are controlled by guanine nucleotide exchange factors (GEFs) and GTPase-activating factors (GAPs). GEFs execute the GDP release and GTP binding while GAPs catalyze the GTP hydrolysis.

Arf proteins are known as important proteins in trafficking processes. They are implicated in recruitment of coat proteins, cargo sorting and they also activate lipid-modifying enzymes such as phosphatidylinositol kinases. The following features are conserved among members of the Arf and Arl family. Their N-terminus contains an amphipathic helix that allows, together with amino-terminal myristoylation or acetylation, tight membrane association. The switch 1 and switch 2 domains are effector regions that can regulate the binding to membranes by conformational changes of the protein followed by either presenting the amphipathic helix or hiding it inside of the GTPase. This process is GTP/GDP dependent. Figure 1.4 depicts these features of Arf and Arl proteins (Souza-Schorley and Chavier, 2006; Gillingham and Munro, 2007; Donaldson and Jackson, 2011).

The GTPase Arl5b is expressed in various tissues such as kidney, heart, spleen and the brain. Results from a recent study imply a role of Arl5b in retrograde trafficking. Upon knockdown of Arl5b in HeLa cells using siRNAs the internalization and retrograde transport of Shiga toxin fragment B (STxB) towards the Golgi apparatus was blocked (Houghton et al., 2012).

In the brain arl5b is upregulated after different activity inducing stimuli. One and six hours after stimulation of cultured hippocampal neurons (DIV10) with KCl a two-fold increase of arl5b mRNA levels was observed while the activation of MEF2 had no influence on Arl5b (Flavell et al 2008). In addition, transcription of Arl5b was strongly upregulated by an AP bursts protocol in dissociated hippocampal neurons which induces transcription-dependent synaptic plasticity (Arnold et al., 2005). In contrast to this synaptic NMDA receptor signaling dependent protocol a different protocol activating extrasynaptic NMDA receptor signaling did not regulate Arl5b transcription (Zhang et al., 2007).

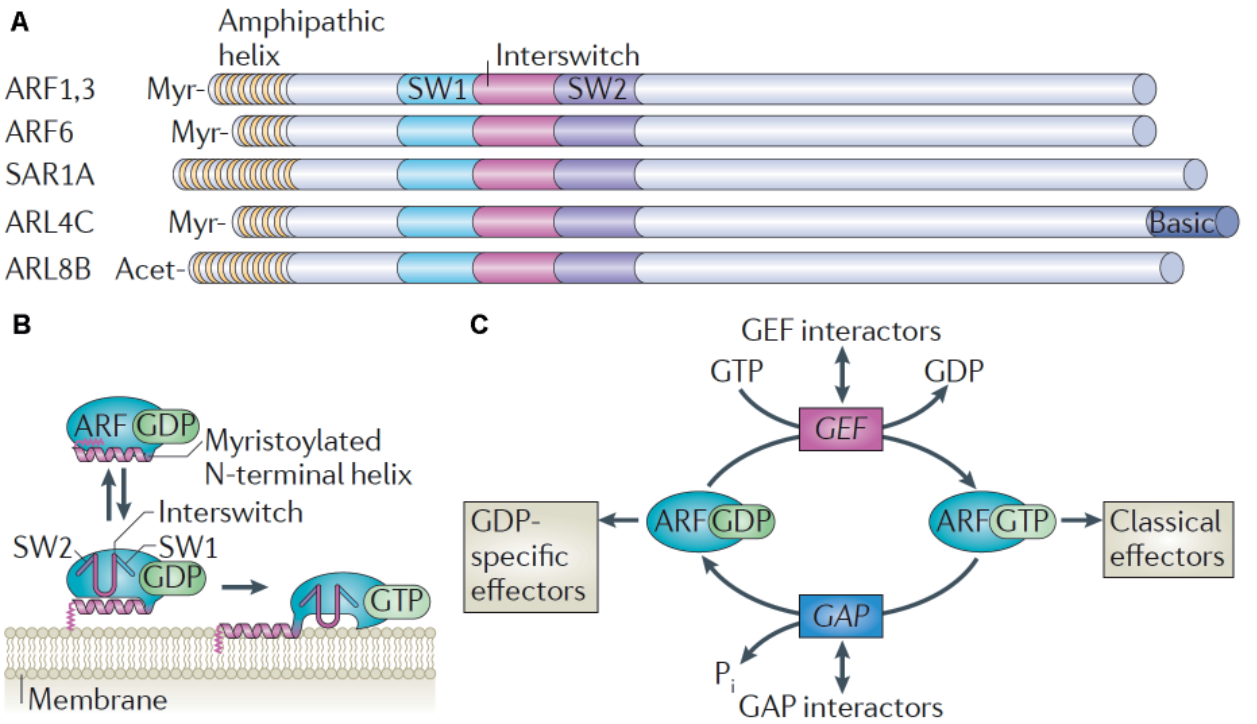

Figure 1.4 Structure and regulation of Arfs and Arls. A Schematic representation of five different members of the Arf family of small GTPases. Highlighted are the conserved N-terminal amphipathic helix which allows myristoylation (Myr) or acetylation (Acet) mediated tight membrane binding and the switch1 and 2 (SW1/2) with intercalating interswitch region which are known as effector regions. GTP binding after GDP release results in a conformational change of the protein. B Exchange of bound GDP to GTP and its hydrolysis reversibly associates Arfs and Arls with membranes. Upon GTP binding the interswitch region of Arf/Arls displaces the amphipathic helix from a hydrophobic pocket where it resides during Arf/Arls are GDP-bound. C Arf family G proteins are regulated by GEFs and GAPs. GEFs exchange GDP by GTP while GAPs catalyze the hydrolysis of GTP to GDP. Arf family proteins interact with GTP and/or GDP specific effectors dependent on their state (modified from Donaldson and Jackson, 2011).

Recent studies from Hermey and colleagues also identified Arl5b as an activity regulated gene. The induction of Arl5b was confirmed by *in vivo* application of kainic acid. The experimental design added knowledge about the regulation of Arl5b after an activity stimulus over a long time period. A sharply controlled strong upregulation in the hippocampus of mice was confirmed by *in situ* hybridization using a radioactively labeled probe of the arl5b open reading frame. While the mRNA levels of Arl5b were increased tremendously after one and two hours after the induced seizure, mRNA levels fall back to baseline after 4 hours (Hermey et al., 2013).

Interestingly the regulation of arl5b is not restricted to neurons. A recently published study identified arl5b as an IFN-β (interferon-beta) response gene. Arl5b exhibits significantly higher baseline transcription levels in peripheral blood mononuclear cells (PBMCs) isolated from patients with a relapsing–remitting form of multiple sclerosis (RRMS) compared to healthy donors (HD). In addition the induction of arl5b after IFN-β treatment is stronger in PBMCs of HD compared to PBMCs of RRMS (Boppana et al., 2013). This result combined with the finding from Houghton and colleagues (Houghton et al 2012) indicates a general role for Arl5b in retrograde trafficking in response to receptor activation. However, these studies were not published at the beginning of the present thesis.

1.6 Aim of this study

In the last decades the role of many activity regulated genes were linked to synaptic plasticity and the formation of long-term memory. Recent screens revealed a multitude of yet uncharacterized activity dependent proteins. One of them is the small GTPase Arl5b. It is among a smaller subgroup of genes which are tightly upregulated after plasticity producing stimulation. Together with its function as small GTPase this makes Arl5b a good candidate to act as a regulator in synaptic trafficking events, as a key molecule in one of the signaling cascades mediating synaptic plasticity and beyond that being required for memory formation. One aim of the study was to investigate the role of Arl5b in the mammalian neuronal cells with the help of molecular and biochemical assays and by studying interaction partners of Arl5b. In addition the importance of Arl5b during memory formation will be investigated by establishing and characterization of an Arl5b knockout mouse model.

2. Material & Methods

2.1 Material

2.1.1 Solutions and growth media

All solutions and media were prepared with purified water (aqua dest.) Unless stated otherwise the pH-value was adjusted by using NaOH, KOH or HCl. For sterilizing solutions were autoclaved for 20 min at 121 °C and 2.1 bar or filtered through a membrane with an exclusion limit of 0.22 µm. Table 2.1 lists used solutions and media and their compositions.

Table 2.1. Buffers and media used in experiments of this thesis.

PBS 10x		
Reagent	Final concentration	Amount
NaCl	1.37 M	80 g
KCl	27 mM	2.01 g
Na_2HPO_4(*$2H_2O$)	81 mM	14.4 g
KH_2PO_4	14.7 mM	2 g
H_2O		Ad 1000 ml

Antibiotics (added to LB media for clone selection)			
Reagent	Stock concentration	Final concentration	Volume for 1 l medium
Kanamycin	50 mg / ml in H2O	50 µg / ml	1 ml
Ampicillin	100 mg / ml in H2O	100 µg / ml	1 ml
Tetracyclin	5 mg / ml in ethanol	10 µg / ml	2 ml
Chloramphenicol	12.5 mg / ml in ethanol	12.5 µg / ml	1 ml

SSC 20x		
Reagent	Final concentration	Amount
NaCl	3 M	175.3 g
Trisodium citrate (*$2H_2O$)	0.3 M	88.2 g
H_2O		Ad 1000 ml
Adjusted to pH 7.0 (add 1000 µl DEPC for RNA)		

Lysogeny broth		
Reagent	Final concentration	Amount
NaCl	0.5 % (w/v)	5 g
Tryptone	0.5 % (w/v)	5 g
Yeast extract	1 % (w/v)	10 g
H_2O		Ad 1000 ml
Adjusted to pH 7.5, autoclaved		

SOC medium			
Reagent	Stock concentration	Final concentration	Volume / amount
Pepton			20 g
Yeast extract			5 g
NaCl	5 M	8.56 mM	1.712 ml
KCl	1 M	2.5 mM	2.5 ml
H_2O			Ad 1000 ml
Adjusted to pH 7.0, autoclaved			
$MgCl_2$	2 M	10 mM	5 ml
Glucose (sterilized by filtration)	1 M	20 mM	20 ml

Buffers used for DNA preparation			
Buffer S1			
Reagent	Stock concentration	Final concentration	Volume / Amount
TrisHCl pH 8.0	1 M	50 mM	50 ml
EDTA pH 8.0	250 mM	10 mM	4 ml
RNAseA		100 µg / ml	100 mg
H_2O			Ad 1000ml
Buffer S2			
NaOH	2 M	200 mM	100 ml
SDS	10 %	1 %	100 ml
H_2O			Ad 1000 ml
Buffer S3			
KAc pH 5.5	10 M	3 M	300 ml
H_2O			Ad 1000 ml

DNA gel loading buffer 10x			
Reagent	Stock concentration	Final concentration	Volume / amoun
TrisHCl pH 7.6	1 M	10 mM	100 µl
Glycerin	100 %	50 %	5 ml
EDTA pH 8.0	500 mM	60 mM	1.2 ml
Bromphenol blue		0.25 %	25 mg
H_2O			Ad 10 ml

Protein sample buffer 5x			
Reagent	Stock concentration	Final concentration	Volume / amount
TrisHCl pH 6.8	1 M	250 mM	25 ml
SDS		10 %	10 g
Glycerin	100 %	50 % (w/v)	50 g
DTT		500 mM	7.715 g
Bromphenol blue	1 %	0.01 %	1 ml
H_2O			Ad 100 ml

Cell lysis buffer (for cell lysis and CO-IP)			
Reagent	Stock concentration	Final concentration	Volume / amount
TrisHCl pH 7.5	1 M	10 mM	500 µl
NaCl	5 M	150 mM	1.5 ml
EDTA	500 mM	0.5 mM	50 µl
NP40		0.5 %	0.25 ml
H_2O			Ad 50 ml
Freshly added:			
PhosSTOP phosphatase inhibitor cocktail (Roche)	10 x	1 x	
cOmplete protease inhibitor cocktail (Roche)	50 x	1 x	

Dilution buffer (for cell lysis and CO-IP)			
Reagent	Stock concentration	Final concentration	Volume / amount
TrisHCl pH 7.5	1 M	10 mM	500 µl
NaCl	5 M	150 mM	1.5 ml
EDTA	500 mM	0.5 mM	50 µl
NP40		0.5 %	0.25 ml
H_2O			Ad 50 ml
Freshly added:			
PhosSTOP phosphatase inhibitor cocktail (Roche)	10 x	1 x	
cOmplete protease inhibitor cocktail (Roche)	50 x	1 x	

HANKS` medium / HANKS` medium plus FCS			
Reagent	Stock concentration	Final concentration	Amount
HANKS balanced salt solution			1 bottle
$NaHCO_3$		4.17 mM	350mg
HEPES		1 mM	238mg
H_2O			Ad 1000 ml
Adjust to pH 7.3-7.4			

HANKS` medium plus FCS (sterilized by filtration)			
HANKS` medium			160 ml
FCS	100 %	20 %	20 ml

Dissociation buffer			
Reagent	Stock concentration	Final concentration	Amount
NaCl	5 M	147 mM	2.74 ml
KCl	1 M	5 mM	500 µl
Na_2HPO_4 (*$2H_2O$)	120 mM	7 mM	5.833 ml
HEPES		25 mM	595.8 mg
H_2O			Ad 100 ml
Adjusted to pH 7.2			

Degestion buffer		
Reagent	Final concentration	Volume / amount
HANKS` medium		100 ml
$MgSO_4$ (7*H_2O)	12 mM	296 mg

Neuronal growth medium		
Reagent	Final concentration	Volume
Lonza PNBM		250 ml
NSF-1		4 ml
L-Glutamine		2 ml
GA-1000 Gentamicine sulfate		200 µl

Coomassie solutions		
Coomassie staining solution		
Reagent	Final concentration	Volume / Amount
Methanol	50 %	500 ml
Acetic acid	10 %	100 ml
Coomassie briliant Blue R-250	0.01 % (w/v)	100 mg
H_2O		Ad 1000 ml
Coomassie destaining solution		
Methanol	5 %	50 ml
Acetic acid	12.5 %	125 ml
H_2O		Ad 1000 ml

Tail lysis buffer			
Reagent	Stock concentration	Final concentration	Volume
Tris pH 8.5	2 M	10 mM	2.5 ml
EDTA	0.5 M	5 mM	0.5 ml
SDS	10 %	0.2 %	1 ml
NaCl	5 M	200 mM	2 ml
H_2O			Ad 50 ml

Permeabilization buffer			
Regent	Stock concentration	Final concentration	Volume /Amount
PBS	10 x	1 x	10 ml
FCS		5 %	5 ml
Saponin		0.5 % (w/v)	0.5 g
H_2O			Ad 100 ml

2.1.2 Antibodies

Primary and secondary antibodies used in this thesis are listed in table 2.2 and table 2.3, respectively. Antibodies were diluted in 1x PBS (WB) or Permeabilization buffer (ICC). Working dilutions were stored at 4 °C and stock solutions according to manufacturer's information.

Table 2.2. Primary antibodies used in Western Blot assays and immunocytochemistry experiments in this thesis.

Antigen	species	Dilution (WB)	Dilution (ICC)	Productcode	Company
Beta actin	mouse	1:100000		A5441	Sigma
DsRed	rabbit		1:500	632496	Clontech
GFP	chicken	1:10000	1:10000	Ab13970	Abcam
GM130	mouse		1:2000	610823	Becton, Dickinson and Company
HA	mouse	1:1000	1:1000	MMS-101R	Covance
MAP2	chicken		1:20000	Ab5392	Abcam
Myc	mouse	1:1000	1:1000	MMS-150P	Covance
Neurofilament	mouse		1:2000	NE1022/NE1023	Millipore
Ribosomal Protein S6 (Phospho)	rabbit	1:1000		#4858	Cell Signaling
Ribosomal Protein S6	mouse	1:1000		#2317	Cell Signaling
Tau	rabbit		1:20000	A0024	DacoCytomation
TGN46	rabbit		1:400	ab16059	Abcam

Table 2.3. Secondary antibodies used in Western Blot assays and immunocytochemistry experiments in this thesis.

Antibody	Species	Dilution (WB)	Dilution (ICC)	Productcode	Company
α-chicken-Alexa488	Goat		1:400	A-11039	Life Technologies
α-chicken-Alexa633	goat		1:400	A-21103	Life Technologies
α-chicken-HRP	goat	1:7500		G135A	Progmega
α-mouse-Alexa488	goat		1:400	A-11001	Life Technologies
α-mouse-Alexa633	goat		1:400		Thermo-scientific
α-mouse-HRP	horse	1:7500		PI-2000	Vector Laboratories
α-rabbit-Alexa488	goat		1:400	A-11008	Life Technologies
α-rabbit-Alexa555	goat		1:400	A21428	Life Technologies
α-rabbit-HRP	goat	1:7500		PI-1000	Vector Laboratories

Antibodies were purchased from the following companies: **Abcam** (Abcam plc, 330 Cambridge Science Park, Cambridge, CB4 0FL, UK); **Becton, Dickinson and Company** (Becton, Dickinson and Company, 1 Becton Drive, Franklin Lakes, NJ 07417-1815, USA); **Cell Signalling Technology** (Cell Signaling Technology, Inc., 3 Trask Lane, Danvers, MA 01923, USA); **Clontech** (Clontech Laboratories, Inc., 1290 Terra Bella Ave., Mountain View, CA 94043 USA); **Covance** (Distributed via HiSS Diagnostics GmbH, Güterhallenstraße 3, 79106 Freiburg i.Br., Germany); **DacoCytomation** (DakoCytomation Denmark A/S, ProdGBtionsvej 42,Glostrup, Denmark) ; **Life Technologies** (Life Technologies Corporation, 5823 Newton Drive, Carlsbad, CA 92008, USA); **Millipore** (Distributed via Merck Chemicals, Am Kronberger Hang 5, 65824 Schwalbach, Germany); **NEB** (New england Biolabs, Brüningstr. 50 Geb. G 810, 65926 Frankfurt am Main, Germany); **Promega** (Promega Corporation, 2800 Woods Hollow Road, Fitchburg, WI 53711, USA); **Thermo Scientific** (Thermo Fisher Scientific Inc. 81 Wyman Street Waltham, MA 02454, USA), **Vector Laboratories** (Vector Laboratories, Inc., 30 Ingold Road, Burlingame, CA 94010, USA)

2.1.3 Technical equipment

Equipment for DNA analysis

DNA Amplification: TGradient, TProfessional Standard/Trio (Biometra)

DNA concentration measurements: NanoDrop2000 spectrophotometer (Thermo Scientific)

Agarose gel electrophoresis: PerfectBlue chambers (Peqlab)

Southern Blot analysis: Victor3 Multilabel counter (PerkinElmer), FLA-3000 (Fujifi lm)

Preparation of embryonic / brain sections: Hyrax C60 Cryostat (Carl Zeiss AG)

Equipment for protein analysis

Protein concentration analysis (BCA assay): SLT Rainbow Scanner (SLT Labinstruments)

Cell lysate preparation: Sonifier 250 (Branson)

SDS-PAGE: Minigel-Twin chambers (Biometra)

Western Blot: iBlot Gel Transfer Device (Life Technologies)

Chemiluminescent detection/ image aquisition: ImageQuant LAS4000mini detector (GE Healthcare)

Microscopes

Confocal laser scanning microscope:

Inverted Olympus Fluoview 1000 (AR Laser (458nm, 476nm, 488nm, 514nm); GreNE Laser (543nm); HeNe Laser (633nm) Three PMTs (epifluorescence, reflection) and one PMT for transmission mode Scanformat up to 2048 x 2048 pixel, 12 bit, scanfield rotatable –5 up to +95 °.

Epifluorescence microscope:

Upright Zeiss Axio Imager.M2 with HXP 120C mercury short-arc lamp.

Spinning disc microscope:

Visitron Systems Spinning Live Cell Confocal, lasers (solid state): 488, 561, 647 or 405. The spinning disc microscope was combined with two charge-coupled device EM-CCD cameras (Hamamatsu Pho tonics) and equipped with an optical image splitter for simultaneous dual image acquisition.

Software

Proprietary software from Olympus, Carl Zeiss AG and Visitron Systems was used to acquire images. ImageJ and Fiji were used for image processing and kymograph plotting. MetaMorph 7.7.5 was used for vesicle tracking. SigmaPlot 12.5 (Systat Software Inc.) was used for statistical analysis. Adobe Illustrator was used to assemble figures and Microsoft Word and Adobe InDesign to write this thesis. Graphs were plotted with Microsoft Excel and processed with Adobe Illustrator. For planning and evaluation of molecular cloning SeqMan, EditSeq and SeqBuilder packeges of DNASTAR Lasergene were used. ClustalW2 was used for sequence alignment. TierBase was used for mouse colony management. Ethovision XT 6.1 (Noldus Technology) and TSE Multi Conditioning System V9.03 were used for automated analysis of animal behavior.

2.2 Molecular biology

2.2.1 Polymerase chain reaction (PCR)

Amplification of DNA by PCR was necessary for different purposes. A basic PCR protocol was used for genotyping, plasmid insert amplification and selection of positive clones by colony PCR. For each reaction shown in table 2.4 the standard PCR reaction mix was set up.

Table 2.4. Composition of a standard PCR mix.

Reagent	Stock concentration	Volume
Forward primer	10 µM	1 µl
Reverse primer	10 µM	1 µl
dNTPs	25 mM	1 µl
10 x reaction buffer (incl. $MgCl_2$)	-	5 µl
Polymerase	-	x µl
Template DNA	-	x µl
H_2O	-	Ad 50 µl

For genotyping and colony PCR purposes 1 U of DreamTaq DNA Polymerase from Thermo Scientific (0.2 µl per PCR reaction) was pipetted to the mix before 1 µl of genomic DNA was added as last component for genotyping PCRs. For colony PCR reactions a single *E. coli* colony was picked with a pipette tip from LB-Agar plates, shortly dipped into 1 ml of the corresponding LB medium and added to the PCR mix. In case of amplification of an insert for plasmid cloning a proofreading polymerase was chosen. 1 U of Pwo DNA Polymerase (1 µl, Rapidozym) was used for amplification of plasmid DNA. For amplification of a coding sequence out of a cDNA library 1 U of High-Fidelity PCR Enzyme Mix (1 µl, Thermo Scientific) the Polymerase of choice. A basic PCR protocol (table 2.5) was modified according to the specific requirements of the experiment.

Table 2.5. Protocol of a standardized PCR.

Step	Time (min:sec)	Temperature	Repeats
Initial denaturation	03:00	95 °C	1
Denaturation	00:30	95 °C	Repeated for 20 to 40 times
Primer annealing	00:30	50 – 70 °C	
Amplification	00:15 – 07:00	72 °C	
Terminal amplification	07:00	72 °C	1
Resting temperature	00:00	4 °C	-

For each primer the melting temperature was calculated according to the following formula.

69,3+((41*# of GC bp)/(# of total bp)-650/(# of total bp))

The primer annealing temperature for each PCR was set to be 2 °C below the lowest melting temperature of the used primers. The length of the amplicon necessitated the time of the amplification step. All used polymerases are capable to amplify with a speed of at least 1000 bp/min. Therefore the amplification time was set up after this value.

2.2.2 Restriction enzyme digestion of plasmid DNA

Plasmid DNA or PCR products were incubated with different restriction endonuclease enzymes according to the specifications of the manufacturer (NEB and Fermentas). If possible 1 Unit of enzyme added per µg of plasmid DNA and the reaction was performed in the recommended buffer. In most cases of double digestions fast digest enzymes and the fast digest buffer (Fermentas) were used for high efficiency.

2.2.3 Separation and purification of DNA fragments

For genotyping and plasmid modification DNA fragments were separated according to its size by agarose gel electrophoresis in horizontal electrophoresis tanks. Agarose was added to 1 x TAE buffer to a final concentration between 0.5 to 2 %. The mix was boiled up in a microwave oven and GelRed (Biotium), 0.5 µl per 100 ml gel, was added to the gel before it was set. Bromphenol blue was used as loading dye in case the PCR or restriction buffer did not already contain a dye (“ready to load”). For electrophoresis the gel was submerged in 1 x TAE buffer and run with 10 V/cm until the desired separation was achieved. GeneRuler 1kb plus DNA ladder (Fermentas) helped to assess the size of the DNA fragments.

To extract separated DNA fragments the NucleoSpin Gel and PCR Cleanup kit (Macherey-Nagel) was used. The DNA was detected with UV-light and the required DNA fragment was excised with a scalpel. DNA Fragments were melted in loading buffer (ratio 1:2) at 50 °C with gentle shaking for 5 to 10 min and loaded to NucleoSpin ion exchange columns. DNA was purified by following the manufacturer’s manual.

2.2.4 Ligation of DNA fragments

For ligation of restriction fragments 20 ng of vector DNA and insert DNA in 5 times excess was incubated together with 1 U T4-DNA-ligase in 1 x ligation buffer over night at 4 °C. In case the vector DNA was digested with one restriction enzyme, the 5'-phosphate groups were removed to prevent relegation. After digestion of the DNA the removal was achieved by incubation with 1 U FastAP Thermosensitive Alkaline Phosphatase (Fermentas) before purification and subsequent ligation.

2.2.5 Gateway cloning

Most expression constructs were generated by Gateway recombination (Life Technologies). Desired coding sequences were amplified by PCR. A Kozak consensus sequence (CACC) in front of the sequence was added by an appropriate primer. The purified DNA fragment was combined with a pENTR_D_TOPO donor vector in a 5 min TOPO reaction (table 2.6). 1 µl of a TOPO reaction was employed for the transformation of competent E.coli Top10. The integration and correct sequence of the coding sequence into the pENTR vector was verified by DNA sequencing after preparation of the plasmid by a midi preparation.

To generate an expression construct of choice a LR reaction was carried out. The pENTR carrying the coding sequence of interest was mixed with a pDEST construct and for recombination LR-ClonaseII was added (table 2.6). After incubation for at least 1 h at room temperature the Enzyme was inactivated by adding 1 µl of ProteinaseK and incubation for 10 min at 37 °C. 2 µl of the LR reaction mix was used for subsequent transformation of competent E.coli Top10.

Table 2.6. Gateway recombination reactions

Gateway TOPO reaction		
Component	Volume	Amount DNA
PCR product	1 µl	10 ng
pENTR_d_TOPO	1 µl	10 ng
TOPO-salt solution	1 µl	
H_2O	Ad 6 µl	
LR Reaction		
pENTR containing sequence of interest	X µl	100 - 200 ng
pDEST vector	1 µl	150 ng
LR-ClonaseII	1 µl	
TE buffer pH 8.0	Ad 10 µl	

2.2.6 Site directed mutagenesis

For the mutation of recombinant proteins a site-directed, Ligase-independent mutagenesis (SLIM) protocol was adapted from Chiu and colleagues (Chiu et al., 2004). Both, the basic PCR mix and protocol were modified. Single nucleotide mutations were introduced by nucleotide exchanges in specifically designed oligonucleotide primers which were sufficient to amplify the entire template plasmid. The principle of SLIM is visualized in figure 2.1.

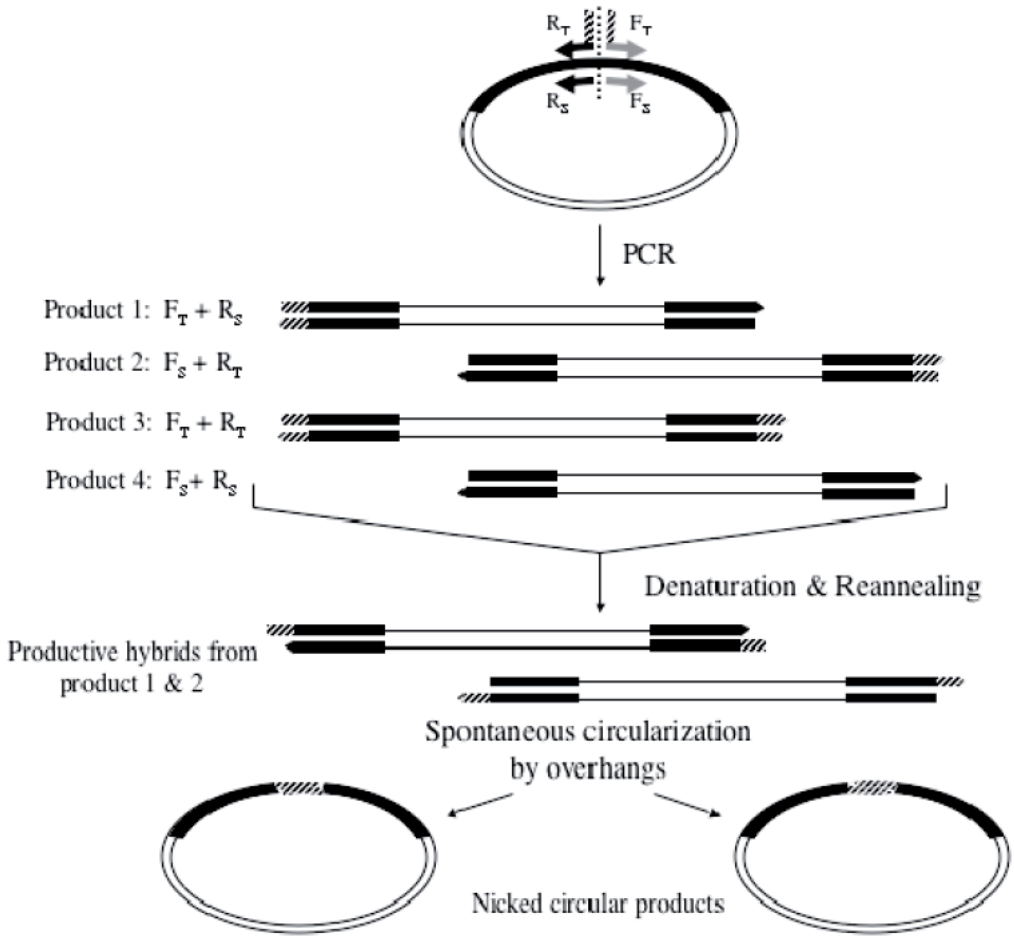

Figure 2.1. Principle of Site directed mutagenesis (modified from Chiu et al., 2004).

Instead of one forward and reverse primer four primers, F^T, F^S, R^T and R^S, were added to the PCR mix. The mutation is introduced through the F^T and R^T primers. F^S and R^S primers were designed as the complement of F^T and R^T but lacked the sequence were the mutation was introduced leading to formation of DNA hybrids with overhangs after a PCR. The design of the primers is shown in figure 2.2 and the modified PCR mix in table 2.7. Table 2.8 shows the protocol for the SLIM PCR amplification.

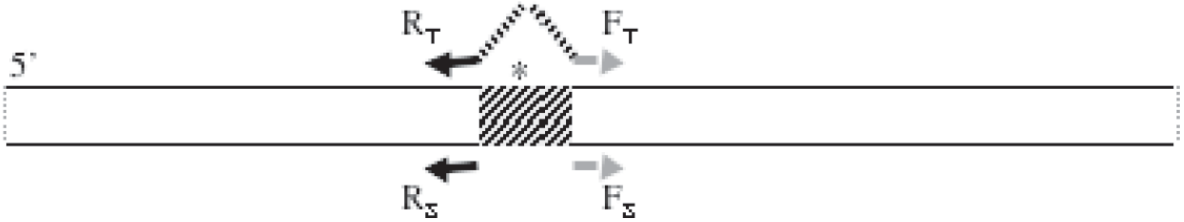

Figure 2.2. Design of the four primers needed for successful SLIM (modified from Chiu et al., 2004).

Table 2.7. PCR mix setup for SLIM.

Reagent	final concentration	Volume
Primer F_T	10 pM	1 µl
Primer F_S	10 pM	1 µl
Primer R_T	10 pM	1 µl
Primer R_S	10 pM	1 µl
dNTPs	200 µM	1 µl
10 x reaction buffer (incl. $MgCl_2$)	-	5 µl
Pwo DNA Polymerase	1U	x µl
Plasmid DNA	100 pg	1 µl
DMSO	2 %	1 µl
H_2O	-	Ad 50 µl

Table 2.8. PCR protocol used for SLIM.

Step	Time (min:sec)	Temperature	Repeats
Initial denaturation	02:00	95 °C	1
Denaturation	00:15	95 °C	Repeated for 25 cylces
Primer annealing	00:20	61 °C	
Amplification	03:30	72 °C	
Terminal amplification	07:00	72 °C	1
Resting temperature	00:00	4 °C	-

For heteroduplex formation the PCR reaction was diluted in 5 µl NEBuffer 4 supplied with 5 U of DpnI (from New England Biolabs). After incubation at 37 °C for one hour the digestion was stopped by heat inactivation at 80 °C for 20 min. For the final hybridization two cycles of 65 °C for 5 min and 30 °C for 15 min were performed and 20 µl were used for transformation of E.coli Top10 bacteria.

2.2.7 Transformation of chemically competent E.coli strains with plasmid DNA

Bacteria were stored in aliquots at -80 °C and were thawed on ice for 15 min before transformation. The E.coli strain for transformation was chosen depending on the needs for further experiments (table 2.9). The appropriate amount of ligation mix or pure plasmid DNA was added to 50 µl of bacteria and mixed by snipping. After incubation for 15 °C on ice the mix was heat shocked for 45 sec at 42 °C and returned to ice for additional 60 sec. For recovery 250µl SOC Medium was added to the bacteria followed by shaking with 250 rpm at 37 °C. Selection of clones was achieved by plating bacteria on LB-agar plates containing antibiotics suitable to the gene mediated resistance.

Table 2.9. Different *E. coli* straines used for transformation with plasmid DNA in this thesis.

E. coli strain	Goal
XL1-Blue	Amplification of plasmid DNA
TOP10	Amplification of plasmid DNA acquired by Gateway recombination reactions
ccdB Survival™ 2 T1R	Amplification of pDEST-vectors of the Gateway cloning system
BL21 (DE3) pLYS	Expression of recombinant fusion proteins

2.2.8 Preparation of plasmid DNA

The method of preparation was chosen after the further experimental use of the plasmid DNA. E.g. to analyze modified plasmids a “mini preparation” by alkaline lysis (Birnboim and Doly, 1979) using a NucleoSpin Plasmid kit (Macherey Nagel) was sufficient. 2 ml of LB medium were inoculated with one colony from a LB-agar plate. After incubation at 37 °C and 250 rpm shaking over night 1 ml of the culture was centrifuged for 30 sec at 13000 rpm. The supernatant was discarded and 250 µl of buffer S1 was added. By vortexing the bacteria were resuspended, 250 µl of buffer S2 were added for lysis and the mixture was neutralized by adding 300 µl ice-cold buffer S3 and inverting for 5 times. The DNA was extracted from the lysate using ion exchange columns following the manufacturer’s specifications.

To isolate larger quantities of plasmid DNA for transfecting a variety of cell types a “midi preparation” was the method of choice. Different kits from Macherey Nagel were used. Depending on the necessary level of purity for future experiments an Endotoxin-free preparation kit (NucleoBond Xtra Midi EF) or the NucleoBond Xtra Midi kit was utilized. In either case a 100 ml overnight culture in DYT medium was prepared. Extraction of highly purified plasmid DNA was carried out after the protocol provided by Macherey Nagel.

The yield of plasmid preparations were determined by a NanoDrop 2000 spectrophotometer (Peqlab). To estimate the purity the OD260 / OD280 ratio was determined.

2.2.9 DNA sequencing

To verify the modification of plasmid DNA all plasmids were analyzed by sequencing by the chain-terminating didesoxy method (Sanger et al., 1977). Sequencing was carried out by Eurofins MWG Operon in Martinsried or the service group Bioanalytics under the direction of PD Dr. S. Hoffmeister-Ullerich at the ZMNH. The software DNASTAR Lasergene SeqBuilder was used for evaluation.

2.2.10Southern Blot

20 µl genomic DNA was restricted with the indicated enzyme (2 µl) over night. On the next day a 1 % agarose gel was cast and the genomic DNA was separated by gel electrophoresis. Afterwards the DNA was detected by UV-light and recorded with a ruler for documentation. The gel was submerged in 0.25 M HCl until the color of the Bromphenol blue marker shifted to yellow. The gel was transferred to 0.4 M NaOH for 15 min. For the Southern Blot a Hybond XL membrane was used. The membrane was washed with H_2O and equilibrated in 0.4 M NaOH. A Plexiglas disc was placed on a basin and the Southern Blot was assembled on it. At the bottom, two pieces of Whatman paper (WP) were used to form a liquid bridge. Two additional pieces of WP of the size of the agarose gel were placed on the bridge. The gel was placed on top and entangled with Parafilm. The membrane formed the next layer covered by two additional pieces of WP. 10-15 cm of tissue paper was placed on top of the blot. A weight was used to ballast. The Southern Blot ran over night. On the next day the membrane was washed with 2 x SSC. After drying it, it was backed for two hours at 80 °C and was set aside.

Plasmids were linearized and purified to subsequently label antisense DNA with [alpha-35S] radioactively by *in vitro* transcription following the instructions of the Megaprime DNA Labeling System kit (GE Healthcare). Per DNA probe 50 µCiα[35S]-UTP were used and the final hybridization solution was set to a value between 500 cpm/µl to 800 cpm/µl.

For the hybridization with the probe the membrane was rinsed with 2 x SSC and put into a hybridization-tube. In a pre-hybridization step 10 ml of Speed Hyb II supplemented with 500 µl salmon sperm were added to membrane and the membrane was incubated for two hours at 65 °C under constant rotation. The probe (500 cpm/µl) was added to 500 µl salmon sperm. After boiling at 95 °C for five minutes the mix was added to 10 ml Speed Hyb II the hybridization mix was used to replace the pre-hybridization solution. Hybridization was performed over night at 65 °C. On the next day the mix was discarded and the membrane was washed three times for 10 min with 2 x SSC + 0.1 % SDS. The membrane was wrapped in clear film and exposed to a PhosphorImager screen for one day.

2.3 Biochemistry

2.3.1 Preparation of cell lysates

After cultivation and transfection/infection in culture dishes lysis of cells (primary neurons / HeLa cells) followed on ice: Cells were washed with ice cold 1x PBS. An appropriate amount of cell lysis buffer was added to the cells which were subsequently scraped off the dishes using a cell scraper. After optional sonication (duty cycle = 20 %, output control = 0.2) cells were rotated for 20 min at 4 °C to complete cell lysis. Cell debris was removed by centrifugation for 5 min at 4 °C with 10000 g.

2.3.2 Recombinant protein expression in *E. coli*

Recominant proteins were expressed in the E.coli strain BL21. 50 µl of competent BL21 cells were transfected with an appropriate expression vector as described above. On the next day a 14 ml preculture (LB-Medium supplemented with antibiotics) was inoculated with one colony of BL21 cells and incubated over night at 37 °C and 250 rpm. 5 ml of the preculture were transferred to 1 l of LB medium on the following morning. The culture was incubated at 37 °C and 250 rpm shaking and the optic density (OD) at 600 nm was checked hourly. At an OD of approximately 0.6 the expression of the recombinant protein was induced by adding 1ml 1M Isopropyl-β-D-thiogalactopyranosid (IPTG) to the culture. After 4 h of incubation the bacteria was harvested by centrifugation at 4 °C and 5000 g for 10 min. The supernatant was discarded and the cells were brought back into suspension in 20 ml ice cold PBS. Aliquots were frozen until further purification/use at -80 °C.

2.3.3 GST-Pulldown

Aliquots of BL21 cells resolved in PBS which expressed either GST or GST fused to a protein of interest were thawed on ice for 20 min. For cell lysis a reasonable amount of lysozyme was added and the samples were incubated for 30 min at 4 °C and inverted every 10 min. Triton-X-100 was added to a final concentration of 1 % and the cells were sonicated 3 times for 10 sec each (duty cycle = 30 %, output control = 0.3). In a centrifugation step (10 min at 14000 g for 10 min) cell debris was sedimented and the supernatant was transferred into a clean microcentrifuge cup. Per GST-Pulldown reaction 2 x 50 µl Pierce Gluthatione Magnetic Beads (GSH beads, Thermo Scientific) were washed in ice cold PBS 3 times and added to the BL21 cell lysate. To allow binding of the GST/GST fusion protein to the GSH beads the mix was incubated for 30 min at 4 °C under constant inversion by rotation. After this coupling step the beads were washed 3 times with lysis buffer and put aside on ice until further use. HEK cells expressing a potential interaction partner of the GST fusion protein were lysed. 1 to 5 % of the lysate was mixed with 5 x protein

sample buffer and is referred was input later on. The rest of the lysate was split equally to microcentrifuge cups containing either the earlier prepared GST or GST-fusion protein beads. The GST-Pulldown was carried out for 10 - 30 min at room temperature or for 2 h or over night at 4 °C under constant rotation. After the incubation the beads were washed three times with lysis buffer for 5 min each. The beads were resuspended in 30 µl 2 x protein sample buffer and all samples were boiled for 5 min at 95 °C. The samples were frozen at -20 °C until further use or directly loaded to an SDS-PAGE gel.

2.3.4 (Co-)-Immunoprecipitation

For Immunoprecipitation of GFP-fusion proteins magnetic GFP-Trap beads (Chromotek) were used. All steps were performed on ice if not stated differently. A protocol provided by Chromotek was modified. For one immunoprecipitation of a GFP-fusion protein approximately 4 x 107 previously (co-)transfected HeLa cells were harvested and suspended in 200 µl cell lysis buffer. For an efficient cell lysis the cells were sonicated for 5 sec (duty cycle = 20 %, output control = 0.2) and incubated at 4 °C for 20 min under constant inversion. Cell debris was removed by centrifugation for 10 min at 4 °C and 20000 g. During this time the GFP-Trap beads and control beads, blocked magnetic particles (bmp), were prepared. For each immunoprecipitation 20 µl beads were equilibrated in dilution buffer by washing for 3 times. The cell lysates were transferred into clean microcentrifuge cups and 1 to 5 % of the lysate was mixed with 5 x protein sample buffer for use as input. The rest of the lysate was filled up to 800 µl with dilution buffer. For the immunoprecipitation one half of the diluted lysate was incubated with the GFP-trap beads for 10 min – 2 h min at room temperature under rotation, the other half was mixed with the bmp. The beads were magnetically separated and the supernatant was discarded. To eliminate residues from the cell lysate the beads were washed three times with dilution buffer. For elution of (co-)precipitated proteins the beads were resuspended in 20 µl 2 x protein sample buffer and boiled at 95 °C for 5 min. SDS-PAGE was subsequently preformed with all samples.

2.3.5 Protein concentration analysis

To normalize samples to total protein levels the BCA method (BCA Protein Assay kit from Thermo Scientific) was used. A standard curve was determined by using a BSA solution with a known concentration. The appropriate amount of BSA and 1 – 2 µl from each cell lysate was filled up to 25 µl with distilled water. Ice cold BCA Protein Assay Reagent A was mixed with BCA Protein Assay Reagent B (ratio 49:1) and 200 µl of this solution was added on ice to each protein sample. The reactions run for 30 min at 37 °C. Afterwards the samples were allowed to cool down to room temperature for 5 min before the OD was measured at 562 nm with a SLT Rainbow Scanner (SLT Labinstruments). The concentration for each protein

sample was determined with help of the calculated standard curve and adjusted to 1 µg/µl with 5 x protein sample buffer and lysis buffer. Samples were stored at -20 °C until further use.

2.3.6 SDS-PAGE

To separate proteins according to their molecular weight sodium dodecyl sulfate – poly acrylamide gel electrophoresis (SDS-PAGE) was carried out. Dependent on the proteins gels were cast with 8 – 12 % acrylamid. Gels were polymerized between two glass plates. First a separating gel was cast. To create a clean edge the poly acrylamide solution was overlaid with isopropanol during the polymerization process. After washing off the isopropanol with water the stacking gel was cast on top of the separating gel and a comb was inserted to provide sample wells. For electrophoresis a voltage of 80 V during focalizing of the protein samples in the stacking gel and 150 V in the separating gel, respectively, was applied. After separation the gel was Coomassie stained or the proteins were transferred by Western Blotting. PageRuler prestained protein Ladder (Thermo Scientific) was used to assess the molecular weight of proteins.

2.3.7 Coomassie Staining

After Western Blotting the gel was transferred into a glass cuvette and shaken in a Coomassie staining solution for 1 h. The Coomassie solution was reused several times. For clear protein bands the gel needed to be washed with a destaining solution multiple times for a several hours or overnight. The destaining solution was filtered through active charcoal and also reused. Gels were either scanned or dried after the destaining procedure.

2.3.8 Western Blot

Transfer of proteins onto a PVDF membrane after successful separation by SDS-PAGE was carried out using an iBlot Gel Transfer Device (Life Technologies). The instructions provided by the manufacturer were followed. The poly acrylamide-gel was placed on the PVDF membrane contained in the bottom stack pack and was overlaid with a water soaked Whatman filter paper. On top the top stack was placed. Air bubbles were avoided during assembly. A Sponge was placed on the intended site and the machine was closed and a appropriate program was started. After protein transfer the membrane was cut with a scalpel and blocked by shaking in 5 % non-fat milk powder solved in PBS-T for 45 min. The membrane was washed with PBS-T two times and incubated with a specific primary antibody overnight at 4 °C and shaking. On the next day the primary antibody was replaced by PBS-T and stored with 1 mM sodium azide at 4 °C until reuse. The membrane was washed for 3 times 10 min in PBS-T followed by incubation with a peroxidase conjugated secondary antibody for 2 h at room temperature. To visualize specific protein bands the

membrane was pivoted for 1 min in freshly prepared Super Signal ECL substrate solution (Pico or Femto, Thermo Scientific). For image acquisition the LAS4000MIini system from GE Healthcare was used. Protein amounts were quantified by using Fiji for digital western blot image analysis.

For some experiments the antibodies were stripped of from western blot membranes to allow for detection with another specific primary antibody. The membrane was washed with PBS-T after detection, incubated with methanol for 5 sec and subsequently dried. Until further use the membrane was stored at -20 °C. For reconstitution the membrane was dipped into methanol for 5 sec and washed in PBS-T. After incubation in stripping buffer at 50 °C under rotation in a hybridization oven the membrane was washed again in PBS-T. The next step was the repeated blocking of the membrane before the second antibody binding was performed.

2.4 Cell culture

2.4.1 Cultivation of immortal, eukaryotic cell lines

Handling of cell lines was always performed under a laminar flow hood (clean bench) according to good laboratory practice guidelines. For cultivation cells were incubated in a gas incubator with 5 % CO2 and 95 % humidity at 37 °C. A list of all cell lines used for this thesis can be found in table 2.10.

HEK and HeLa cells were maintained in 10 cm cell dishes in Dulbecco's modified eagle medium (DMEM) with 10 % added fetal calf serum (FCS). Cells were split upon ~90 % confluency. After washing with PBS, one ml trypsin solution (10 mg / ml trypsin in Ca^{2+} / Mg^{2+} free PBS) was added to the cells until they contracted and detached from the culture dish. The cells were collected in 10 ml DMEM + FCS in a 15 ml falcon tube and sedimentation at 1200 g for 2 min was performed. Supernatant medium was discarded and the cell pellet was resuspended in 10 ml DMEM. 500 µl of the cell suspension was added to 9.5 ml of DMEM + FCS in a culture dish for further cultivation.

For long-term storage cells were frozen. Cells from a ~90 % confluent 10 cm culture dish were re-suspended in 2 ml DMEM + FCS and mixed with 2 ml freshly prepared 2 x cryoprotectant medium (20 % dimethyl sulfoxide, 40% FCS, 40 DMEM). The cell suspension was slowly frozen in cryo vials in a Styrofoam box at -80 °C. On the following day the vials were transferred into a liquid nitrogen tank.

Cells were thawed by adding DMEM + FCS (pre-warmed at 37 °C). After thawing cells were sedimented at 500 g for 5 min. After discarding the supernatant medium the cell pellet was resuspended in 10 ml DMEM + FCS. Cells were cultivated in a 10 cm dish in a cell culture incubator.

Table 2.10. List of cell lines used for experiments of this thesis.

Cell line	Origin
HEK 293 (Human embryonic kidney)	Established by Graham and colleagues from a human primary embryonic kidney which was transformed by adenovirus type 5 (AD5) (Graham et al., 1977)
HEK 293T (Human embryonic kidney)	Derived from the HEK 293 cell line. Highly transfectable. cells contain a temperature sensitive mutant of SV-40 large T-antigen. According to the German Central Commission for Biological Safety (ZKBS) the cell line is classified as risk group 1 (Pear et al., 1993)
HeLa	This cell line is the first aneuploid, continously cultured human cell line. It was established from an adenocarcinoma of a 31 year old woman (Henrietta Lachs) in 1951. Originally the carcinoma was classified as epitheloid cervix carcinoma (Gey et al., 1952).
SH SY5Y	Clonal subline of the neuroepithelioma cell line SK-N-SH which was established in 1970. Origin is a bone marrow biopsy of a 4 year old girl with metastatic neuroblastoma (Biedler et al., 1973).

2.4.2 Embryonic stem cells

Embryonic stem cells were ordered from European Conditional Mouse Mutagenesis (EUCOMM) program. Upon delivery on dry ice they were immediately stored in liquid nitrogen. All further handling and injections were performed by PD I Hermans-Borgmeyer and Sarah Homann.

2.4.3 Preparation of dissociated hippocampal neuron cultures

For generation of primary cell cultures wild type C57Bl/6J or Arl5b knockout mice were sacrificed. For the preparation brains of either 16 – 17 days old embryos (E16/17) or pups at P1 were dissociated. Pregnant mice were sacrificed by cervical dislocation. Embryos, collected out of the uterus of the mother, and pups were sacrificed by decapitation. All buffers used during dissociation were cooled to 4 °C if not stated otherwise. Brains were removed using microscissors and forceps and stored in HANKS buffer supplemented with 20 % FCS for immediate dissociation of pooled wild type cultures or single knockout preparation Alternatively the brains were stored in Hibernate-E medium (Life Technologies) for pooling of hippocampi of the same genotype in knockout preparations. In this case a small sample of the cortex of each mouse was lyses with QuickExtract™ DNA Extraction Solution (Epicentre) for rapid genotyping. The hippocampi were isolated in the medium under 4 – 10 x magnification. The hippocampi were pooled in

10 ml of HANKS with 20 % FCS. After sedimentation the upper buffer was collected and the hippocampi were washed twice with 10 ml HANKS buffer. The tissue was incubated for 30 min in 2 ml Digestion buffer containing ~2.5 mg Papain and 40 µl (3000 U) DNAase at 37 °C. Following two additional washing steps with 10 ml HANKS buffer the cells were dissociated. For this purpose the buffer was replaced by 2 ml of Dissociation buffer supplemented with 40 µl of DNAse and were triturated gently for 15 times with a Pasteur pipette and additionally with a second Pasteur pipette with its opening narrowed to a ¼ diameter by fire polishing. The reaction was stopped by adding 10 ml Hanks + 20 % FCS and dissociated cells were pelletized by centrifugation for 5 min at room temperature and 1000 g. Supernatant was removed and cells were resuspended in neuronal growth medium. 20 µl of Cells mixed with 20 µl of trypan blue to distinguish dead and live cells during counting using a Neubauer cell counting chamber. Depending on the experimental purpose neurons were seeded on previously prepared and Poly-L-Lysin (Sigma) coated glass coverslips, cell culture dishes with glass bottom or cell culture plastic dishes with a density between 105 to 106 cells / cm2. Glass cover slips needed to be treated before Poly-L-Lysin coating. After incubation of 24 h in 1 M HCl they were washed twice with pure acetone and ethanol each before sterilizing them by baking. For Poly-L-Lysin coating glass cover slips and plastic dishes were incubated with Poly-L-Lysin solved in water (1 mg/ml, Sigma) overnight and subsequently washed three times with sterile H_2O before seeding of neuronal cells.

2.4.4 Infection of primary neurons with lentiviruses

The protocol for the production of lentiviruses was modified from Lois and colleagues (Lois et al., 2002). About 4 million Hek 293-T cells were transferred into a 6 cm cell culture dish and cultivated over night in DMEM + FCS. On the next day cells were washed with DMEM. Until transfection with Lipofectamine2000 (Life Technologies) cells were incubated with 3 ml DMEM. Four plasmids were mixed for transfection in 0.5 ml OptiMEM. 4 µg expression-plasmid DNA was combined with 2.4 µg pLP1, 1.2 µg pLP2 and 0.8 µg pLVSVG (curtesy of P. Osten). 22.5 µl Lipofectamine2000 were mixed with 0.5 ml OptiMEM using a vortex mixer. 5 min later the Plasmid-mix was added drop-wisely to the Lipofectamine2000-mix and the mix was blended gently. After 20 min the transfection-mix was added drop by drop to the prepared Hek 293-T cells. Cells were incubated for 4 to 6 hours in a cell culture incubator. The DMEM was replaced by 4 ml neuronal growth medium and the cells were incubated over night. After 24 hours the supernatant was harvested and filtered through a 0.22 µm PES filter and aliquots of 100 µl were immediately frozen in liquid nitrogen. The lentiviruses were stored at -80 °C until further use. For infection of dissociated hippocampal neurons aliquots were thawed at RT. Dependent on the efficiency of the produced batch of viruses an appropriate amount of the aliquot was added to neuronal cells.

2.4.5 Transfection of primary neurons and secondary cell lines

An appropriate amount of Hek or HeLa cells was seeded into a 6 well plate on the day before transfection. Prior to transfection the cells were washed with DMEM. 4 µg of plasmid DNA was mixed with 250 µl OptiMEM and set aside. In a micro centrifuge cup 10 µl Lipofectamine200 was added to 250 µl OptiMEM. After mixing and incubation for 5 min at RT the DNA-mix was added drop by drop to the Lipofectamine2000-mix. After gentle shaking the mix was incubated for 20 min at RT before it was pipetted drop-wisely to the cells. After 4-6 hours incubation in a cell culture incubator the medium was replaced by DMEM + FCS.

For transfection of primary neurons the required quantity of cover slips were transferred into a 6 cm dish containing 1.5 ml neuronal growth medium immediately before transfection. The described procedure for transfection was performed with a few modifications. 1.5 µg of plasmid DNA was mixed with 1.5 µl Lipofectamine2000 in a total volume of 300 µl OptiMEM. The cells were incubated for 30 to 60 min and afterwards transferred back into their neuronal growth medium. For live cell imaging neuronal cultures the medium was replaced after 30 to 60 minutes with pre-warmed neuronal growth medium.

2.4.6 Generation of stably transfected cell lines

To generate monoclonal stably transfected cell lines HeLa cells were transfected with Lipofectamine2000 as described in 2.4.5. One day after transfection the cells were separated by trypsin and suspended in 65 ml of DMEM + FCS. Per well 200 µl of the cell suspension were seeded into 96 well plates. After 24 hours medium was replaced by selection medium (DMEM + 10 % FCS + 250 µg/ml Zeocin). Single, successfully transfected cell clones were selected by eye and the culture was transferred into a 24 well plate upon confluency. Cells were tested by appropriate method to verify transfection. Cells were cultured in 10 cm culture dishes in selection medium.

2.4.7 Immunocytochemistry

Primary neurons were cultivated on glass cover slips with a diameter of 12 mm. For immunocytochemistry staining the cells transferred to 24 well plates and washed with 1 x PBS for two times. Cells were treated with paraformaldehyde (4 % w/v in PBS) for 15 min. After an additional washing step with PBS cells were premeabilized with saponin by covering the cells with permeabilization buffer for one hour. Primary antibodies were diluted in permeabilization buffer and for each cover slip a drop of 35 µl was pipetted onto parafilm. Coverslips were transferred to the drop on the parafilm (cell side down). With wet tissue paper and a light proof box a humid environment was constructed. To let the antibodies bind antigens the cells were incubated for two hours. Afterwards cells were transferred back into the 24 well plate and

washed with permeabilization buffer for three times for 5 minutes each. The procedure was repeated for incubation with secondary antibodies. Following the two hours incubation cells were washes two times with PBS and an additional washing step with water was performed to remove salt residues. Four parts Immu-Mount were mixed with one part ProlongGold anti fade with DAPI. For each cover slip a drop of this mounting mix was placed on a glass microscope slide. Using a forceps the coverslips were transferred to the mounting mix, avoiding air bubbles and with the cell side facing down.

2.4.8 Detection of myristoylation by radioactively labeled Tritium

For the myristoylation assay 4 million HeLa cells were seeded into a 6 well plate and incubated in a cell culture incubator over night. On the next day cells were starved for 1 h in OptiMEM and were transfected with Lipofectamine2000 (2.4.5). After 6 hours of incubation the medium was replaced with OptiMEM supplemented with: 100 µg / ml BSA, 10 mM NaPyrovate, [^{3}H]-myrisic acid (2 % v/v, 50 µCi/ml). After incubation for 16 h cells were washed two times with and harvested in ice cold 1 x PBS. After cell lysis the exogenous expressed protein was purified by immunoprecipitation. Western blot analysis was used to verify expression and IP. The PVDF membrane was exposed to an x-ray film. After different durations of exposure the film was developed.

2.4.9 Differentiation of SY5Y cells

SY5Y cells were grown in DMEM/F-12 supplemented with 15% FCS, 1 x MEM Non-Essential Amino Acids (Gibco) and 1% Penicillin/Streptomycin. Cells were maintained at 37 °C in a gas incubator with 5 % CO2 and 95 % humidity. For the differentiation experiment cells were seeded with an initial density of 104 cells per cm2 in 24 well plates. The day after plating retinoic acid was added at a final concentration of 10 µM. The cells were cultures for five days. During this time HeLa cells stably transfected with BDNF-GFP grown in DMEM without serum for four days. On the fourth day the conditioned medium was harvested and 20-fold concentrated using AMICON Ultra 15 ml filters (Millipore) with a cut-off at 10 kDa. Control medium was added to non transfected HeLa cells and conditioned and concentrated in parallel. After five days of pre-differentiation of the SY5Y cells by retinoic acid the cells were washed three times with DMEM/F-12. To test the biological activity of BDNF-GFP DMEM/F-12 (without serum) was supplemented with the conditioned or control medium (1 µl per 500 µl DMEM/F-12). The differentiation of SY5Y cells was examined after additional 10 days of cultivation.

2.5 Animals and behavioral experiments

2.5.1 Animal breeding

All animal breeding, handling and experiments were conducted in accordance with institutional guidelines. Organ harvests were performed with the §6 TierSchG permission "ORG 443", Kainic acid injections with "G11/020 Aktivitäsregulierte Gene" and perfusions (supervised or performed by Dr. Guido Hermey) with "A6/499 Perfusion". Animals were sacrificed either by cervical dislocation for biochemical and cell culture experiments or cardiovascular perfusion with paraformaldahyde for histochemical experiments.

For genotyping tail tips of mice were cut and DNA was extracted by incubation with 25 µl of tail lysis buffer containing ProteinaseK over night at 37 °C under moderate shaking at 300 rpm. The ProteinaseK was heat inactivated by boiling at 95 °C for 15 min. 175µl TE-buffer (pH 7.6) was added to the mix of which 1 µl was used for genotyping PCR reactions subsequently. For each strain different primers were used for genotyping (table 2.11).

Table 2.11. List of primers used for genotyping of Arl5b knockout and conditional knockout mice.

Primer	Mouse strain(s)	Sequence
Arl5b_KO_For1	Constitutive Arl5b KO	GGCCTTCACATCACCACTTTCTAC
Arl5b_KO_Rev1	Constitutive Arl5b KO	GGGCAGCAGATGGTTTGCTG
LacZ2	Constitutive Arl5b KO	ATTCAGGCTGCGCAACTGTTGGG
Arl5b-5'Arm	$Arl5b^{KO}$, $Arl5b^{FL}$	ATACATGTTATCATGGAATGTTA
Arl5b-3'Arm	$Arl5b^{KO}$, $Arl5b^{FL}$	AACAGTGCAATCCCTGAAGACT
LAR3	$Arl5b^{KO}$	CAACGGGTTCTTCTGTTAGTCC
EMXCreFor	$Arl5b^{FL}$	AAACGTTGATGCCGGTGAACGTCC
EMXCreRev	$Arl5b^{FL}$	TAACATTCTCCCACCGCTAGTACG
Flip For	$Arl5b^{KO}$, $Arl5b^{FL}$	GTCACTGCAGTTTAAATACAAGACG
Flip Rev	$Arl5b^{KO}$, $Arl5b^{FL}$	GTTGCGCTAAAGAAGTATATGTGC
Rosa26-Seq1	$Arl5b^{FL}$	AAAGTCGCTCTGAGTTGTTAT
Rosa26-Seq2	$Arl5b^{FL}$	GCGAAGAGTTTGTCCTCAACC
Rosa26-Seq3	$Arl5b^{FL}$	GGAGCGGGAGAAATGGATATG

2.5.2 Seizure induction

For seizure induction kainic acid from Ascent was used. Aliquots of Kainic acid solved in PBS at a concentration of 4 mg/ml were stored at -20 °C. Each mouse was injected with 25 mg/kg body weight kainic acid i.p.. Following the injection mice were under permanent surveillance at low light conditions. Behavioral cues (cramping, crouched stance, "piano player") were used to determine the onset of seizures and animals were sacrificed after a certain amount time – indicated for each experiment – passed by.

2.5.3 Preparation of mouse hippocampal lysates

After scarification the mouse brain was dissected and hippocampi were isolated on ice. All following steps were performed on ice or at 4 °C. Both hippocampi of a mouse were pooled in 500µl pre-cooled brain lysis buffer. The tissue was dissociated by processing through cannulas of three different sizes for 10 times each. Afterwards 50µl 10% Triton-X100 was added to the homogenate which was subsequently sonicated for 3 x 10 sec (duty cycle = 20 %, output control = 0.2). Cell lysis was completed by 15 min of incubation under rotation and cell scrape was removed by centrifugation for 5 min at 1000 g. The supernatant was transferred in a new Eppendorf cup and 2 µl was used for protein concentration analysis by a BSA based assay. For further use samples were adjusted to 1µg/µl with brain lysis buffer and 5 x protein sample buffer, boiled for 5 min at 95 °C and stored at -20 °C.

2.5.4 Perfusion of mice

For Perfusion all tubes and the perfusion needle were rinsed with water for several minutes before it was exchanged entirely with 0.01% Heparin/PBS. Ketamine/Xylazine was used for anesthesia at 2.65 µl/kg body weight (100 mg/ml Ketamine, 20 mg/ml Xylazine). 10 to 15 min after i.p. injection of the solution the depth of the anesthesia was tested by toe-reflex testing. In case the mouse still showed a reaction, a second dose, half as much as the original dose, was injected. Additional 10 minutes later the mouse was fixed at the limbs on a Styrofoam board using needles. The fur was cut from the chest and the chest cavity was opened with forceps and scissors followed by fixation of the exposed heart with forceps. The perfusion needle was injected into the left ventricle. To prevent a drop out the needle was fixed on the Styrofoam board. A small cut in the right atrium was made to allow the outflow of liquid. Afterwards the animal was perfused with 10 – 15 ml Heparin solution before the solution was changed to 4 % Paraformaldahyde (pH 7.4, filtered to prevent unsolved PFA from clogging arteries) and perfusion was continued for another 50 ml. Following the perfusion the brain of the mouse was collected and stored in 4 % Paraformaldehyde overnight at 4 °C for additional fixation.

2.5.5 In situ hybridization

Plasmids were linearized and purified with Sure Clean Plus (Bioline) to subsequently label antisense RNA with [alpha-35S] radioactively by *in vitro* transcription following the instructions of the DNA 5’ End-Labeling System kit (Promega). Per RNA probe 80 µCi [35S]-UTP were used and the final hybridization solution was set to a value between 5000 cpm/µl to 8000 cpm/µl.

Mouse brains and embryos were flash frozen in liquid nitrogen and stored until cryosectioning at -80 °C. A cryostat was used to slice the brains in 20 µm thick sections. The sections were mounted on

microscopy slides and dried for 15 min at room temperature followed by fixation with 4 % paraformaldehyde for 15 min and washing in PBS for 3 times 5 min. Subsequently the sections were acetylated by i) equilibrate them in 0.1 M Triethanolamine (pH 8.0) for 3 min and ii) submerging them in fresh 0.1 M Triethanolamine (pH 8.0) immediately after adding 350 µl acetic anhydride. After acetylating for 10 min the sections were dehydrated by immersion in an ethanol-series of 30, 50, 80, 95 and 100 % ethanol and dried at room temperature.

For hybridization the sections were covered in 100 µl hybridization mix supplemented with 5000 cpm/µl of the radioactive probe, covered with a glass coverslip and mounted with DPX. After incubation at room temperature for 30 min the hybridization continued at 55 °C over night.

On the following day the DPX mount was removed and the glass slide was submerged in 4 x SSC for 20 min at room temperature. The coverslip is detached during this step. After two additional 10 min washing steps in 4 x SSC sections were treated for 30 min with RNAse-buffer at 37 °C. Subsequently the sections were washed in 2 x SSC, 1 x SSC and 0.5 x SSC for 15 min each followed by 30 min in 0.1 x SSC at 55 °C and 10 min at room temperature. After dehydrating in 70 and 95 % ethanol for 5 min the slides were air-dried. A Kodak BioMax MR autoradiography film was exposed to the sections for the indicated number of days.

2.5.6 Nissl staining

Coronal cryosections of brains were mounted on Superfrost™ Plus Microscope slides (Thermo Scientific) and put aside for two hours to air-dry. To prepare the staining solution 4.5 g of cresyl-violet was mixed with 45 ml ethanol. After 30 min of incubation 450 ml of water were added and the solution was heated to 50 °C before filtration. The air-dried brain sections were submerged in the cresyl-violet solution for 4 min and washed once with in a ethanol/glacial acetic acid solution (2 ml glacial acetic acid per 98 ml pure ethanol) followed by two additional washes in ethanol. Finally the brain sections were cleared with xylene and mounted with Di-n-butyl phthalate.

2.5.7 Housing conditions for behavioral experiments

All behavioral experiments were performed with adult male Arl5b$^{EMX\text{-}KO/EMX\text{-}KO}$ mice (KO) mice and wild type litter mates. All animals were progeny from heterozygous mating pairs. Weaning was on day 21 after birth. Male and female mice were kept separate from each other. Four weeks prior to experimental work the animals were transferred to an installation for keeping the animals with a switched 12 hour light-dark daily rhythm (light phase from 8 pm to 8 am). Two weeks before the experimental handling started the mice were single caged. All animals had direct accession to food and water. All experiments were performed during the dark cycle. Prior to the experiments the animals were habituated to the experiment-

ers by handling each mouse for approximately 2 minutes two times a day during the two days before the actual experiment was performed.

2.5.8 Open field

The open field test was used for a quantitative analysis of the mobility, anxiety levels and exploratory behavior in a new, unknown environment (Crawley, 1985). The open field arena was a 50 x 50 x 50 cm box constructed from white forex plates. The test was performed at a constant temperature of 21 °C ±1 and defuse light conditions. Each mice was placed carefully in the box and their behavior was documented with a video camera for 10 minutes. For automated analysis of the documented behavior Ethovision XT (Noldus Technology) software was used. Before examination of the next mice the box was cleaned with 70% ethanol

2.5.9 Elevated plus maze

The elevated plus maze was used to assess the spontaneous anxiety of mice. This experiment based on the innate behavior to avoid open and elevated spaces (Crawley, 1985). The elevated plus maze was placed on a 50 cm high stand. It was assembled of four arms (5 x 30 cm) of the same size and a center plate (5 x 5 cm). One pair, opposite to each other, of the arms was surrounded on three sides by 15 cm high arms made of non-transparent walls and were accessible from the center. Both other arms had only an 3 mm high edge. The elevated plus maze was performed in a room with defuse light conditions and constant temperature of 21 °C ±1. Each mice was placed at the center of the maze with the head pointing to an open arm. The animals were let alone for exploration for five min before they were transferred back into their home cage. Their traveled path was traced with a video camera. For automated analysis the Ethovision XT (Noldus Technology) software was used. Before examination of the next mice the elevated plus maze was cleaned with 70% ethanol.

2.5.10Fear conditioning

For fear conditioning the TSE Multi Conditioning System V9.03 was used. On training day the animals were placed in a cage with Opaque walls with a grid floor with ethanol odor. The cage was lightened by white light. The mice were acclimatized to the conditioning chamber for two min. In the following 20 seconds a tone (10 kHz, 75 dB) was presented paired with a foot shock (0.5 mA) for the last 2 seconds. The conditioning was repeated three times with a 60 sec intertrial interval. For a contextual fear testing the mice were transferred to the conditioning chamber for 3 minutes without a tone or shock. For the cued fear testing the chamber was modified. A plastic foil strewn with bedding material covered the grid. The

shape of the cage was altered to a triangular shape by adding an oblique wall. The animals were placed in the box and allowed to explore the new environment for 120 sec. Subsequent the tone (10 kHz, 75 dB) was presented for 120 sec. The testing was performed in dim red light and in the presence of acetic acid smell. Fear response was automatically quantified by the TSE software my measuring the duration of freezing.

2.5.11Morris water maze

For the Morris water maze a circular tank with a diameter of 150 cm was filled with opaque water. The temperature of the room and the water was constantly at 21 °C ±1. A hidden platform made of Plexiglas with a abrasive surface and a diameter of 14 cm was installed 10 to 12 mm below water level in the pool. The swimming path of the mice was recorded by video camera. For automated analysis Ethovision XT (Noldus Software) was used. All mice were between 3 to 4 month old during training. Mice were trained to stay on the platform for 20 sec prior to water maze training (two days, four trials per day). Two training trials were given per day for six days and the latency for each trial was recorded. The mice were allowed to search the platform for 90 sec. If they did not find the platform in this time they were guided to it. On the seventh day a probe trial was performed. The platform was removed from the tank and the mice were allowed to swim for 90 sec. Performance was assessed in three ways: latency until first crossing of the platform area, total crossings of the platform area in 90 sec and time spent in the quadrant the platform was originally located (target quadrant).

2.5.12Novel object recognition

In the novel object recognition task 3 to 4 month old mice were habituated to the open field box on day 1 for 10 minutes. The environmental conditions were described in 2.5.8. On day 2 the mice were allowed to explore the box again. On this day two identical objects were placed in the box (sample phase). After 24h one of the objects (familiar) was replaced with a novel object. The mice were allowed to explore the objects for 10 min (choice phase). The familiar/novel objects were counterbalanced. The behavior of the mice was recorded by a video camera and was analyzed automated by Ethovision XT (Noldus Technology) software. The center and nose-point of the mice were tracked. Exploration was defines as a situation when the nose-point was closer than 2.5 cm to the object. Rearing and climbing of the mice were excluded from the exploration time.

2.5.13Data analysis

Sigma Plot 12.5 was used for all statistical analysis. Prior to further analyses data was tested for normal distribution by a Shapiro-Wilk test. All values are shown as mean ±SEM. In behavioral experiments p values were determined for conditional Arl5b knockout mice against their littermate controls or the indicated hypothesized mean using a (paired) two-tailed Student's t-Test (involving two experimental conditions) or an ANOVA (involving three or more experimental conditions) if not stated otherwise.

3. Results

At the beginning of this thesis, Arl5b function was undescribed. Its activity regulated expression in neurons suggested that it may play a role in synaptic plasticity related events. Moreover, since Arl5b belongs to the family of small GTPases it suggested on the cellular level a regulatory function in signaling or transport processes. Three approaches were pursued to investigate Arl5b function. The first was an examination of Arl5b on a cellular level. The second strategy focused on putative interaction partners. The third aimed at revealing the functional role by generating and analyzing an Arl5b knock out mouse model.

3.1 Cellular functions of Arl5b

3.1.1 Arl5b is expressed during embryonic development in mice

Many activity-regulated genes were linked to the development of the brain, suggesting that similar cellular mechanisms are involved during neuronal development and plasticity (Leslie and Nedivi, 2012). In situ hybridization was used to answer the question if the activity-regulated Arl5b gene is expressed during embryonic development. Sagittal sections of embryonic mice (embryonic day 16 and 18) were hybridized with a radioactively labeled antisense mRNA probe complementary to the open reading frame (ORF) of Arl5b. At both developmental stages Arl5b is expressed in the prenatal brain. In addition high levels of transcripts were detected in the heart, kidney, duodenum, thymus and spinal cord (figure 3.1).

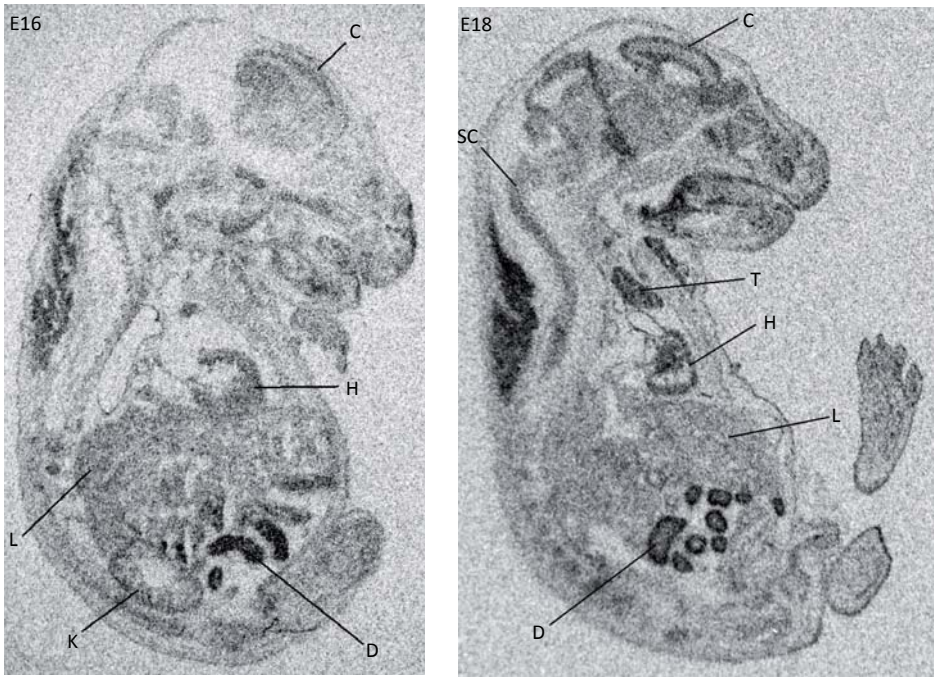

Figure 3.1. The mRNA of Ar-Arl is expressed in various tissues during embryonic development. Autoradiograms of Arl5b mRNA of sagittal sections of an embryo 16 days p.c. (left image). Autoradiograms of Arl5b mRNA of sagittal sections of an embryo 18 days p.c. (right image). C = Cortex; D = Duodenum; H = Heart; K = Kidney; L = Liver; SC = Spinal cord.

3.1.2 Subcellular localization of Arl5b in primary neurons

One way to gain insights into the function of a protein is to determine its subcellular localization as a starting point for further experiments. Based on the expression of Arl5b in the brain during development and its activity regulated expression in the hippocampus (Hermey et al., 2013), first experiments assessed subcellular localization of Arl5b in dissociated primary cultures of hippocampal neurons. This was achieved by C-terminal fusion of Arl5b with fluorescent markers and overexpression of the fusion proteins after transfection. Fluorophores and other tags used to localize the protein were always fused to the C-Terminus of Arl5b, because the N-terminus harbors a consensus site for N-terminal myristoylation which is shared with other Arf-like proteins and is thought to be important for proper function and subcellular localization. N-terminal modifications of Arl5b were investigated in detail (compare 3.1.3).

Expression of Arl5b-tdTomato in developing hippocampal neurons revealed a ubiquitous distribution pattern. In general the subcellular pattern of Arl5b was assessed with various Arl5b fusion proteins and it did not vary based on the tag fused to Arl5b. For example Arl5b-tdTomato, Arl5b-eGFP, Arl5b-mKate2 and Arl5b-HA exhibit very similar subcellular distribution in HeLa cells and neurons. Arl5b was found to be present in the neurons soma, dendrites and axon. In this experiment the axon was visualized by counterstaining with an axonal marker, an antibody against neurofilament, and dendrites with the dendritic marker MAP2 (figure 3.2).

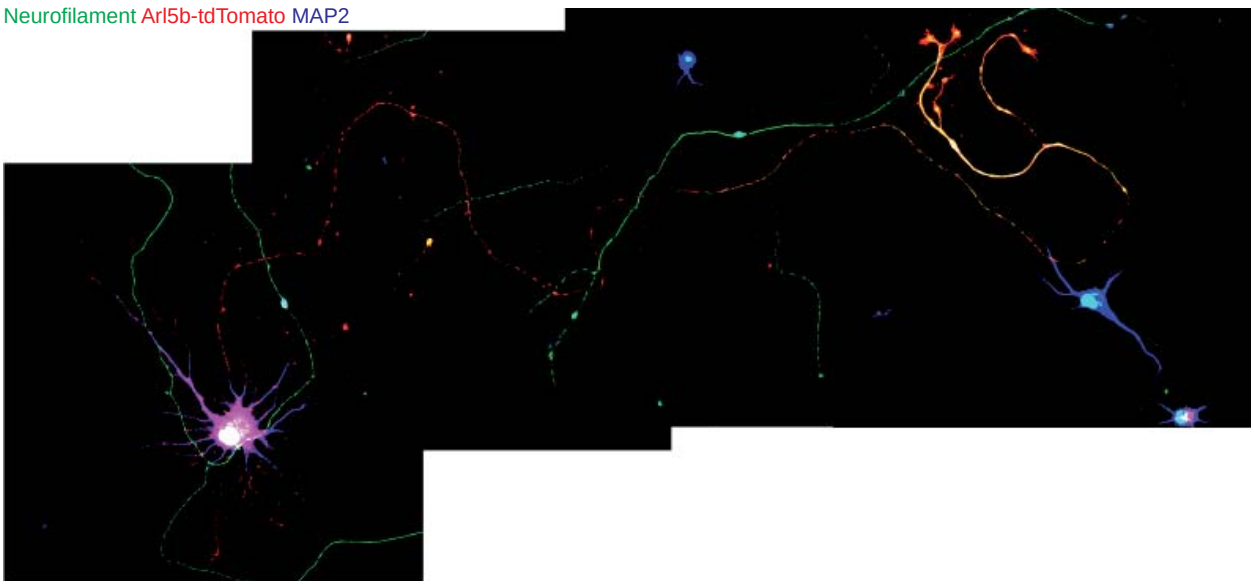

Figure 3.2 Arl5b is localized to the soma, dendrites and axon in principal hippocampal neurons. Cultured hippocampal neurons after 4DIV were transfected with Arl5b-tdTomato. One day later neurons were immunostained for Neurofilament and MAP2, an axonal and a dendritic marker, respectively. Magenta colored regions depict Arl5b located in dendrites and the soma while yellow color indicates Arl5b distribution to the axon of developing dissociated hippocampal neurons. The scale bar indicates 20 µm.

Following this first overview the subcellular localization of Arl5b was examined in more detail. In the soma a strong accumulation near the nucleus was prominent. To further characterize the structure hippocampal neurons overexpressing Arl5b-GFP were immuno-stained for two residential proteins of the Golgi apparatus, the cis-Golgi marker GM130 and the trans-Golgi maker TGN46. Figure 3.3 shows a strong overlap of the accumulated Arl5b-GFP signal and both Golgi marker proteins.

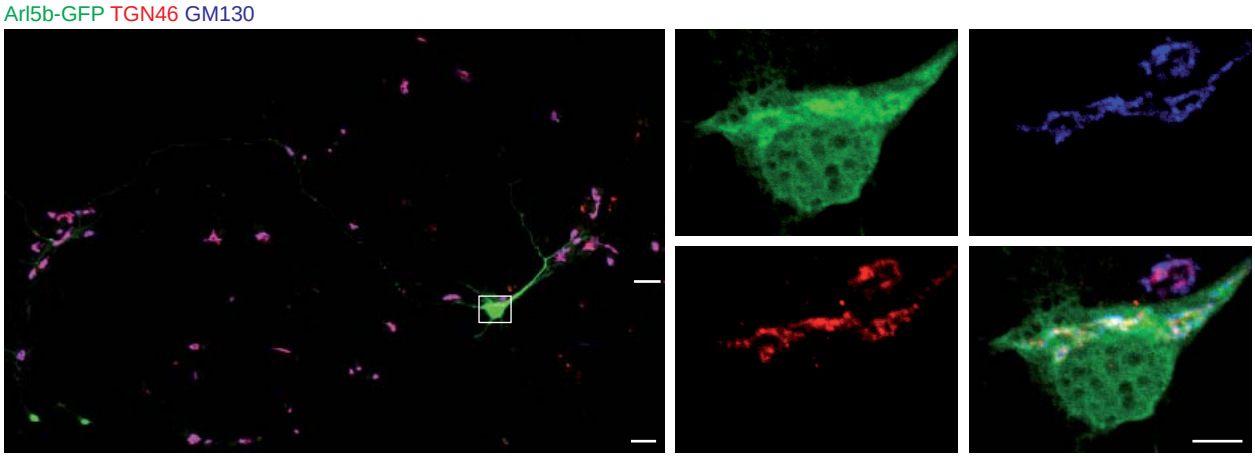

Figure 3.3. Arl5b resides in the Golgi network in the soma of hippocampal neurons. Dissociated neurons were cultivated for four days and transfected with Arl5b-GFP. One day after transfection cultures were counterstained for TNG46, a trans-Golgi network resident protein, and GM130, a protein localized in the cis-Golgi. The white box in the overview (left) indicates the magnified region (right). Arl5b staining is enriched in the cis- and trans-Golgi. White bar in the overview indicates 20 µm and 5 µm in the magnification.

This experiment revealed that Arl5b is localized to the Golgi apparatus. Due to the dense packing of the stacks in the Golgi apparatus it was difficult to assess to which stack of the Golgi the protein is localized. One way to address this problem is to disperse the Golgi apparatus. This was achieved by treatment of the cells with Nocodazole. This agent interferes with the polymerization of microtubules which is essential for the proper architecture of the Golgi apparatus. However, the polarization of the dispersed Golgi vesicles remains preserved. After dispersion each Golgi fragment consists of two polarized parts, a cis- and a trans-side. Arl5b co-localized in these structures with both markers, TGN46 and GM130, after dispersion of the Golgi (figure 3.4). Therefore Arl5b seems not to be exclusively present in one of these specialized compartments of the Golgi apparatus, but is rather distributed throughout the Golgi network.

After clarifying where Arl5b predominantly resides in the soma, the subpopulation of Arl5b that was targeted to the neurites of hippocampal neurons was examined. In dissociated hippocampal neurons 21 DIV Arl5b was not diffusely distributed, but accumulated in aggregates (figure 3.5). However, it did not co-localize with GM130 positive Golgi outposts in dendrites (data not shown).

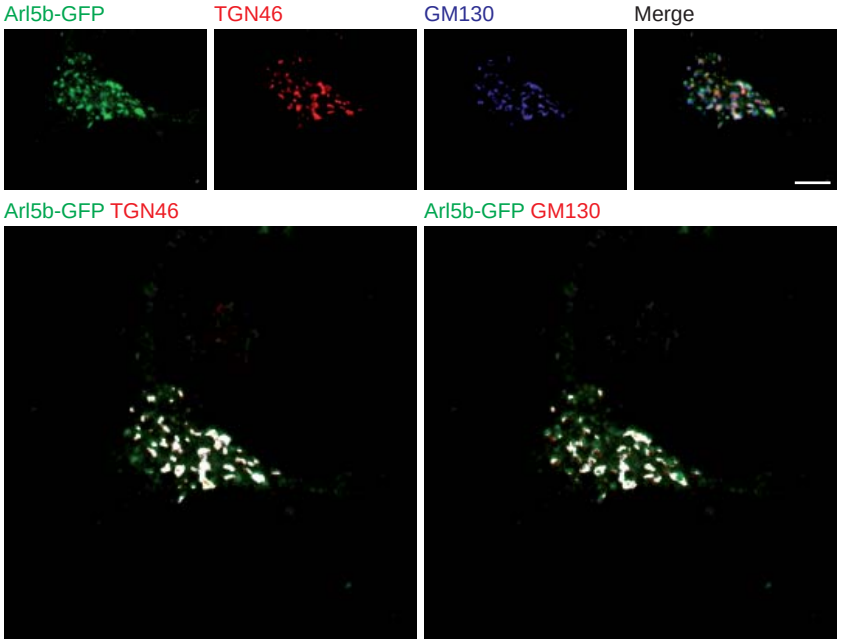

Figure 3.4. Arl5b is not specifically enriched in the trans- or cis-Golgi network. For an improved analysis of Arl5bs distribution in the Golgi apparatus dissociated hippocampal neurons were cultivated and transfected as indicated in figure 3.3. Before counterstaining with TGN46 and GM130 neurons were incubated with 5µg/ml Nocodazole for 2 h for Golgi dispersion. Subsequent co-localization analysis of Arl5b either with TGN46 or GM130 confirms overlapping signals with both markers. Co-localization is labeled in white in overlay analysis of Arl5b/TGN46 and Arl5b/GM130. The scale bar indicates 5 µm.

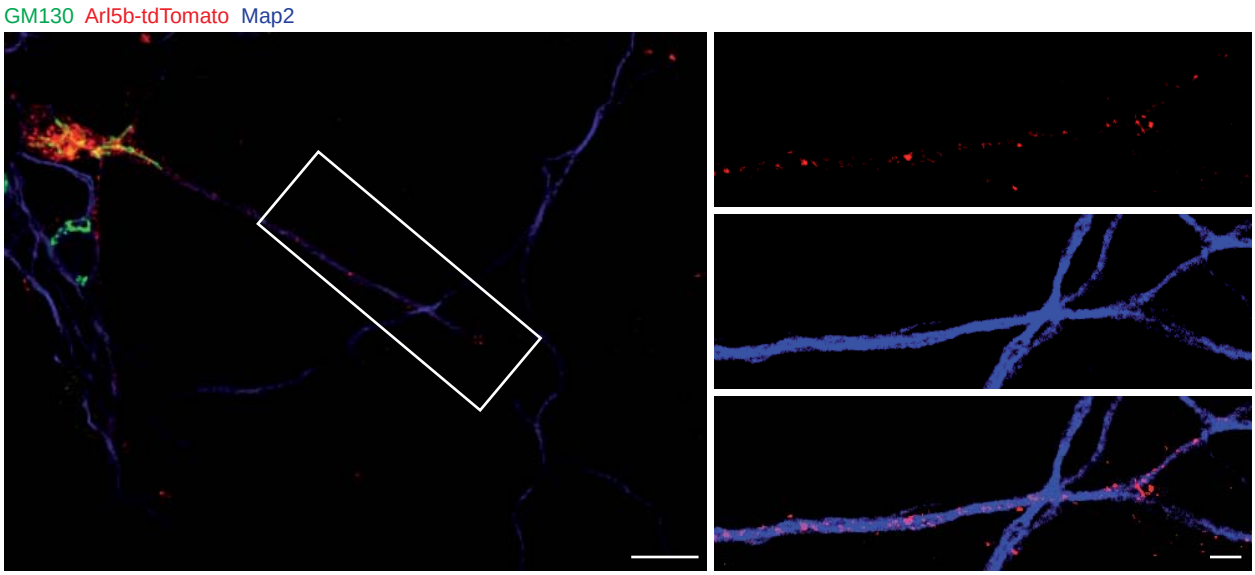

Figure 3.5. Arl5b is recruited to vesicular like structures in dendrites. Dissociated hippocampal neurons were transfected with Arl5b-tdTomato and cultivated until 21 DIV. Dendrites were visualized by immunostaining with MAP2 (blue) and somatic GM130 (green) highlights the Golgi apparatus. In the apical dendrite Arl5b (red) accumulates in vesicular structures. The white box in the overview (left) indicates the magnified dendrite (right). White bar in the overview indicates 20 µm and 5 µm in the magnification.

Additionally, Arl5b was found in small, vesicular like structures at the leading edge of the growth cone of the developing axon (red arrows, figure 3.6). These vesicular like Arl5b aggregates were also enriched in the shaft of the growth cone (blue arrow, figure 3.6) and along neurites (yellow arrows, figure 3.6).

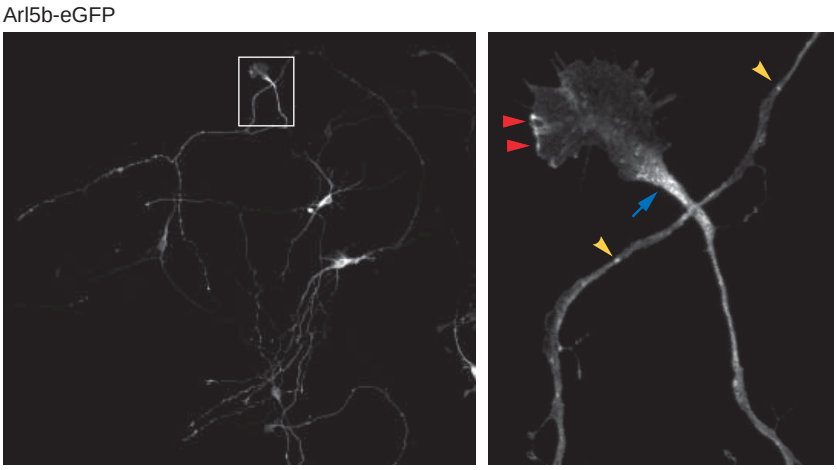

Figure 3.6. Arl5b aggregates in the growth cones and along neurites of dissociated hippocampal neurons. Confocal microscopy image of Arl5b-eGFP transfected cultured hippocampal neurons at DIV5. The depicted neuron was imaged 24 h after transfection. The white box in the overview (left) marks the enlarged growth cone shown to the right. Red arrows mark accumulation of Arl5b at the leading edge of a growth cone, the blue arrow points out an accumulation of vesicle like aggregates of Ar5lb in the shaft of the growth cone and the yellow arrows show vesicular structures of Arl5b distributed along the neurite. White bar in the overview indicates 20 µm.

With a spinning disk live cell imaging setup the Arl5b positive vesicular like structures were tracked over time. These previously observed structures displayed a highly dynamic behavior during live cell imaging. For example aggregation of Arl5b at the tip of a filopodium was recorded. The formed Arl5b positive structure subsequently was targeted out of the filopodium and trafficked along the neurite (figure 3.7).

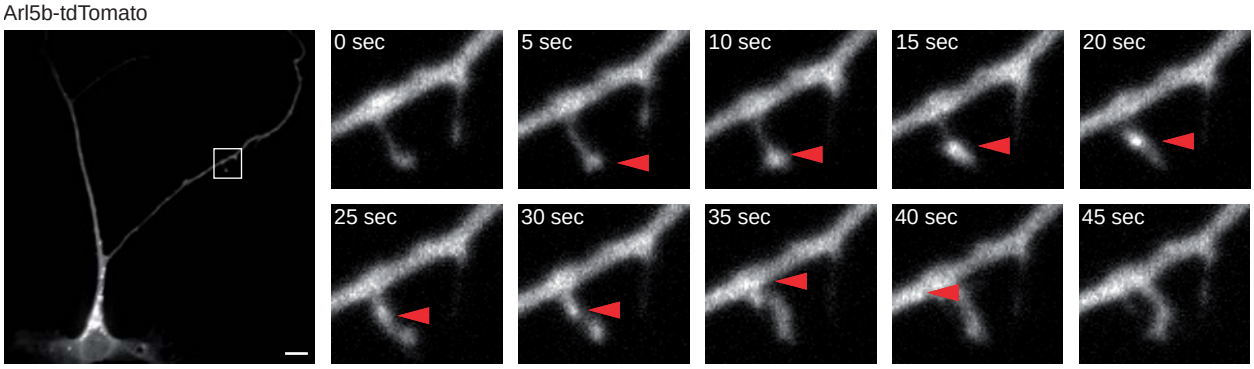

Figure 3.7. Representative live imaging time series showing accumulation of Arl5b followed by transportation of the aggregate out of the filopodium. Spinning disk live microscopy reveals dynamic relocation of Arl5b enriched puncta in neurites of cultured hippocampal neurons (transfected at DIV4 with Arl5b-tdTomato). Cells were recorded at DIV5 with 0.2 fps for a total of 20 minutes. The sequence visualizes how Arl5b is enriched at a vesicle like structure in a filopodia (enlarged images) and is transported out of the filopodium into the neurite and towards the soma over time during the indicated time course. The scale bar indicates 10 µm.

After their formation most of the mobile vesicular like structures moved retrogradly along the developing axon until they reached the soma of the neuron. This was observed in more than three independent experiments and in over 20 neurons in total. An example for the predominantly retrograde trafficking of Arl5b is visualized in a kymograph (figure 3.8). In conclusion, the results showed that Arl5b resides in the Golgi apparatus in the soma and in addition is recruited to vesicular like structures in dendrites and axons of dissociated hippocampal neurons.

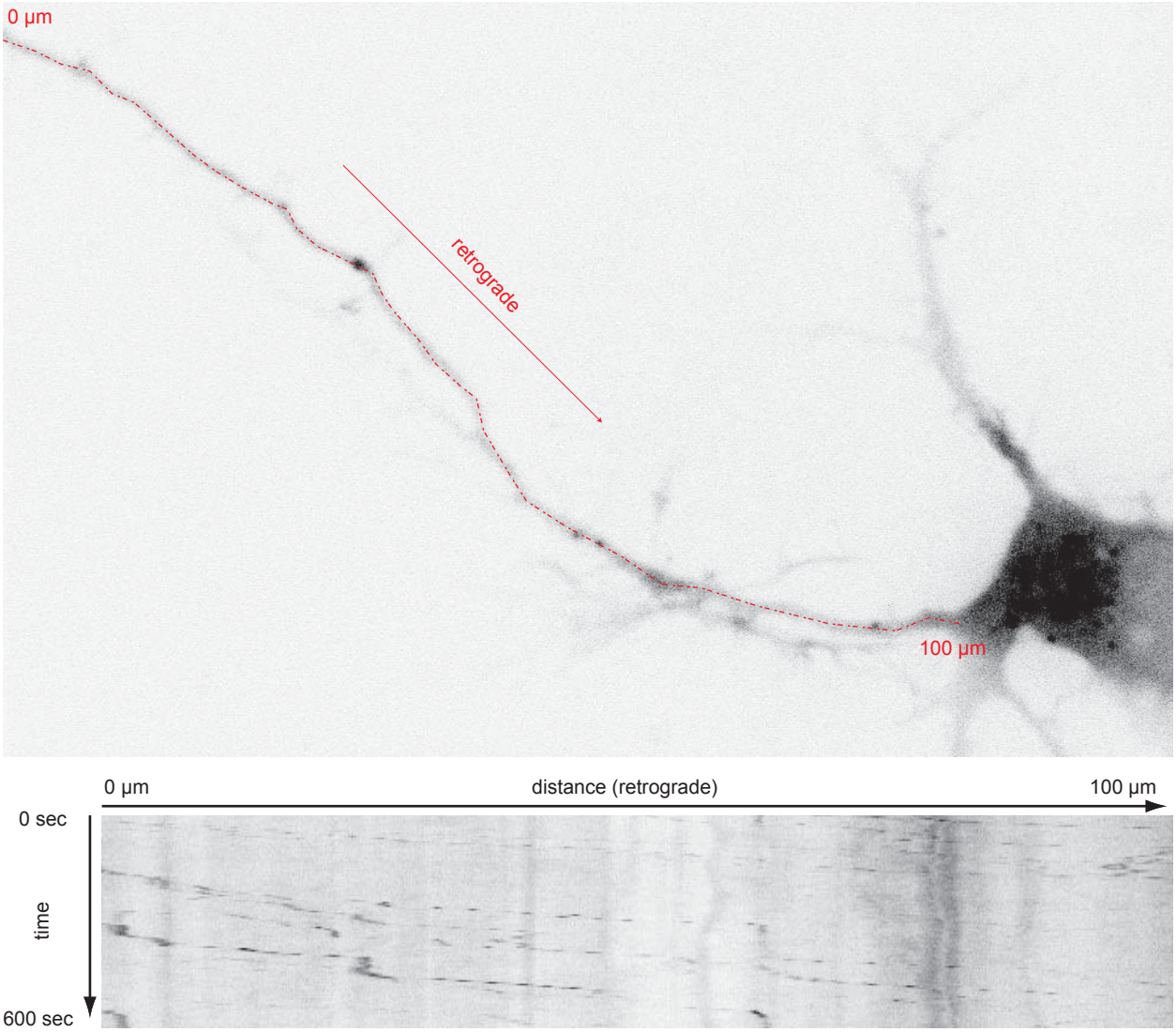

Figure 3.8. Long-range retrograde trafficking of Arl5b aggregates in neurites. Spinning disk live microscopy was performed using dissociated hippocampal neurons 5 DIV transfected with Arl5b-tdTomato. Cells were imaged with 0.2 fps for a total of 10 minutes. Above a single image out of a time series is shown and the dashed red line indicates the path used for kymograph generation. Below the kymograph shows long-range retrograde movement of Arl5b vesicular like structures along the neurite.

3.1.3 Recruitment of Arl5b to membranes is GTP-dependent and requires N-terminal myristoylation

The previous experiments established that Arl5b is localized to membranes of the Golgi apparatus and of mainly motile vesicles. To address the question what posttranslational modifications and structural determinants may regulate the membrane localization of Arl5b a number of mutant expression constructs of Arl5b were generated. Members of the Arf family of small GTPases are often anchored in membranes by myristoylation, an irreversible posttranslational modification. If the protein carries an N-terminal myristoylation motif, the N-myristoyltransferase can attach a myristoyl group to the N-terminal Glycine of an Arf protein after methionylaminopeptidases removed the initiator Methionine (Farazi et al., 2001). Additionally the attachment to membranes is often controlled by GTP binding and subsequent hydrolysis to GDP. Analogous to mutations of other Arf family proteins which result in constitutive active (GTP-restricted) or

dominant negative (GDP-locked) variants (Gillingham and Munro, 2007), I generated constitutive active and dominant negative Arl5b recombinant mutants.

In a series of experiments the factors which are responsible for attachment of Arl5b to membranes were examined. In this regard different recombinant mutant forms of Arl5b were generated. The mutation of a Glutamine (Q^{70}) to Leucine (L^{70}) results in a constitutive active form of Arl5b by mimicking the GTP bound form (Arl5b-Q^{70}L). Opposed to this, mutating a Threonine (T^{30}) to Asparagine (N^{30}) results in a mutant version of Arl5b with a locked in GDP-molecule which acts as dominant negative (Arl5b-T^{30}N). Both mutations were generated by SLIM-mutagenesis (Chiu et al., 2004). For a third mutant a point mutation was introduced to the ORF by using a mutated primer in a PCR. In this case the N-terminal Glycine (G) was exchanged by an Alanine (A). This mutation prevented the predicted myristoylation of Arl5b (Arl5b-G^{2}A). TdTomato tagged versions of Arl5b or each of the three mutants were overexpressed in cultured hippocampal neurons. In addition to the detection of the exogenous Arl5b-tdTomato (red in figure 3.9 and 3.10) the neuronal cultures were immunostained against MAP2 (blue in figure 3.9 and 3.10) and GM130 (green in figure 3.9) or Tau, an axonal marker (green in figure 3.10). The subcellular localization of the constitutive active mutant, Arl5b-Q^{70}L, matched the localization pattern of Arl5b. A clear enrichment in the soma-located Golgi and aggregates of Arl5b-Q^{70}L along the axon were detected. For both of the other mutants this distinct localization was not found. The dominant negative mutant as well as the Arl5b-G^{2}A variant was distributed diffusely throughout the cytoplasm of imaged neurons. Neither the overlap with GM130 in the soma, nor the accumulation in vesicular like structures were observable for either of the two mutants. Representative examples of these findings are depicted in figure 3.9 and 3.10.

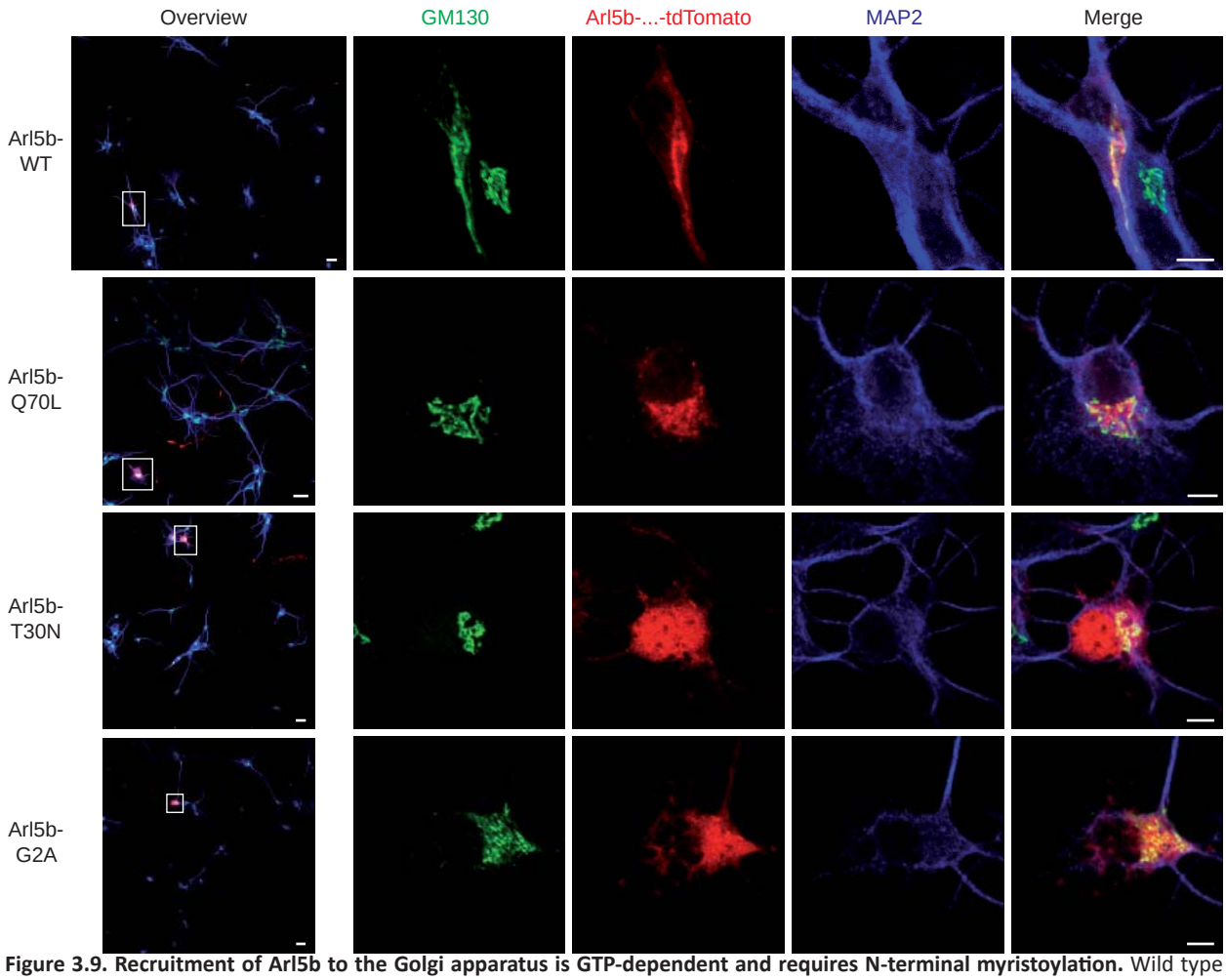

Figure 3.9. Recruitment of Arl5b to the Golgi apparatus is GTP-dependent and requires N-terminal myristoylation. Wild type Arl5b-tdTomato or three mutants, the constitutive active Arl5b-Q^{70}L, the dominant negative Ar5lb-T^{30}N and Arl5b-G^{2}A, incapable of binding myristic acid, were transfected into cultured hippocampal neurons at DIV4. On the next day the neurons were immunostained for the cis-Golgi marker GM130 and the dendritic MAP2. The white boxes in the overview images (left row) indicate the magnified regions. While Arl5b and Arl5b-Q^{70}L strongly accumulate in the Golgi, Arl5b-T^{30}N and Arl5b-G^{2}A are diffusely distributed in the soma. White bars in the overview images depict 20 µm and 5 µm in the magnifications.

Radioactively labeled myristic acid was added to the medium after the transfection. The cells were allowed to recover over night. After cell lysis, immunoprecipitation using an antibody against GFP was followed by Western Blot analysis to confirm the successful precipitation of Arl5b-GFP and Arl5b-G^{2}A-GFP, respectively (figure 3.11, upper panel). To examine whether myristic acid was incorporated into Arl5b-GFP or Arl5b-G^{2}A-GFP the western blot membrane was exposed to an x-ray film for 7.5 weeks. The film was developed and a strong signal was detected in the Arl5b-GFP transfected cell lysate with a molecular weight corresponding to Arl5b-GFP, whereas no signal was detected in the lane loaded with the Arl5b-G^{2}A-GFP transfected cell lysate (figure 3.11, lower panel). From this experiment I conclude that Arl5b is in fact N-terminally myristoylated and the mutation of the first Glycine blocks this posttranslational modification of Arl5b at its N-Terminus. Thus two modifications seem to determine the attachment of Arl5b to membranes, myristoylation of the N-terminus and the reversible binding of GTP.

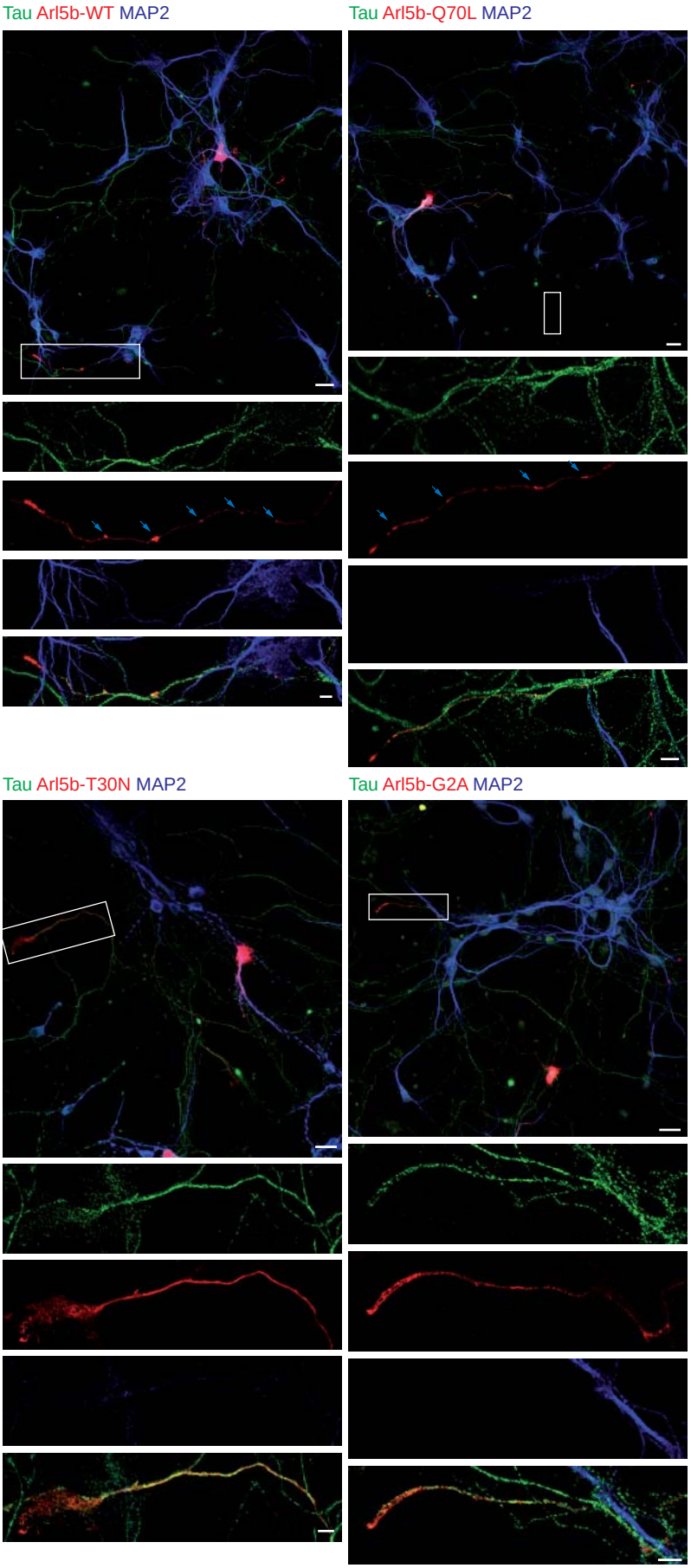

Figure 3.10. GTP-dependent activation and N-terminal myristoylation are required for Arl5b aggregation into vesicular like structures. Dissociated hippocampal neurons were transfected as described in 3.7., but immunostained for Tau, which localizes to axons, and the dendritic localized MAP2. The white boxes in the overview images indicate the magnified regions which are depicted below. Enlarged are sections of the axon of transfected neurons, identified by the staining for Tau and the absence of MAP2. In axons the recruitment of Arl5b to vesicular like structures as shown in figures 3.6-8 is confirmed. The localization pattern of the Arl5b-Q^{70}L mutant matches with the described Arl5b distribution in vesicular like structures in transfected dissociated hippocampal neurons (blue arrows in images depicting overexpressed Arl5b and Arl5b-Q^{70}L). Neither Arl5b-T^{30}N nor Arl5b-G^{2}A aggregates were spotted in analyzed neurons. White bars in the overview illustrate 20 µm and 5 µm in the magnifications.

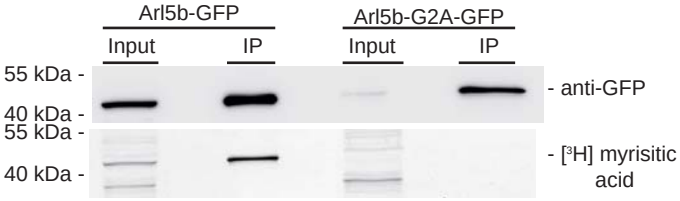

Figure 3.11 Arl5b is myristoylated at its N-terminal glycine. HeLa cells were transfected with either Arl5b-GFP or Arl5b-G^2A-GFP. Tritium labeled myristic acid was added to medium allowing incorporation during new protein synthesis over night. On the next day cell lysis and subsequent immunoprecipitation using an antibody against GFP followed. By Western Blot analysis successful precipitation of both, Arl5b-GFP and Arl5b-G^2A-GFP was confirmed (upper picture). The same membrane was used for an autoradiogram (lower picture). The missing band in the Arl5b-G^2A-GFP IP lane compared to the strong band in the Arl5b-GFP IP lane demonstrate the attachment of myristic acid to the N-terminal Glycine of Arl5b during translation.

3.1.4 Arl5b is present in late endosomes but not early endosomes

While the co-localization of Arl5b together with GM130 and TGN46 proved the residence of Arl5b in the Golgi apparatus in the soma, the identity of the compartments at which Arl5b aggregates in the neurites of neurons remained unspecified. For another subgroup of small GTPases, the Rab protein family, it has been established that specific members of the family are present in functionally different classes of endosomes (Ng and Tang, 2008). For example nascent endosomes become positive for Rab5 shortly after endocytosis. During sorting proceedings the Rab5 is removed from the endosome and dependent on the future fate of the endosomes other Rab proteins become enriched. For recycling endosomes that are sorted back to the plasma membrane Rab4 or Rab11 are specific markers. Other endosomes, so called late endosomes and also multivesicular bodies, are characterized by the presence of Rab7 before they end up at the Golgi apparatus or mature to lysosomes. To identify if Arl5b is present at the membrane of one of the described endosomes Arl5b-tdTomato was co-transfected together with tagged variants of Rab4, Rab5, Rab7 and Rab11 in HeLa cells. For Rab4, Rab5 and Rab11 no co-localization was observed by confocal microscopy, in contrast the Arl5b signal overlapped with Rab7 (data not shown). These results were subsequently confirmed in cultured hippocampal neurons. Developing hippocampal neurons (DIV4) were co-transfected with Arl5b-tdTomato and Venus-Rab7 or eGFP-Rab5. Most of the Arl5b punctuate signals in the longest neurite overlapped with Rab7 positive vesicles (figure 3.12). This kind of co-localization was rarely observed for Arl5b and Rab5 (figure 3.13). All experiments were performed at least three times and confirmed by analysis of multiple neurons.

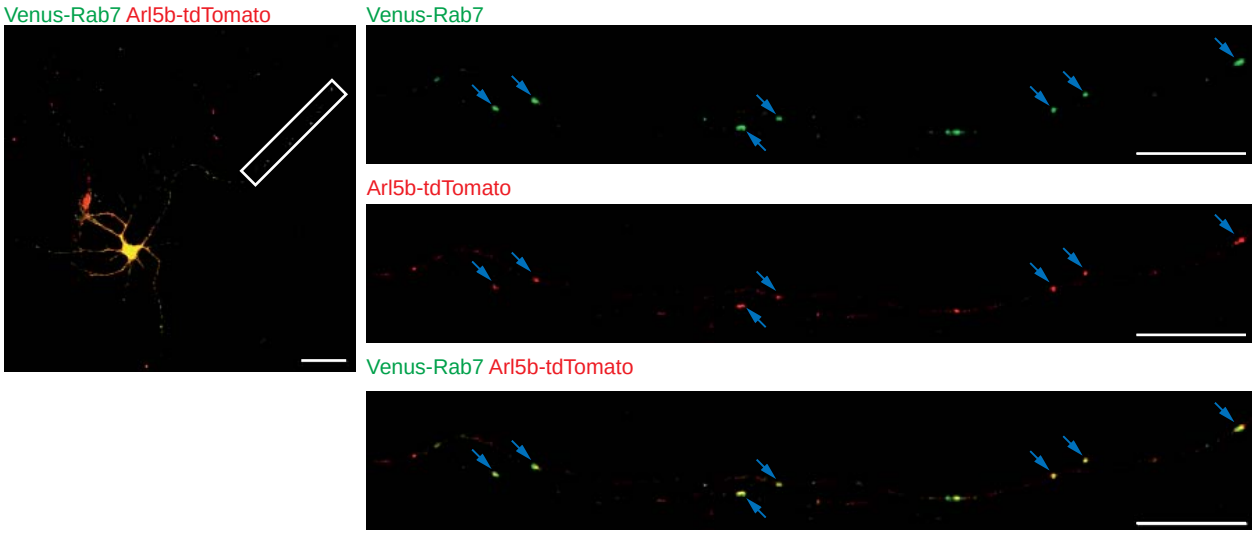

Figure 3.12. Arl5b is recruited to retrogradly transported Rab7 positive late endosomes. Confocal microscopy images of cultured hippocampal neurons (DIV5) co-transfected with Venus-Rab7 and Arl5b-tdTomato at DIV4. The white box in the overview on the left marks the enlarged region depicted in the right images. Blue arrows indicate areas were the Arl5b-tdTomato signal overlaps with the signal of Venus-Rab7. Scale bars indicate 10 µm.

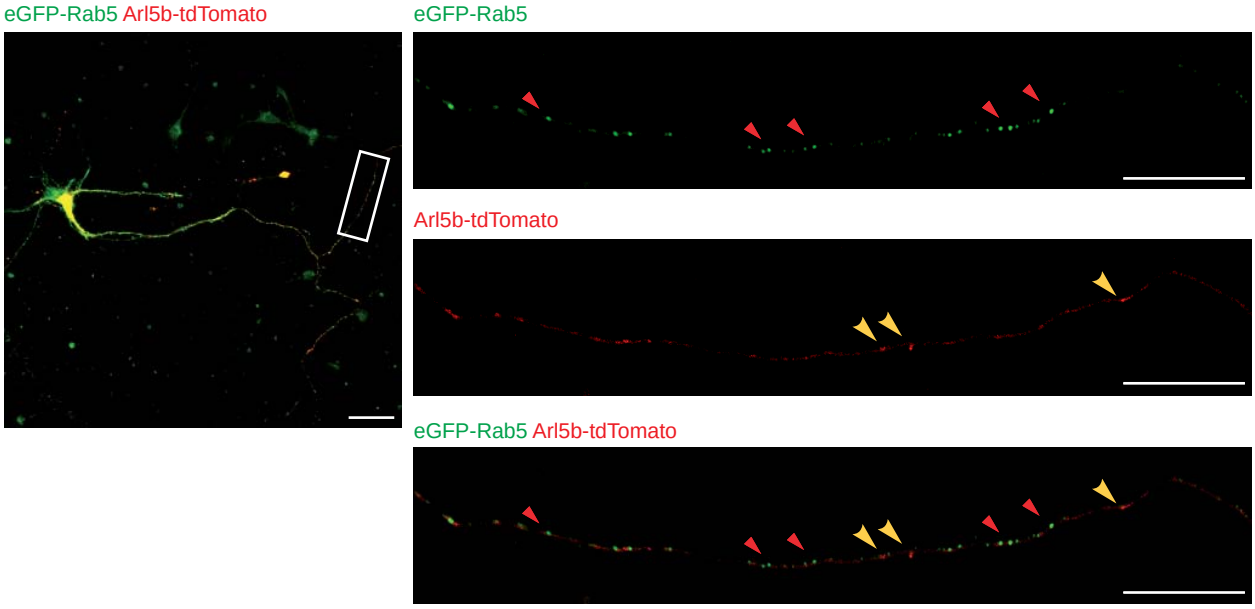

Figure 3.13. Arl5b is absent in Rab5 labeled early endosomes. Confocal microscopy images of cultured hippocampal neurons (DIV5) co-transfected with Venus-Rab5 and Arl5b-tdTomato at DIV4. The white box in the overview on the left marks the enlarged region depicted in the right images. Arl5b positive vesicles (yellow arrows) do not co-localize with the early endosomes marker Rab5 (red arrows). Scale bars indicate 10 µm.

To further validate that Arl5b is recruited to late endosomes live cell imaging was performed. Rab7 positive endosomes are thought to undergo retrograde long-range transport in the axon of developing spinal cord motor neurons while Rab5 positive early endosomes are relatively stable and are trafficked over comparably short distances (Deinhardt et al., 2006). Figure 3.14 shows a kymograph which supports the results obtained from confocal microscopy: most of the detected Arl5b and Rab7 proteins were retrogradly transported together over a long distance in the same vesicles in the imaged axon. This was not true for Rab5 positive vesicles which indeed are only trafficked over short distances in the axon. These vesicles

are not enriched with Arl5b which again showed the expected long-range movement (figure 3.15). Both results were observed in more than three independent experiments and the acquired data strongly suggests a role for Arl5b at late endosomes in the retrograde transport pathway in neurons.

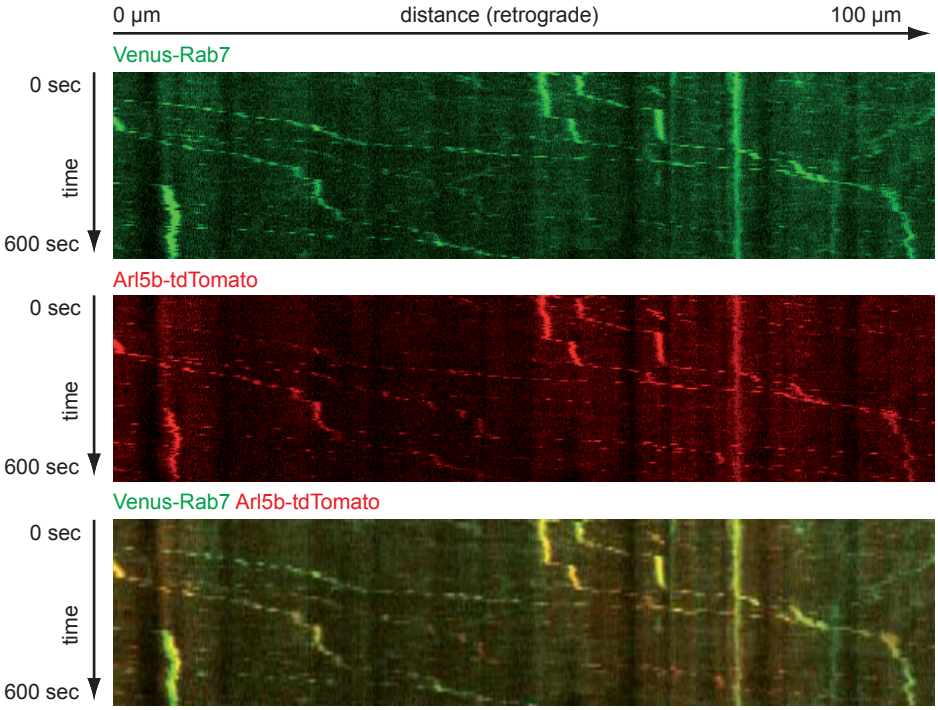

Figure 3.14 Arl5b is dynamically co-trafficked in late endosomes together with Rab7. Kymographs of spinning disc live microscopy of cultured hippocampal neurons at DIV4, co-transfected with Venus-Rab7 and Arl5b-tdTomato on the day before live imaging. The time series was recorded with 0.2 fps over 10 minutes. Yellow staining in the image of the merged channels (bottom) represents co-trafficking of Rab7, signal depicted in green, and Arl5b, signal depicted in red, positive vesicles.

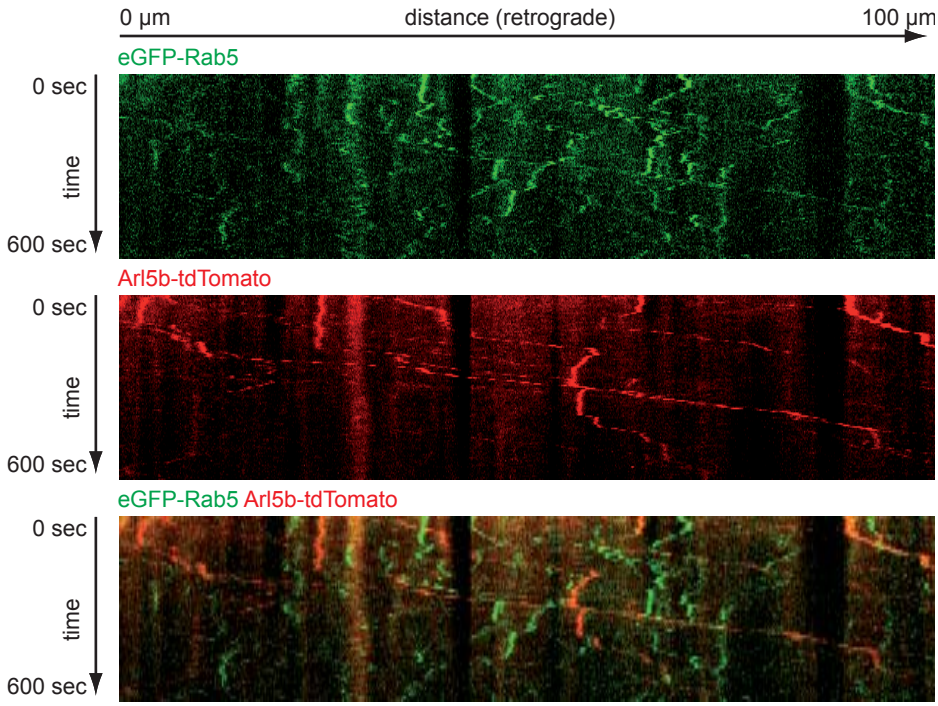

Figure 3.15 Rab5 marked early endosomes are not enriched in Arl5b. Spinning disk live imaging recordings (0.2 fps, 10 min) of cultured hippocampal neurons at DIV5, co-transfected with eGFP-Rab5 and Arl5b-tdTomato at DIV4. Depicted is a kymograph showing vesicle trafficking in a representative neurite of a dissociated hippocampal neuron. Vesicles are either Arl5b (red) or Rab5 (green) positive, almost no co-trafficking (yellow) was observed.

3.1.5 TrkB is present in Arl5b positive vesicles and both proteins are co-transported

Combining the previous described results of Arl5b being present in most Rab7 positive late endosomes and the knowledge that Rab7 is involved in sorting of receptors such as TrkB led to the next hypotheses. Is Arl5b present in late endosomes that are enriched for TrkB? To test this assumption Arl5b-tdTomato and TrkB-eGFP were co-expressed in hippocampal neurons and fixed for confocal microscopy at DIV8 or imaged with a spinning disk microscope at DIV3. The overlap of Arl5b (red) and TrkB (green) signals after fixation and immunostaining in the axon is marked by blue arrows in figure 3.16. During live imaging at least a part of the retrogradely moving Arl5b positive vesicles contained the tagged TrkB receptor (figure 3.17). The observed co-trafficking of Arl5b and TrkB provide a hint that Arl5b may be involved in the signaling pathways downstream of BDNF.

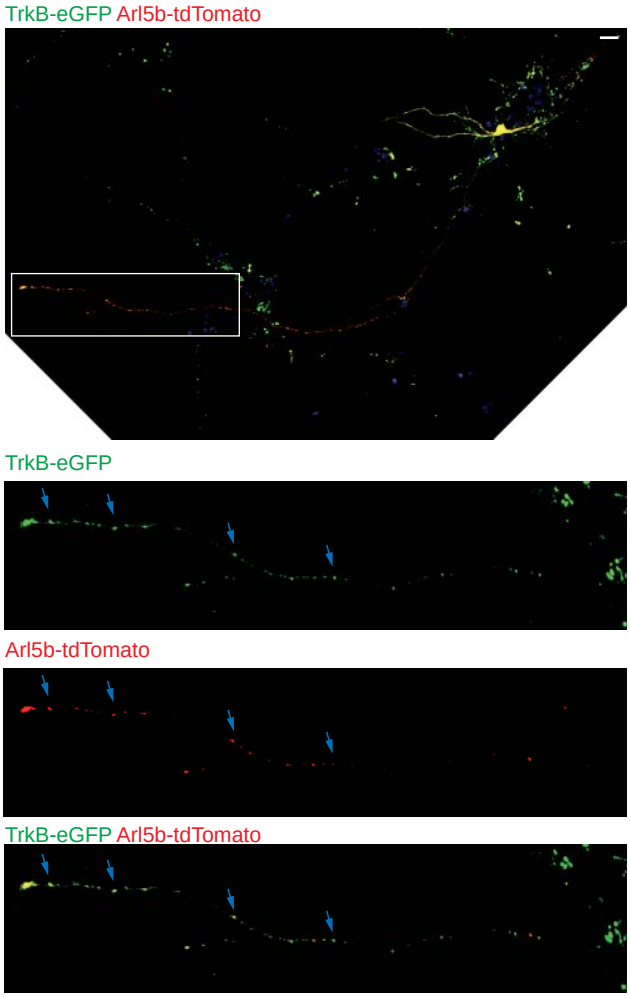

Figure 3.16. The BDNF receptor TrkB is attached to Arl5b positive vesicles. Images of cultured hippocampal neurons after DIV8 acquired by confocal microscopy. Neurons were co-transfected with TrkB-eGFP and Arl5b-tdTomato. The white box in the overview (top) marks the enlarged region (lower images). The enlarged region shows the axon of a developing neuron. TrkB signals are depicted in green, Arl5b signals in red. Co-localization of Arl5b and TrkB at vesicles (visualized by yellow staining in the overlay image) in the neurite is marked by blue arrows. Scale bars indicate 20 µm.

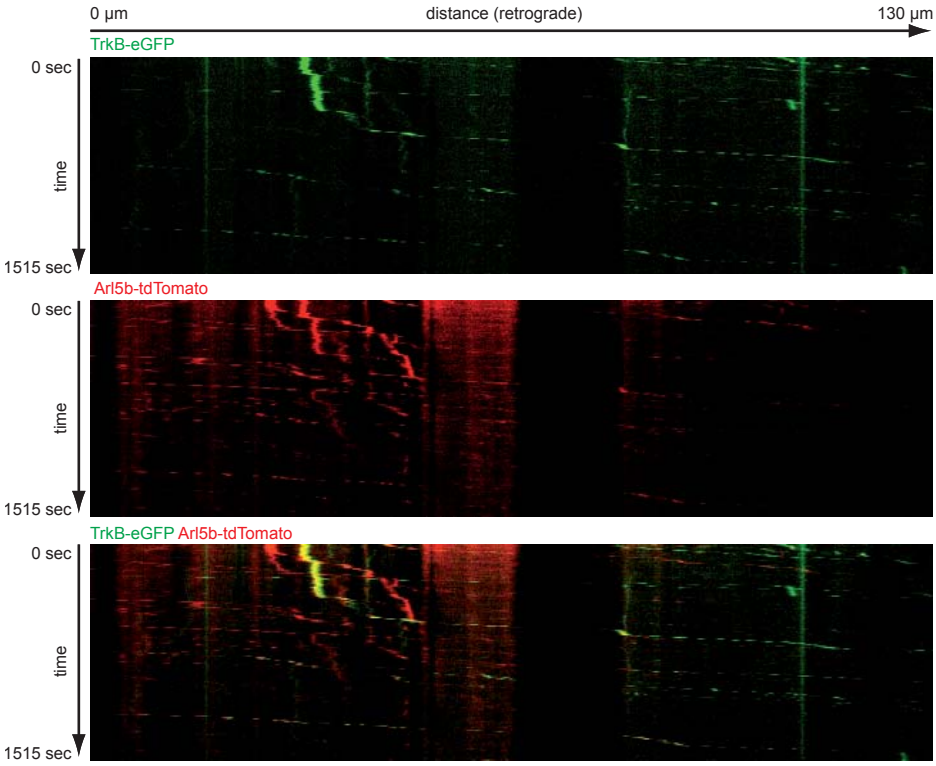

Figure 3.17. Long-range retrograde transport of TrkB is associated with Arl5b positive vesicles. Kymograph of a spinning disc live microscopy time series. Cultured hippocampal neurons at DIV3, co-transfected with TrkB-eGFP and Arl5b-tdTomato on the day before imaging, were imaged with 0.2 fps for ~25 min. Partial retrograde co-trafficking of Arl5b (red) and TrkB (green) is visualized by yellow staining. Cells were imaged with 0.2 fps for the indicated time.

3.1.6 BDNF is sufficient to recruit Arl5b to vesicles

Arl5b-tdTomato was found to co-localize with Rab7 in late endosomes not only in neurons but also in HeLa cells (data not shown). However, this recruitment of Arl5b was serum dependent: after serum starvation for 24h only a low percentage of HeLa cells exhibited Arl5b attached to vesicles (26%), instead Arl5b was distributed diffusely in the cytoplasm in most HeLa cells (74%). Addition of 10% FCS to the cell culture medium altered the localization of Arl5b. 60 min after serum addition Arl5b was recruited to endosomes in almost all analyzed HeLa cells (75%) (figure 3.18). The experiment was performed three times independently from each other and the amount of cells displaying vesicular Arl5b staining before and after addition of FCS differed significantly from each other (***, $p < 0.001$, two-tailed Student's t-Test).

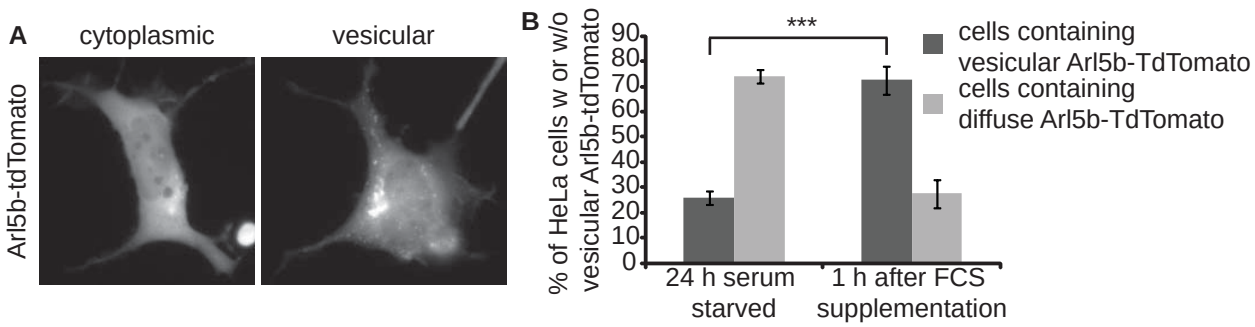

Figure 3.18. Recruitment of Arl5b to vesicles is serum-dependent in HeLa cells. A, Representative images of HeLa cells stably expressing Arl5b-tdTomato (HeLa Arl5b-tdTomato). HeLa cells were analyzed for localization pattern of Arl5b. Distribution of Arl5b was characterized to be either cytoplasmic (left) or vesicular (right). **B,** Quantification of HeLa cells analyzed for the distribution of Ar5lb after serum starvation for 24 h and one hour after supplementation of 10 % FCS. Addition of FCS significantly increased the percentage of cells in which Arl5b was recruited to vesicles (n = 3 experiments, ***, $p < 0.001$, two-tailed Student's t-Test).

To assess a possible role of Arl5b in BDNF transport or signaling a HeLa cell line stably expressing recombinant BDNF-GFP under the CMV promoter was generated (HeLa BDNF-GFP). Proper secretion of the GFP-tagged mature BDNF by the stably transfected cells was analyzed by seeding cells in a 10 cm cell culture dish, harvesting the cell culture medium after three days, subsequent concentration of the medium and immunoprecipitation with an antibody against GFP. The successful purification of BDNF-GFP was confirmed by Western blotting (figure 3.19). As a control non transfected HeLa cells (HeLa ctrl) were treated the same way. There was no detectable band at the expected height in the control Western Blot. These experiments showed that the generated HeLa BDNF-GFP cell line secrets BDNF-GFP into the medium.

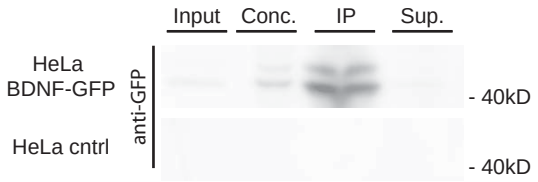

Figure 3.19. BDNF-GFP was expressed stably in and secreted by HeLa cells. Either stable expressing BDNF-GFP or non transfected HeLa cells were incubated for 3 d with DMEM. Western blot analysis was performed using anti-GFP and samples of the conditioned DMEM. After collecting the different DMEM from the cells (Input) their volumes were 20 fold concentrated using 30 kDa cutoff Amicon Ultra 15 mL centrifugal filter devices (Conc.). In a first step the BDNF-GFP was immunoprecipitated using an antibody against GFP (IP). Supernatant was loaded to examine the efficiency of the IP (Sup.). BDNF-GFP is enriched during the experiment in the medium preconditioned with BDNF-GFP secreting HeLa cells (upper image) but not in DMEM from non-transfected HeLa control cells (lower image).

The secreted BDNF-GFP was tested for its biological activity. For this purpose neuroblastoma cells were analyzed for differentiation. SY5Y cells were seeded and pre-differentiated by incubation with retinoic acid for 5 days. In parallel, medium was preconditioned by BDNF-GFP HeLa cells or HeLa ctrl cells. This preconditioned medium was concentrated and 1µl was added to 500µl fresh DMEM. The pre-differentiation medium of the SY5Y cells was replaced by BDNF-GFP conditioned or control medium. After 10 days the SY5Y cells treated with the control medium were dead while the BDNF-GFP treated cells survived and further differentiated (figure 3.20). This proved that the generated HeLa cells secreted an active, mature form of BDNF.

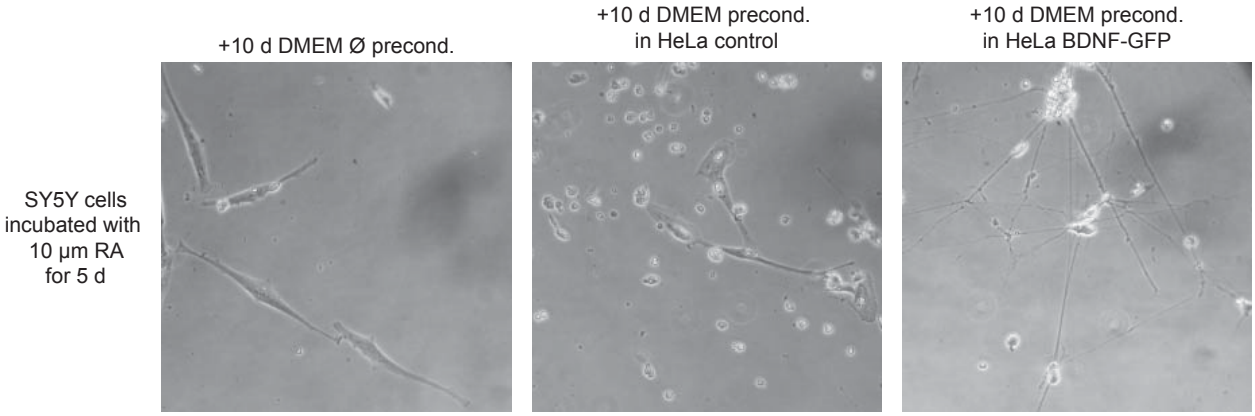

Figure 3.20. BDNF-GFP secreted by a stably transfected HeLa cell line is biologically active. SY5Y cells were pre-differentiated in DMEM supplemented with 10 µm retinoic acid (RA) for 5 d. DMEM was preconditioned by incubation with HeLa cells expressing BDNF-GFP or non transfected control HeLa cells. After 20 fold concentration and purification the SY5Y cells were incubated with fresh DMEM supplemented with the preconditioned medium (1 µl per 500 µl). Shown are representative images of SY5Y cells after additional incubation for 10 days. SY5Y cells treated with BDNF-GFP containing medium were differentiated (right). Almost all control cells incubated non preconditioned medium (left) or medium preconditioned with control HeLa cells (middle) died.

HeLa cells expressing Arl5b-tdTomato were co-cultivated either with the HeLa BDNF-GFP cell line or with HeLa control cells in medium without serum for 3 days. The stably Arl5b expressing HeLa cells were analyzed for Arl5b distribution by live microscopy. The number of cells exhibiting activated, vesicular Arl5b was significantly higher in the presence of BDNF compared to the control experiment (n = six experiments, ***, $p < 0.001$, two-tailed Student's t-Test, figure 3.21). The evidence that the presence of BDNF is sufficient to recruit Arl5b to vesicular structures further reinforces the hypothesis that Arl5b acts downstream of BDNF.

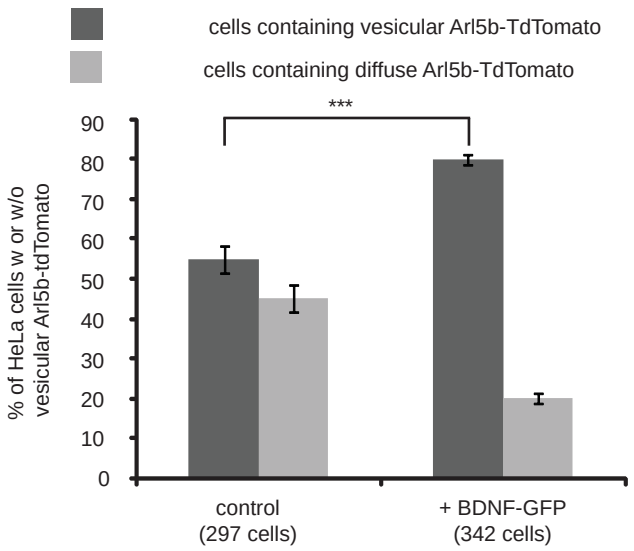

Figure 3.21. BDNF is sufficient to activate Arl5b. Quantification of recruitment of Arl5b-tdTomato to vesicles. HeLa cells stably expressing Arl5b-tdTomato were co-cultured with HeLa control cells or HeLa BDNF-GFP cells in DMEM without FCS for 3 days. Recruitment of Arl5b-tdTomato to vesicles in each cell was determined visually by live cell imaging. In total 342 HeLa cells growing in presence of BDNF and 297 HeLa cells growing in control medium were examined in six independent experiments. The percentage of HeLa cells containing Arl5b recruited to vesicles was significantly increased in BDNF supplemented medium compared to the percentage of cells with "vesicular Arl5b" incubated in control medium. Statistical significance was determined by two-tailed Student's t Test (***, $p < 0.001$, n = 6 experiments).

3.1.7 Rab7 retrograde trafficking is impaired upon overexpression of dominant negative Arl5b

It has been demonstrated in a different experiments that Rab7 is required for proper transport of TrkB. Overexpression of a dominant negative variant of Rab7 abolishes TrkB long-range transport in spinal cord motor neurons (Deinhardt et al., 2006). In a live cell imaging experiment the effect of Arl5b on Rab7 trafficking was investigated by analyzing hippocampal neurons (DIV5) overexpressing Rab7 by spinning disk microscopy. The left upper panel in Figure 3.22 shows representative kymographs of a series of recordings of Venus-Rab7 in the axon of a primary neuron which was co-transfected with Arl5b-tdTomato. A fraction of Rab7 undergoes fast retrograde trafficking. In contrast the left lower panel shows a kymograph of Rab7 in presence of the dominant negative version of Arl5b, Arl5b-T^{30}N-tdTomato, where less Rab7 vesicles are transported retrogradely along the axon. This effect of the dominant negative Arl5b on the transport of Rab7 was analyzed in three experiments (n = 19 neurons for each group). Neither the number of immobile nor of slowly moving vesicles was different ($p > 0.05$, two-tailed Student's t-Test) in presence of the dominant negative Arl5b. However the number of fast moving Rab7 vesicles was significantly reduced (**, $p < 0.01$, two-tailed Student's t-Test). Apparently Arl5b influences Rab7 dependent retrograde trafficking of late endosomes, even though the transport of Rab7 is not completely blocked (figure 3.22).

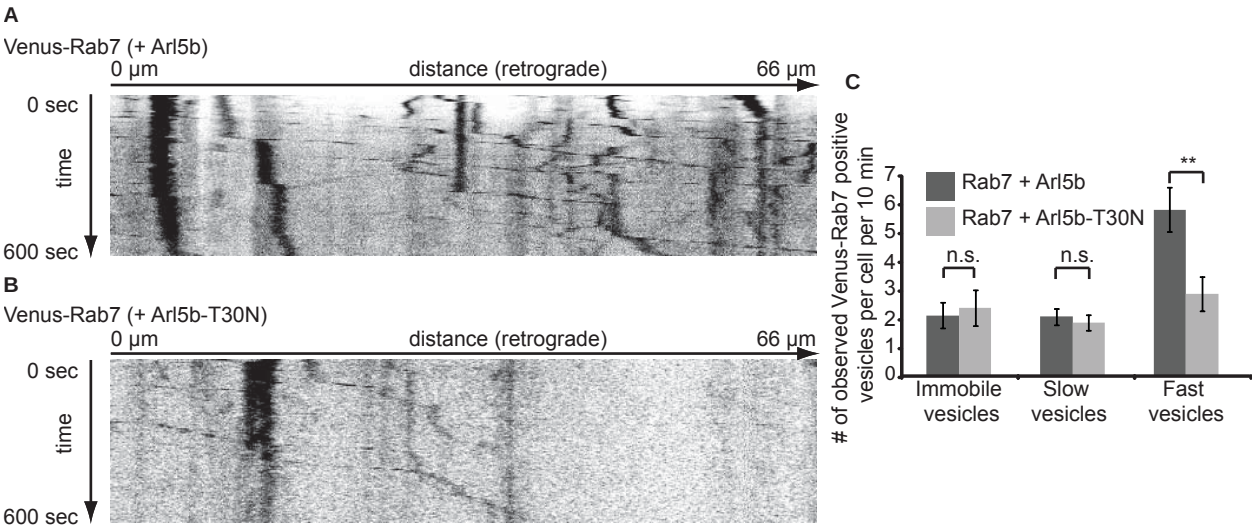

Figure 3.22. Rab7 trafficking is impaired by overexpression of dominant negative Arl5b in neurons. A-B, Representative kymographs of time series acquired by spinning disk live microscopy of cultured hippocampal neurons (DIV5). Neurons were co-transfected before with Venus-Rab7 and either wild type Arl5b-tdTomato **(A)** or dominant negative Arl5b-T^{30}N-tdTomato **(B)**. Cells were recorded for 10 min with 0.2 fps. **C,** Quantification of the number of retrogradly transported Rab7 positive vesicles over a timeframe of 10 min. Vesicles were classified as immobile (<0.1 µm/sec), slow moving (0.1 to 0.4 µm/sec) or fast moving (>0.4 µm/sec). In each case, co-transfected with Arl5b or Arl5b-T^{30}N, 19 neurons and a total of 192 and 137, respectively, vesicles were analyzed. The # of detected immobile and slow Rab7 vesicles per neuron and 10 minutes was not significantly different between neurons co-transfected with Arl5b or Arl5b-T^{30}N. A significant reduction of fast traveling Rab7 vesicles was observed in neurons co-transfected with Arl5b-T^{30}N compared to co-transfection with Arl5b (** $p < 0.01$). Statistical significance was determined by two-tailed Student's t tests. The data was acquired in three independent experiments.

3.1.8 A close homolog of Arl5b, the small GTPase Arl5a, is recruited to Rab7 positive late endosomes

The dominant negative variant of Arl5b reduces but does not completely block Rab7 retrograde transport. An explanation might be an independent or redundant mechanism for Rab7 trafficking. It is possible that only a part of the Rab7 trafficking is mediated by Arl5b. Other proteins of the Arf family could regulate Rab7 trafficking by a similar mechanism. Arl5a shares approximately 80% similarity on the amino acid level with Arl5b (Figure 3.23).

```
Arl5a     MGILFTRIWRLFNHQEHKVIIVGLDNAGKTTILYQFSMNEVVHTSPTIGSNVEEIVVNNT 60
Arl5b     MGLIFAKLWSLFCNQEHKVIIVGLDNAGKTTILYQFLMNEVVHTSPTIGSNVEEIVVKNT 60
          **::*:::* ** :********************** ********************:**

Arl5a     RFLMWDIGGQESLRPSWNTYYTNTEFVIVVVDSTDRERISVTREELYKMLAHEDLRKAGL 120
Arl5b     HFLMWDIGGQESLRSSWNTYYSNTEFIILVVDSIDRERLAITKEELYRMLAHEDLRKAAV 120
          :*************.******:****:*:**** ****:::*:****:**********.:

Arl5a     LIFANKQDVKECMTVAEISQFLKLTSIKDHQWHIQACCALTGEGLCQGLEWMMSRLKIR 179
Arl5b     LIFANKQDMKGCMTAAEISKYLTLSSIKDHPWHIQSCCALTGEGLCQGLEWMTSRIGVR 179
          ********:* ***.****::*.*:***** ****:**************** **: :*
```

Figure 3.23. Arl5a and Arl5b are homologous proteins. Shown is a multiple sequence alignment of Arl5a and Arl5b generated using ClustalW. ~80% of the amino acids are conserved in both proteins.

A prerequisite for Arl5a to fulfill a role similar to Arl5b is a comparable subcellular localization. Arl5a-tdTomato was overexpressed in dissociated hippocampal neurons together with Venus-Rab7. In figure 3.24 the observed co-localization of Arl5a and Rab7 in vesicles in an axon is depicted. Arl5a and Arl5b are recruited to the same population of vesicles in neurons. As both homologs are present in Rab7 positive late endosomes one cannot exclude that Arl5a acts redundantly in Rab7 trafficking.

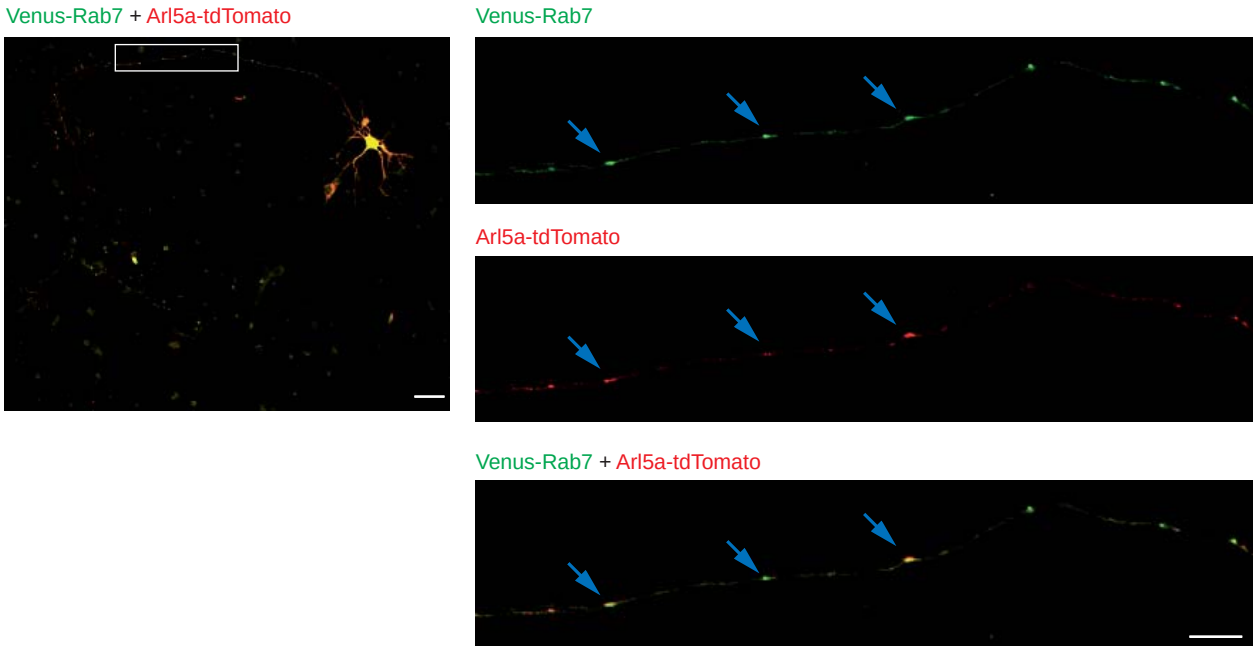

Figure 3.24. Arl5a is localized in the same late endosomes as Arl5b. Representative confocal microscopy image of cultured hippocampal neurons co-transfected with Venus-Rab7 (green) and Arl5a-tdTomato (red). The white box in the overview on the left marks the enlarged region (right). Blue arrows mark vesicles which are double positive for Rab7 and Arl5a (yellow staining in the image with merged channels). White bars in the overview illustrate 20 µm and 5 µm in the magnifications.

3.2 Interaction partners of Arl5b

The second approach to examine Arl5b function was carried out in parallel. The knowledge about the interaction network of a protein can significantly contribute to solve the role of this protein. One aim of the study was the identification of interaction partners of the small GTPase.

3.2.1 A Yeast-Two-Hybrid screen revealed potential interaction partners of Arl5b

Since its invention in 1989 by Songs and Fields the Yeast-Two-Hybrid (Y2H) screen proved its power to examine interactions between a protein of interest and large groups of other proteins in a short period of time (Song and Fields, 1989).

In a Y2H screen a protein of interest (bait) is fused to the DNA-binding domain (DBD) of a transcription factor, originally Gal4 from *Saccharomyces cerevisiae*. The DNA-binding domain on its own is

not sufficient to activate transcription of reporter genes. For initiation of transcription a second protein, the activation domain (AD), must be in close proximity to the DBD. The AD can than recruit the required transcriptional machinery. The AD alone without the DBD is also unable to activate transcription. These facts are exploited in the Y2H assay. A second protein of interest (prey) is fused to the AD. Upon interaction between bait and prey the DBD and AD can initiate transcription. Commonly used reporter genes are markers such as beta galactosidase (lacZ) or *HIS3*. Expression of lacZ results in a blue staining of positive colonies in the presence of X-gal which is cleaved by beta galactosidase. *HIS3* can be used to select positive clones given that histidine is not provided in the medium (figure 3.25).

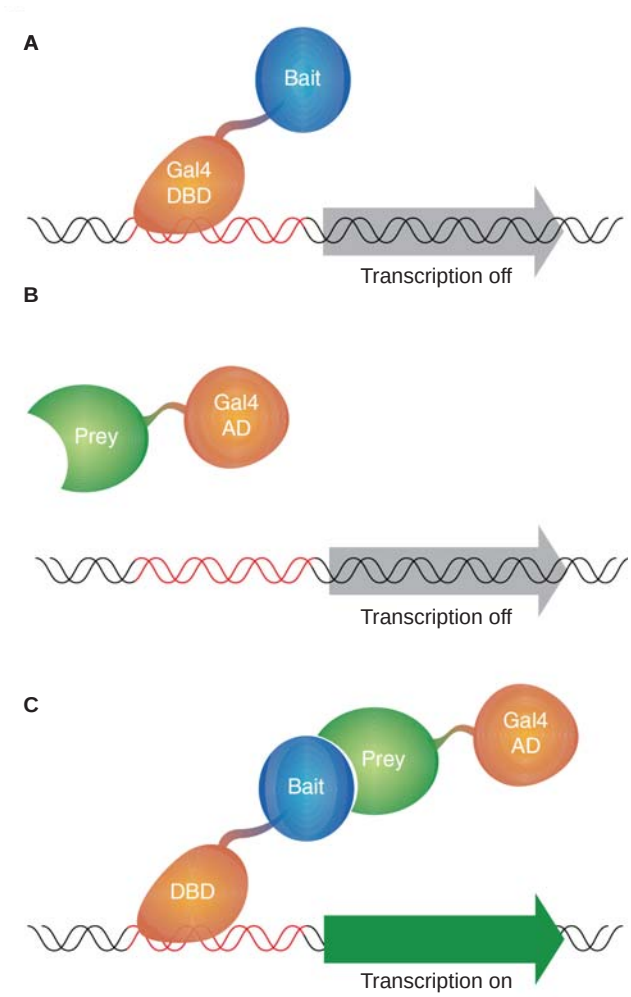

Figure 3.25. Schematic diagram of the Yeast-Two-Hybrid assay. A transcription factor, in the schematic diagram this is Gal4, consists of two independent protein domains, the DNA binding domain (DBD) and the activation domain (AD). Each of two proteins of interest (called bait and prey) are fused to either the DBD or AD. **A,** The DBD-bait fusion protein binds near the transcription start of a reporter gene, but it is not sufficient to switch on transcription. **B,** As well as the AD-Prey fusion protein is not able to turn on transcription. **C,** If both fusion proteins are expressed and The bait and prey proteins interact with each other the AD of Gal4 is located close enough to the transcription start and can recruit additional transcription machinery to switch on transcription of the reporter gene. Often used reporters are LacZ or *HIS3* (modified from Lentze and Auerbach, 2008).

To screen for interaction partners the complete open reading frame of Arl5b was used as bait. It was cloned into the pB27 vector resulting in a LexA-Arl5b fusion. The actual Y2H screens were carried out by the company Hybrigenics. Two different prey libraries were screened for Arl5b interaction partners. In the first approach a library of cDNA purified from embryonic mouse brain tissue was screened, in a second approach the library consisted of fragments from proteins expressed in the adult mouse brain. In total 142 million interactions were analyzed in the first screen and 68.4 million in the second screen. As a result

267 and 186 positive clones were processed, respectively. Sequencing revealed that the prey fragments of these clones coded for 43 and 14 unique proteins. After exclusion of prey domains with known non-specific interactions and proven artificial interactions a total of 53 different proteins remained as putative interaction partners of Arl5b. As far as possible the proteins were classified into ten different functional groups by assessing their cellular function described in the literature, their homology to other genes or, if available, annotations to Gene Ontology termini (see Figure 3.26).

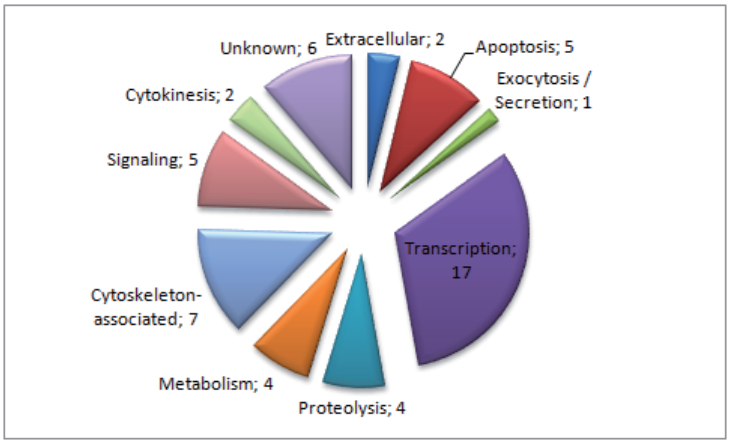

Figure 3.26. Categorization of putative interaction partners of Arl5b. Proteins identified in the Y2H screen are involved in a variety of different cell biological functions. Most interesting interaction partners are part of the two large groups of proteins with a role in intracellular signaling or which are associated with the cytoskeleton.

The largest group of putative interaction partners (transcription associated proteins) was excluded from further investigations because proteins in this category are very likely false positive hits in Y2H screens. Many small GTPases are integral elements of signaling cascades. Therefore Arl5b, as a member of a GTPase family, is likely to fulfill a function in signaling and members of this category of proteins were considered interesting interaction partners. In addition, a lot of signaling cascades require active transport along microtubules and also Actin polymerizing proteins drive trafficking in cells. Moreover remodeling of the cytoskeleton is essential for synaptic plasticity. Taken together the relationship between signaling and cytoskeleton-associated proteins led to the decision to include cytoskeleton-associated proteins in the in-depth analysis.

Based on the analysis 10 candidates identified in the Y2H screens were chosen as targets of interest. As the Y2H assay is known for a high rate of false positive results the validation of interactions between the candidates and Arl5b by biochemical assays complementing the Y2H results is a requisite.

To achieve this goal the ORFs of the genes were cloned into the pENTR vector of the gateway system using cDNA libraries or verified cDNA clones as template. This allowed fast cloning into different destination vectors to obtain suitable fusion proteins needed for different biochemical assays.

3.2.2 Validation of an Arl5b interacting protein by GST-pulldown and Co-immunoprecipitation

Casein kinase 1 alpha (CK1α), a regulator of glutamate-induced neuronal excitation (Chergui et al., 2005), was one of the selected targets of interests. Two distinct biochemical assays, GST-Pulldown and Co-Immunoprecipitation, were performed to verify the interaction between Arl5b and CK1α.

For a GST-Pulldown assay HA tagged CK1α was overexpressed in HeLa cells. Arl5b-GST bound glutathione beads were used to purify CK1α from a respective cell lysates. Control beads, loaded with GST, were not sufficient to precipitate CK1α in comparable amounts. Figure 3.27 shows a representative Western blot assay result for this experiment.

To co-immunoprecipitate Arl5b-HA by CK1α-YFP both proteins were transiently expressed in HeLa cells. Precipitation of CK1α-YFP was performed with ChromoTek GFP-Trap beads. In figure 3.28 the successful immunoprecipitation of CK1α-YFP is depicted. The precipitation of CK1α co-purified Arl5b. Altogether the interaction of Arl5b and CK1α was demonstrated utilizing three different assays.

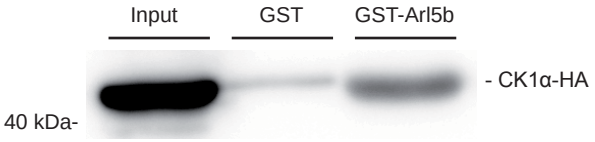

Figure 3.27. Verification of the interaction between Arl5b and CK1α-HA by GST-Pulldown assay. Depicted is a western blot analysis of a GST-Pulldown assay. HeLa cells were transfected with CK1α-HA. On the next day GST or GST-Arl5b bound magnetic GSH beads were incubated with cell lysate from the transfected cultures. A fraction of the HeLa cell lysate was used as input to confirm expression of CK1α-HA. While CK1α-HA was specifically pulled down by a GST-Arl5b fusion protein it was not purified by GST alone.

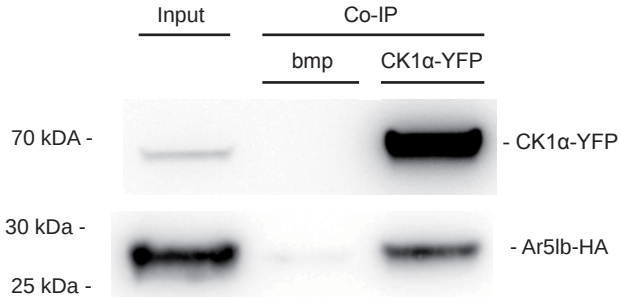

Figure 3.28. Co-immunoprecipitation of Arl5b by purification of CK1α. HeLa cells were co-transfected with CK1α-YFP and Arl5b-HA. Cell lysate were used for a co-immunoprecipitation (Co-IP) after expression of both constructs for 24 h. Western Blot analysis confirmed immunoprecipitation of CK1α-YFP by GFP-Trap beads, blocked magnetic particles (bmp) were used as control and a fraction of the cell lysate to confirm expression of Arl5b-HA and CK1α-YFP (input). By IP of CK1α-YFP Arl5b-HA was successfully co-purified. Arl5b was not enriched by incubation of lysate with bmp.

3.2.3 Casein Kinase 1 alpha co-localizes with Arl5b in cultured hippocampal neurons

All performed assays confirmed the interaction of Arl5b and CK1α *in vitro*. To assess if a physiological relevant interaction of both proteins is possible they were co-expressed in dissociated hippocampal neurons (DIV5). Arl5b and CK1α signals partly overlapped. Figure 3.29 shows co-localization of Arl5b and CK1α at vesicular like structures in neurites.

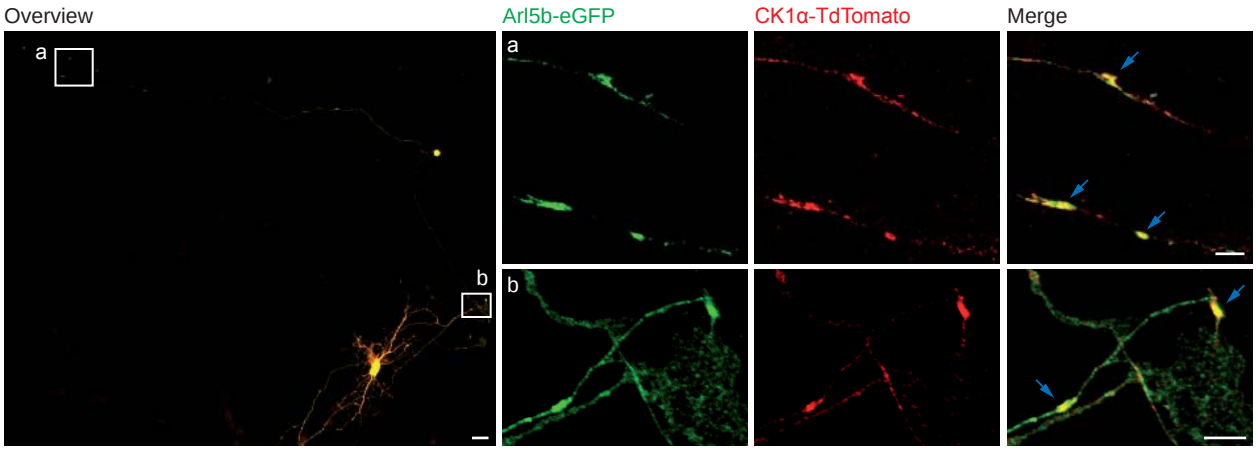

Figure 3.29. Arl5b co-localizes with CK1α at vesicles. Cultured hippocampal neurons were co-transfected with the indicated constructs at DIV4 and incubated for additional 24 h. Depicted are confocal microscopy images. The white boxes in the overview images (left) indicate the magnified regions which are depicted on the right. Arl5b-eGFP (green) and CK1α-tdTomato (red) co-localize at vesicular like structures (areas appearing yellow in the images with overlays of both channels) as indicated by blue arrows. White bars in the overview illustrate 20 µm and 5 µm in the magnifications.

Notably, the co-expression of Arl5b and CK1α can lead to unusual strong aggregation of both proteins in growth cones of developing neurites of hippocampal neurons. The extreme clustering is shown exemplarily in figure 3.30.

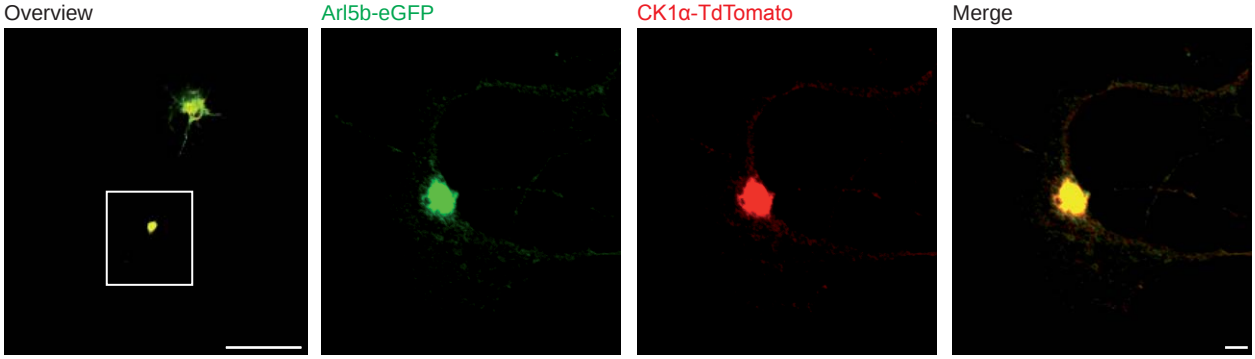

Figure 3.30. Arl5b massively aggregates at growth cones upon overexpression of CK1α. Cultured hippocampal neurons were co-transfected with the Arl5b-eGFP and CK1α-tdTomato constructs at DIV4 and incubated for additional 24 h. Depicted are confocal microscopy images. The white box in the overview image (left) indicates the magnified region (right). Massive aggregates of Arl5b-GFP (green) in the shaft of growth cones are observed in case of overexpression together with CK1α-tdTomato which is also present in the undefined structure. In the merged image the co-localization of Arl5b and CK1α results in a yellow staining. White bars in the overview illustrate 20 µm and 5 µm in the magnifications

Interestingly co-expression of TrkB and CK1α also facilitates exaggerated accumulation of TrkB in the shaft of the growth cone (figure 3.31). This pattern is similar to the above described redistribution of Arl5b.

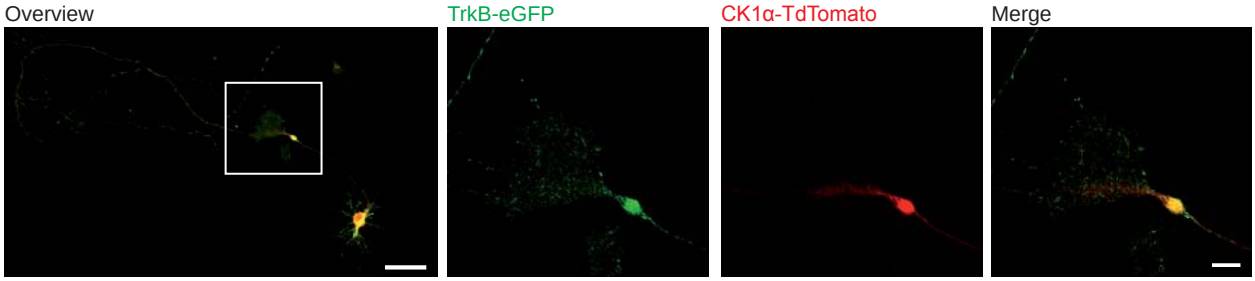

Figure 3.31. CK1α overexpression leads to aggregation of TrkB comparable to Arl5b. Confocal microscopy imaging was performed using dissociated hippocampal neurons after DIV5. Neurons were co-transfected with TrkB-eGFP and CK1α-tdTomato. The white box in the overview image (left) indicates the magnified region (right). As observed for Arl5b the receptor TrkB is heavily enriched in large abnormal structures near growth cones if CK1α-tdTomato is overexpressed in the same neuron. White bars in the overview illustrate 20 µm and 5 µm in the magnifications

3.3 Generation of Arl5b-deficient knockout mice

The third aim of the present thesis was the generation of an Arl5b knockout mouse line to evaluate the relevance of Arl5b *in vivo*. In order to achieve this goal ES cell clones were ordered from the European Conditional Mouse Mutagenesis (EUCOMM) program. At the beginning of this thesis the only available ES cells were derived from gene trapping mutations. A knockout cassette was integrated into the genome by random insertion of a modified retrovirus. ES cells were screened for successful integration of the knockout cassette in a specific gene locus. The ordered ES cell clones were verified to carry the mutation between Exon 1 and Exon 2 of Arl5b. The constitutive knockout of Arl5b is based on the introduction of a new Exon to the gene. The knockout cassette contained a splice acceptor site of the murine Engrailed2. Downstream in this Exon a transcriptional termination sequence (polyadenylation sequence, pA) was introduced mediating a premature termination of Arl5b mRNA translation. Due to this manipulation a truncated polypeptide is expressed instead of functional Arl5b. Therefore manipulated Arl5b alleles are considered “knockout” (figure 3.32).

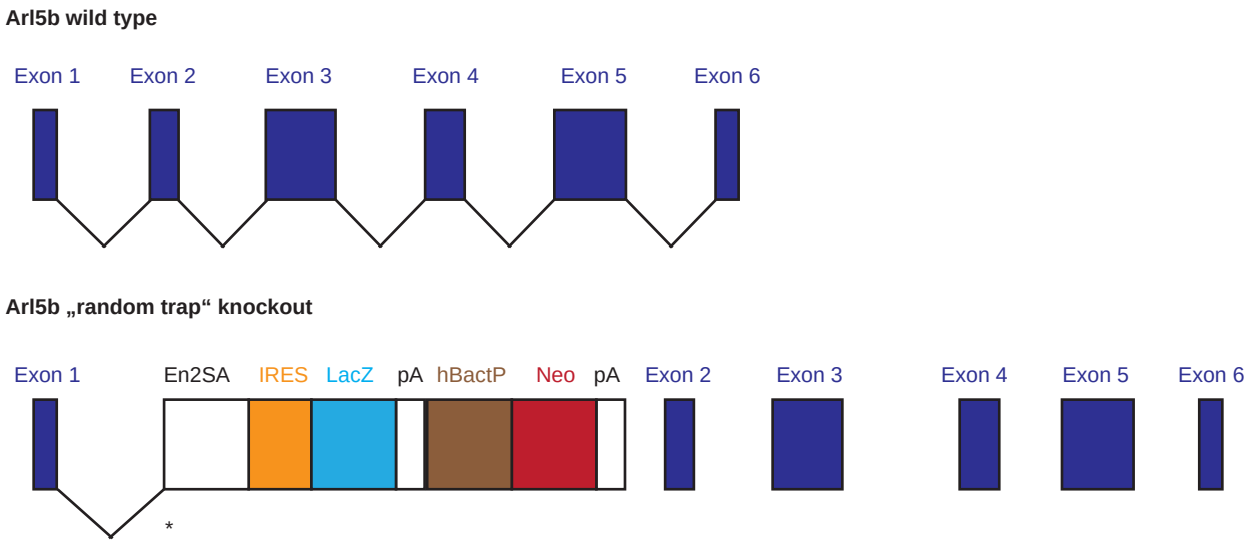

Figure 3.32. Schematic representation of the gene locus of Arl5b. The gene arl5b is composed of six exons (Arl5b wild type). A constitutive knockout allele was constructed by gene trapping. A knockout cassette was inserted to the genome by using a modified retrovirus. By insertion of the knockout cassette between the first and second Exon of Arl5b the splicing of the Arl5b mRNA is alternated. An Engrailed 2 splice acceptor site (En2SA) is inserted. Downstream of this splice acceptor a transcriptional termination sequence (polyA) results in a premature stop of transcription. In consequence instead of Arl5b a truncated version of Arl5b is translated or the mRNA is degraded due to Nonsense-mediated decay.

3.3.1 Arl5b-defienct mice die during early embryogenesis

Arl5b knockout mice were generated by blastocyst injection of the previously thawed and expanded ES cells. The chimeric progeny were cross-bred with C57Bl/6J mice. Further experiments were carried out to verify the successful knockout of Ar5lb. While integration of the gene trap cassette in the arl5b locus between Exon 1 and Exon 2 in the ES cells was validated before, the exact integration site remained unclear. To answer this question the first Intron of Arl5b was sequenced using genomic DNA isolated from a heterozygous mouse from the Arl5b knockout line as template. Various 5’-primers were designed to bind approximately every 500 bp covering the whole first Intron of Arl5b. For each of the 5’-primer primers a PCR reaction with a 3’-primer binding in the En2 domain of the gene trap cassette was set up. This allowed amplifying a DNA fragment where the genomic sequence transitioned to the sequence of the integrated cassette. This fragment was cloned into the pGEM-T Easy vector and the fragment was sequenced. The exact integration site was determined by sequence alignment (data not shown). Based on this result a fragment directly upstream of the gene trap cassette insertion site was amplified, cloned into the pBluescript II vector and used as probe in a Southern Blot assay to validate the knockout of Arl5b in the mouse line. After restriction of wild type, genomic DNA with the enzymes BamHI or PvuII this probe labeled fragments of 12 kb or 7 kb respectively. DNA isolated from progeny of the Arl5b KO Chimera treated the same way additionally produced labeled fragments of DNA with a length of 2 kb (BamHI restriction) and 2.8 kb (PvuII restriction). Figure 3.33 A shows a schematic representation of the genomic region of Arl5b, the location of the probe and the restriction sites in the wild type and knockout situation. Figure 3.33 B shows an au-

toradiogram of a Southern Blot with DNA from a wild type mouse (left) and a heterozygous mouse (right) were one copy of the gene carried the KO insertion. In this way the integration of the gene trap cassette was proven and positively tested progeny were bred with C57Bl/6J mouse to establish the new Arl5b KO mouse line. For further colony management genotyping was performed by PCR (data not shown).

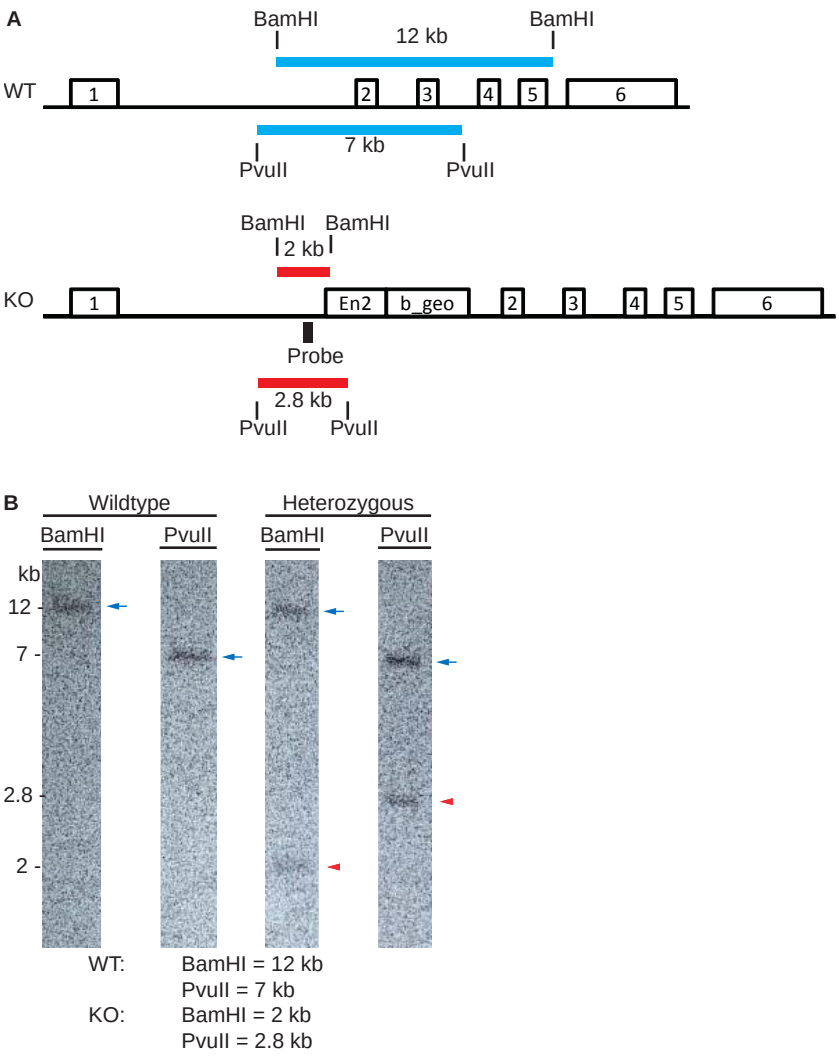

Figure 3.33. Verification of the successfully targeted Arl5b gene locus. A, Depicted is a schematic representation of the Arl5b gene locus and the Southern Blot strategy. Shown are the wild type (WT) and the knockout situation after integration of the targeting cassette (KO). A black square marks the probe used for Southern Blot analysis. BamHI and PvuII restriction sites are indicated. Dependent on the situation DNA fragments of different size were labeled by the probe after restriction with the corresponding restriction enzyme. Fragments are depicted in blue in the wild type locus and red in case of successful integration of the targeting cassette. **B,** Southern Blot analysis with DNA isolated from offspring of an Arl5b/WT Chimera mated with a C57Bl/6J mouse. On the left the DNA fragments have the length predicted for the wild type gene locus (blue arrows) while on the right additional fragments are visible (red arrows) confirming the integration of the knockout cassette in one allele.

The Arl5b KO line was crossbreed into the genomic C57Bl/6J background by repeated breeding with C57Bl/6J mice. After several generations heterozygous mating pairs were set up to obtain homozygous Arl5b knockout mice. In total 121 littermates were analyzed. Out of these 121 mice none was found to be homozygous for the knockout of Arl5b (figure 3.34). A more detailed analysis revealed the lethality of the knockout during an early stage during development. Embryos were isolated during different stages of development. The earliest investigated age of embryos was embryonic day 9.5. None of the analyzed embryos were found to be a homozygous KO. Interestingly the time between E7.5 and E9.5 is a critical phase during development of the heart (Kaufman and Bard, 1999). Due to the high expression levels of Arl5b in the heart the role of Arl5b during cardiogenesis should be examined in future investigations. The early

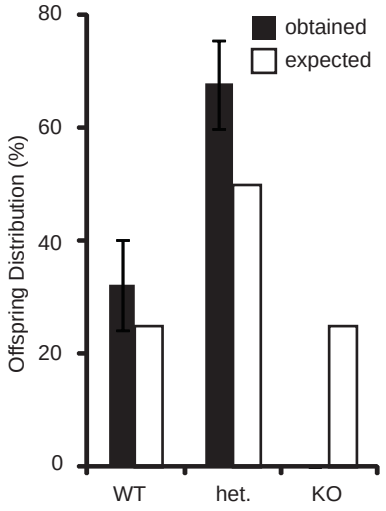

Figure 3.34. Embryonic lethality of the Arl5b knockout was observed. Quantification of offspring from heterozygous mating pairs. The expected offspring distribution is 25% WT, 50% het., 25% KO mice according to the Mendelian laws of inheritance. None of over 121 analyzed littermates was found to be an Arl5b knockout mouse.

embryonic lethality of the homozygous Arl5b KO mice pronounces the importance of the Arl5b protein but another genetic tool was needed to assess the protein function *in vivo*.

3.3.2 Generation of a conditional Arl5b knockout mouse line

A second approach to investigate the role of Arl5b in the living mouse was the generation of a conditional knockout of Arl5b (Arl5b cKO line). This concept has the power to restrict the knockout to a certain tissue or at a certain time point during/after development of the organism. Targeted embryonic stem cells clones, derived from C57Bl/6N mice, became available by this time and were ordered from EUCOMM. In these ES cells the Arl5b gene locus (figure 3.35 A) was replaced by a sequence of a targeting vector by homologous recombination. After the integration the locus consists of all original exons of Arl5b. Additionally loxP sites up- and downstream of exon 3 and a selection cassette between exon 2 and 3, flanked by FRT (flippase recognition target) sites were integrated (figure 3.35 B). On the one hand this cassette mediated resistance against neomycin to select correctly targeted ES clones. On the other hand a splice acceptor site was present in the cassette. This splice acceptor is followed by a LacZ and a stop codon. As a result of the LacZ insertion all Arl5b expressing cells are detectable by X-Gal staining. Additionally the insertion of the constructs generates a “knockout first” situation and a shortened, non functional version of Arl5b is translated in all cells. The allele can be considered as constitutive knockout. To generate an allele with conditional knockout potential the flippase (FLP), a recombinase, was used (figure 3.35 C). This enzyme specifically recognizes the FRT sites and removes the base pair sequence between them by recombination. The loxP sites remain in the genome flanking Exon 3, it is “floxed”. They supposedly do not interfere with splicing of Arl5b and thereby have no effect on Arl5b. Mice that carry the “floxed” Exon 3 ($Arl5b^{WT/FL}$ or $Arl5b^{FL/FL}$) should express Arl5b like wild type mice. In a last step a knockout allele is generated (figure 3.35 D). Cre is a recombinase similar to FLP. Instead of FRT sites it recognizes loxP sites and excises DNA flanked by two loxP sites. Excision of Exon 3 can be triggered tissue specific in progeny of a mating pair of an $Arl5b^{WT/FL}$ mouse and a second mouse which expresses the Cre recombinase under a tissue specific promoter. The result is a tissue specific knockout of Arl5b if the allele was “floxed”. Beyond missing Exon 3 the

mRNA sequence contains a frame shift due to splicing from Exon 2 directly to Exon 4 and additionally runs into a premature stop codon (* in figure 3.35). The resulting mRNA is either degraded due to non-sense mediated decay or a non functional truncated polypeptide is translated.

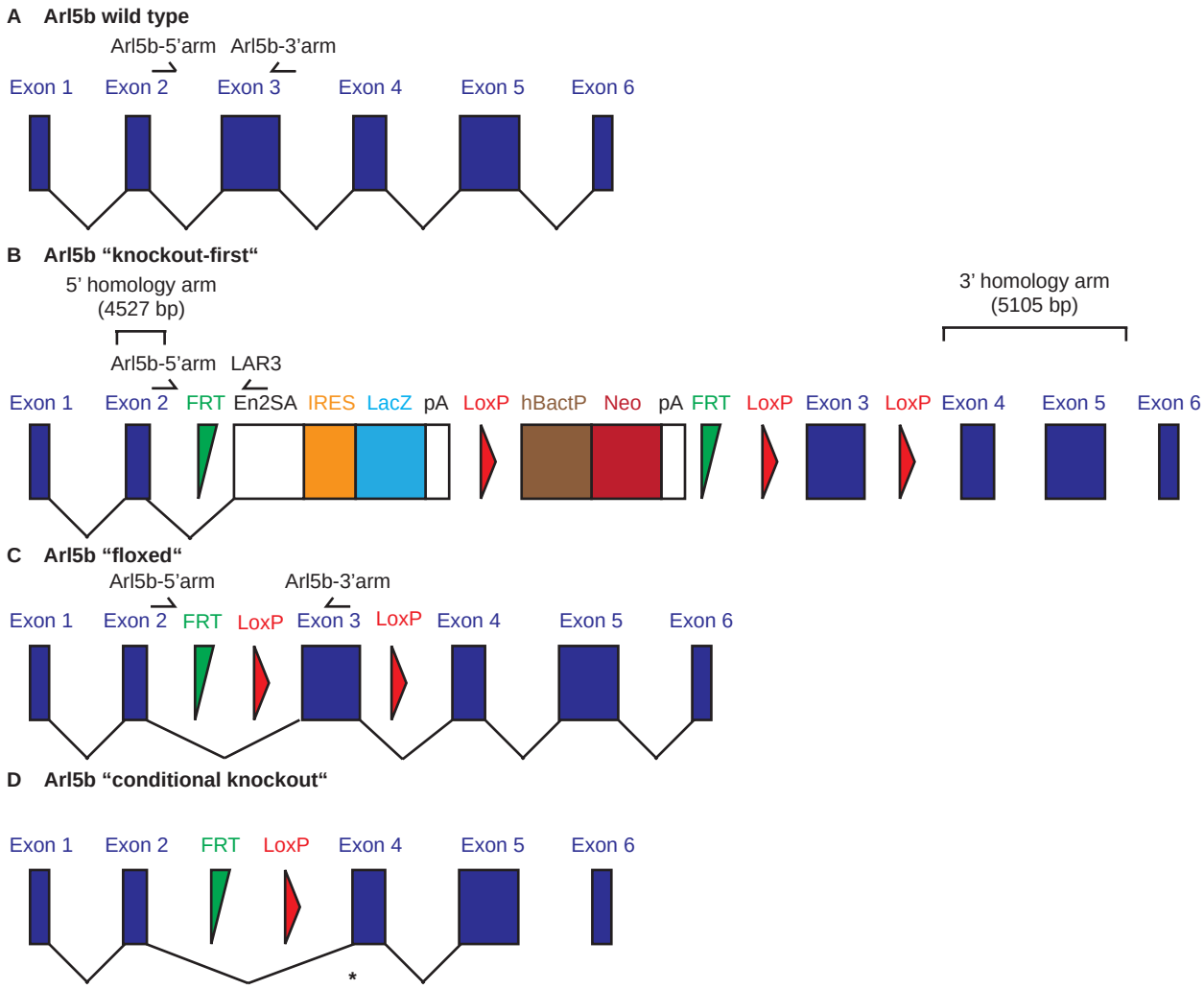

Figure 3.35. Schematic representation of the Arl5b gene locus in the wild type and targeted condition. A, Non modified Arl5b gene locus. **B,** Insertion of the targeting cassette between Exon 2 and Exon 3. The integration of the En2 splice acceptor site (En2SA) generates a nonsense transcript resulting in a constitutive knockout of Arl5b. **C,** By expression of flipase 1 the targeting cassette is excised. The remaining FRT and both loxP sites do not interfere with transcription of Arl5b. **D,** Exon 3 of Arl5b can be excised by the Cre recombinase. As a result of the excision of Exon 3 a frameshift mutation (*) due to alternated splicing a premature stop codon is present in the manipulated ORF. The remaining transcript codes for a non functional polypeptide. Loss of Arl5b gene function depends on the expression pattern of the cross-breed Cre mouse line. Genotyping primers are indicated by halfed arrows. PCR products are: 501 bp for WT, 685 bp for "floxed" and 368 bp for "knockout-first". En2SA = Splice acceptor site of the murine Engrailed2 exon 2; FRT = Flippase recognition target; hBactP = human beta-Actin promoter; IRES = Internal ribosome entry site; LacZ = beta-galactosidase; LoxP = LoxP recognition site; Neo = neomycin resistance gene; pA = SV40 polyadenylation signal

Three manipulated ES clones (HEPD0516_5_C07/D07/F) were thawed and expanded. Blastocyst injections of the ES cells resulted in chimeric progeny (figure 3.36). Chimers were mated with C57Bl/6J mice and litters were genotyped for integration of the targeting cassette by PCR (data not shown). Additionally the integration of the cassette into the Arl5b locus was tested by LacZ staining. The expression pattern of LacZ in the brain of heterozygous litter was comparable to that described for Arl5b (data not shown). To breed homozygous conditional Arl5b knockout mice several mating cycles were required (figure 3.38). A flip deleter mouse line, heterozygous for the recombinase FLP1, was crossed into the Arl5b cKO line to eliminate the targeting cassette, reverting the Arl5b allele from “knockout first” to wild type but “floxed”. FLP1 was expressed under a constitutive promoter, removing the cassette in all cells of the progeny, including the germline cells. Therefore the FLP1 required to be present in future generations to maintain the “floxed” genotype and was crossed out of the Arl5b cKO after successful elimination of the target cassette. Wild type (WT) and “floxed” (FL) alleles of the litter were distinguished by a ~180 bp size shift of the DNA fragment in genotyping PCRs (figure 3.37).

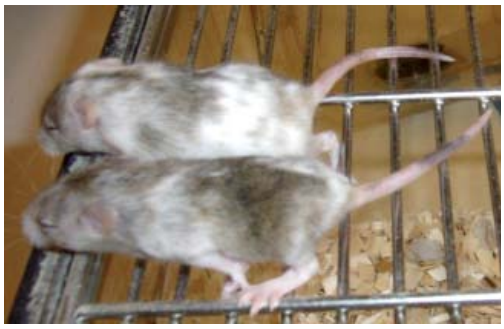

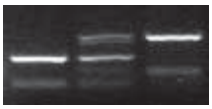

Figure 3.37. Successful excision of the targeting cassette. Representative agarose gel of a genotyping PCR confirming targeting of the Arl5b locus and excision of the knockout cassette. Shown are the PCR products for a wild type (left), a heterozygous littermate (middle) and a floxed mouse (right).

Figure 3.36. Chimeric animals were born after injection of ES clone HEPD0516_5_C07 into blastocysts. Different degrees of ES-cell integration is indicated by the amount of black fur color of the photographed chimeric animals.

To generate a forebrain specific Arl5b knockout a Cre driver line was crossed with Arl5b$^{WT/FL}$ mice. Figure 3.38 outlines the mating scheme for the generation of conditional Arl5b knockout mice (Arl5b$^{EMX\text{-}KO/EMX\text{-}KO}$) by cross-breeding with the EMX1-Cre knock-in mouse line. Cre driven by the EMX1 promoter is not expressed in the germline therefore all progeny of Arl5b$^{EMX\text{-}KO/EMX\text{-}KO}$ do not lack Arl5b gene expression in the case Cre is not inherited.

The EMX1-Cre knock-in mice starts to express the Cre recombinase during the development of the forebrain. Cre is specifically expressed in progenitor cells of pyramidal neurons of the cortex, hippocampus and olfactory bulb (Iwasato et al., 2000). The distinct expression pattern of Cre caused loss of Arl5b in excitatory neurons of the forebrain. Efficacy and specificity of the Cre mediated conditional knockout of Arl5b was verified by *in situ* hybridization experiments using a probe complementary to the sequence of exon 3 of Arl5b. Arl5b$^{EMX\text{-}KO/EMX\text{-}KO}$ mice and WT animals were sacrificed either one hour after onset of kainic acid induced seizures or without injection of kainic acid. In coronal sections of the WT mice the

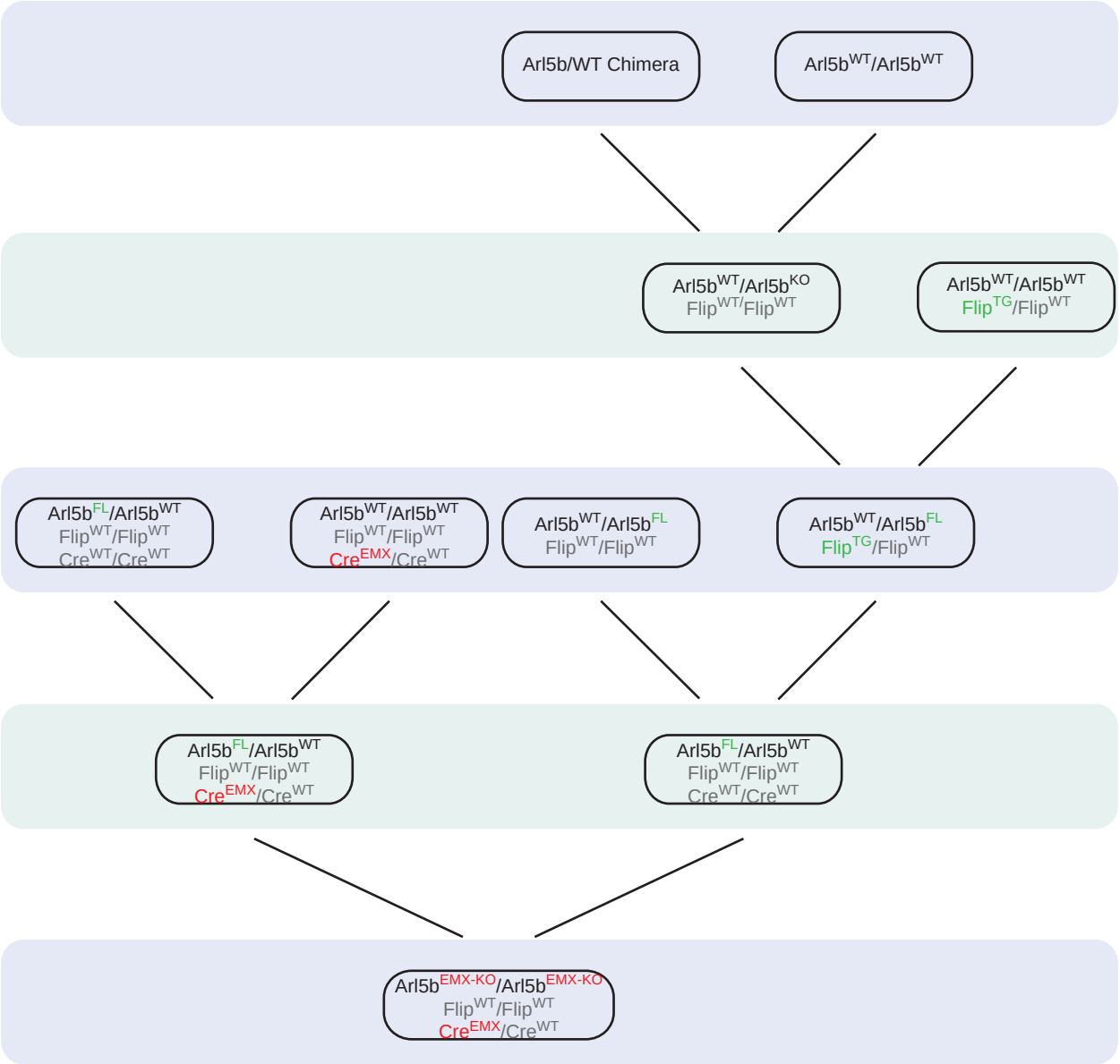

Figure 3.38 Breeding of Arl5b knockout mice. Schematic overview of the different mating pairs necessary to breed homozygous Arl5b$^{EMX-KO/EMX-KO}$ mice beginning with the chimeric animals born after blastocyst injections.

typical upregulation of Arl5b mRNA was observed in the hippocampus. The signal was not detectable in the hippocampus and cortex of Arl5b$^{EMX-KO/EMX-KO}$ mice, though Arl5b mRNA remained in the amygdala. This experiment proved the specific deletion of the floxed Exon by EMX1 promoter driven Cre and consequently loss of functional Arl5b mRNA (figure 3.39).

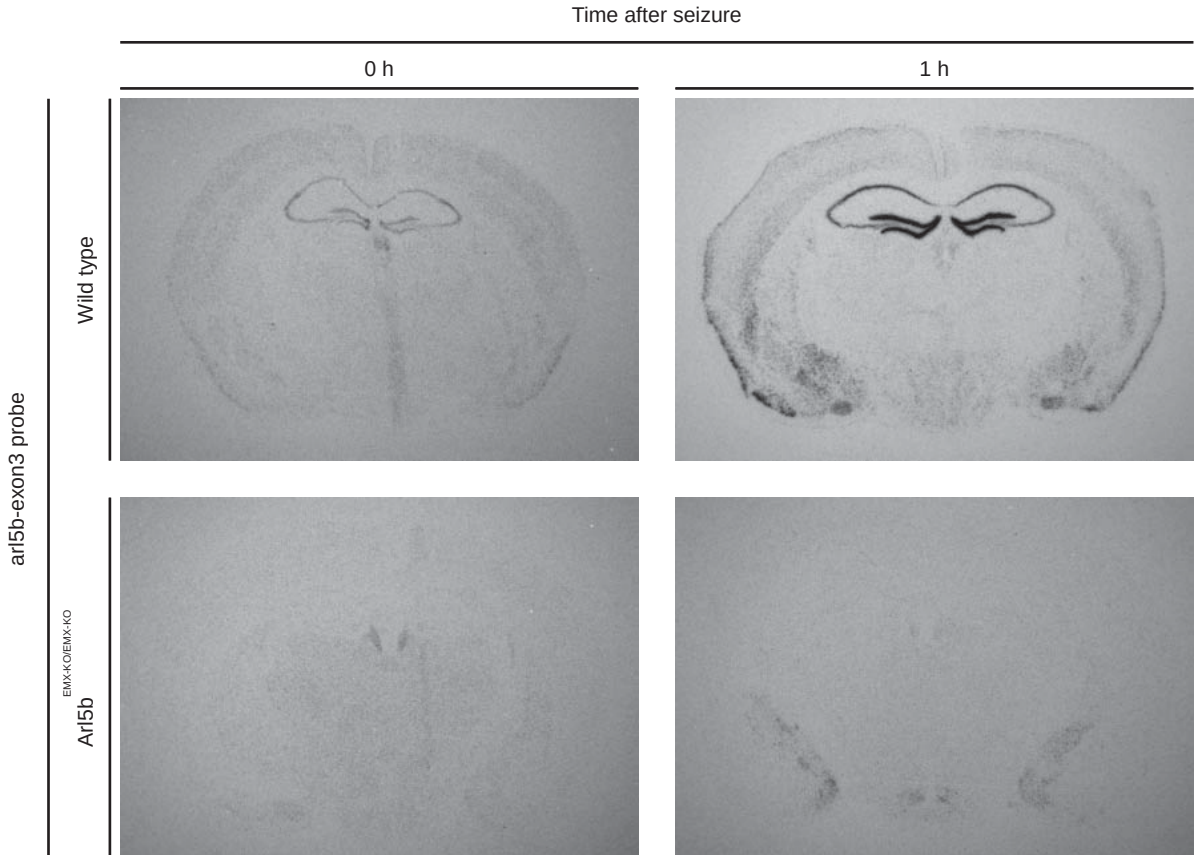

Figure 3.39. Successful knockout of Arl5b in the forebrain of mice. The conditional knockout of Arl5b in pyramidal neurons was shown by *in situ* hybridization. Depicted are autoradiograms of coronal sections of mouse brains 1 h after kainic acid induced seizures. Control mice were not injected (0 h). Radioactively labeled antisense RNA probes specific for Exon 3 were used to mark arl5b mRNA. Arl5b transcript levels rise in WT mice 1 h after seizure, a lack of staining in the Arl5b$^{EMX\text{-}KO/EMX\text{-}KO}$ mice confirms efficient excision of Arl5b Exon3.

3.3.3 Conditional knockout of Arl5b in principal neurons has no effect on the gross morphology of the hippocampus and the cortex

After the successful verification of the efficient forebrain specific knockout of Arl5b homozygous Arl5b$^{EMX\text{-}KO/EMX\text{-}KO}$ and WT mice were bred for analysis of the loss of Arl5b in excitatory neurons in the forebrain during development. After 13 weeks mice were sacrificed and decapitated. The brain was removed and frozen by submersion in liquid nitrogen. Nissl staining was used to visualize brain structures after coronal cryosectioning. No obvious differences were detected by comparing the morphology of the forebrain of Arl5b$^{EMX\text{-}KO/EMX\text{-}KO}$ and WT mice (figure 3.40 left). The inspection of the Nissl stained hippocampi of both mice in a higher magnification did not reveal any visible morphological deficiencies based on the loss of Arl5b (figure 3.40 right).

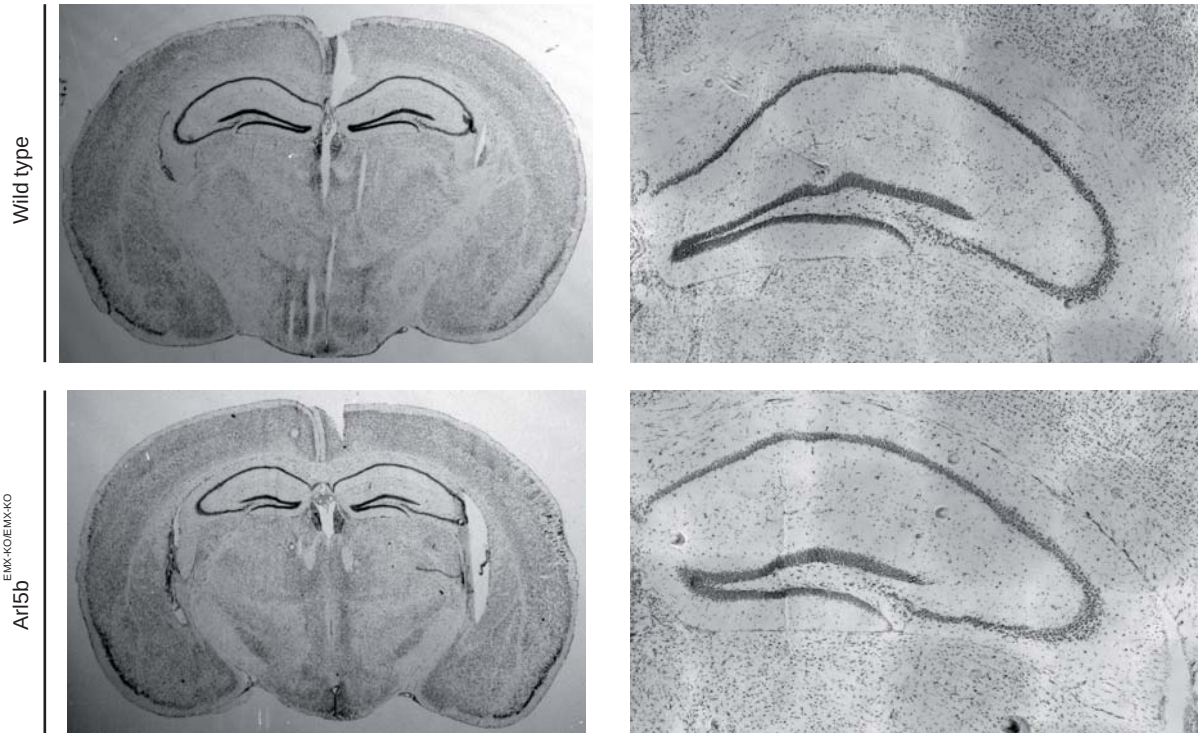

Figure 3.40. Loss of Arl5b does not impair the development of the forebrain in mice. Representative images of Nissl stained coronal sections (left) from 13 weeks old WT and Arl5b$^{EMX-KO/EMX-KO}$ mice. The hippocampi of both mice were imaged in a higher resolution (right). The morphology of the forebrain and hippocampus of Arl5b$^{EMX-KO/EMX-KO}$ mice was not changed compared to WT mice.

3.3.4 Arl5a mRNA levels are unaltered in the brain upon Arl5b loss in mice

To further investigate the possibility that Arl5a can compensate for Arl5b deficiency the regulation of the Arl5a mRNA in WT and Arl5b$^{EMX-KO/EMX-KO}$ mice was compared. Seizures were induced in mice of both genotypes, WT and Arl5b$^{EMX-KO/EMX-KO}$, as described in 3.3.2. In situ hybridization experiments with a radioactively labeled antisense RNA probe specific for the ORF of Arl5a were performed. The transcription levels of Arl5a one hour after or without seizure induction in wild type and Arl5b$^{EMX-KO/EMX-KO}$ background were assessed. The mRNA of Arl5a was equally expressed in untreated animals of both genotypes and was not up- or downregulated in wild type or Arl5b knock out mice 1h after the onset of seizures (figure 3.41).

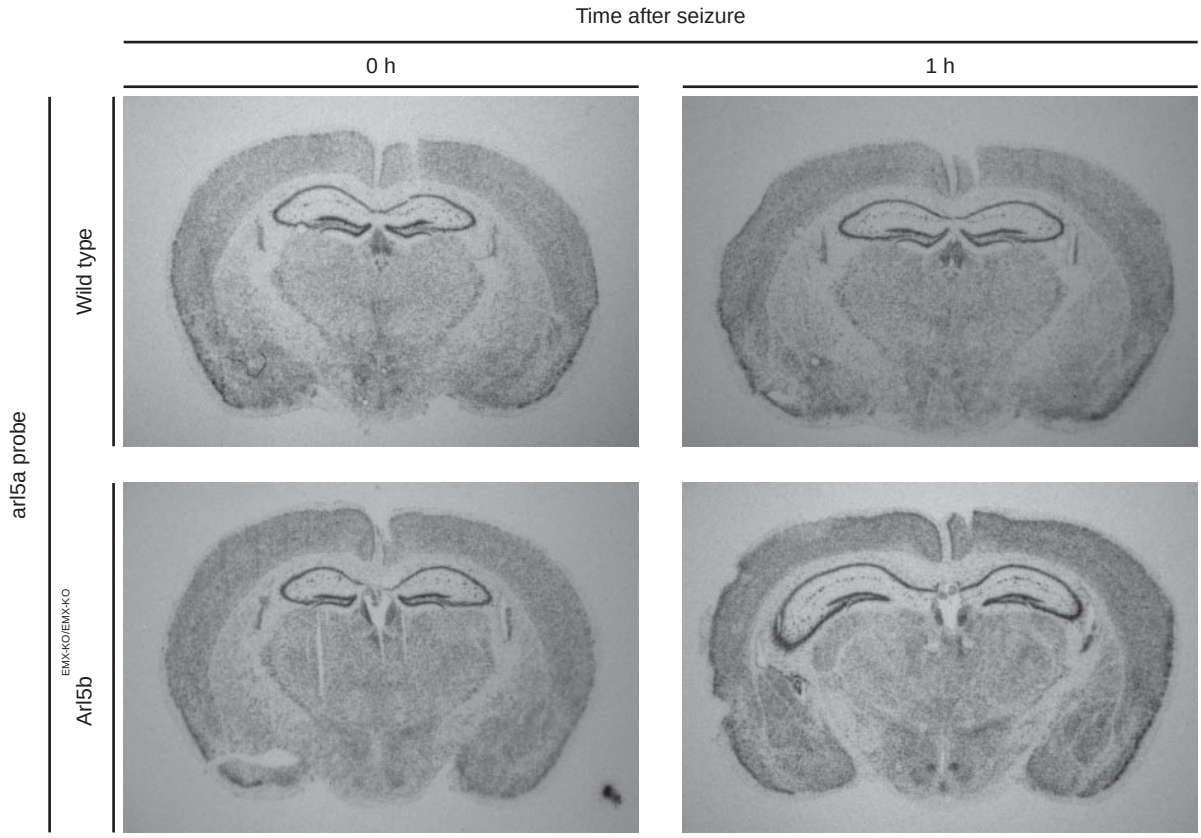

Figure 3.41. Knockout of Arl5b does not change Arl5a transcript levels. Depicted are autoradiograms of coronal sections of mice brains 1 h after kainic acid induced seizures. Control mice were not injected (0 h). An arl5a specific RNA probes was used for radioactive *in situ* hybridization of either WT or Arl5b$^{EMX\text{-}KO/EMX\text{-}KO}$ mice. Neither kainic acid induced seizures nor loss of Arl5b in excitatory neurons in the forebrain affected mRNA levels of Arl5a.

3.3.5 Phosphorylation of ribosomal protein S6 is impaired in the hippocampus of Arl5b knockout mice

The growth factor mediated activation of the PI3-K/AKT/mTOR signaling cascade stimulates translation. This synthesis of new protein is essential for some forms of plasticity. In response to BDNF the translation of CamKIIα, LIML1, NMDA receptor subunit NR1 and PSD95 is upregulated in a PI3-K/AKT/mTOR dependent manner (Schratt et al., 2004; Lee et al., 2005; Akama and McEwen, 2003). The recruitment of Arl5b by BDNF to late endosomes at which it co-localizes with TrkB combined with the finding that dominant negative Arl5b impairs long-range transport of late endosomes led to the hypothesis that Arl5b could mediate signaling downstream of BDNF. One of the targets of BDNF induced PI3-K/AKT/mTOR signaling is the ribosomal protein S6. Phosphorylation of ribosomal protein activates the translation of the above mentioned proteins. Investigation of a putative role of Arl5b in this signaling cascade with ribosomal protein S6 as one of the effector proteins was made possible by the establishment of the Arl5b$^{EMX\text{-}KO/EMX\text{-}KO}$ mouse line. Kainic acid injection induced seizures were used as an activity stimulus. WT and Arl5b$^{EMX\text{-}KO/EMX\text{-}KO}$ mice were sacrificed one hour after beginning of seizures. Cell lysates were prepared of the hippocampi of the mice. 20 µg samples were utilized in western blot analysis. Phosphorylation of the ribosomal protein S6 was successfully increased after the strong activity inducing stimulus, but the activation of ri-

bosomal protein S6 in the hippocampus of Arl5b$^{EMX\text{-}KO/EMX\text{-}KO}$ mice was significantly weaker compared to wild type littermates (Student's t test, ** $p < 0.01$, $n = 4$). The total amount of ribosomal S6 protein was reduced by approximately 10 % in the Arl5b$^{EMX\text{-}KO/EMX\text{-}KO}$ mice. This reduction was not significant (Student's t test: $p = 0.64$, $n = 4$) (figure 3.42). This result provided a hint for a possible impairment of synaptic plasticity in the hippocampus of Arl5b$^{EMX\text{-}KO/EMX\text{-}KO}$ mice.

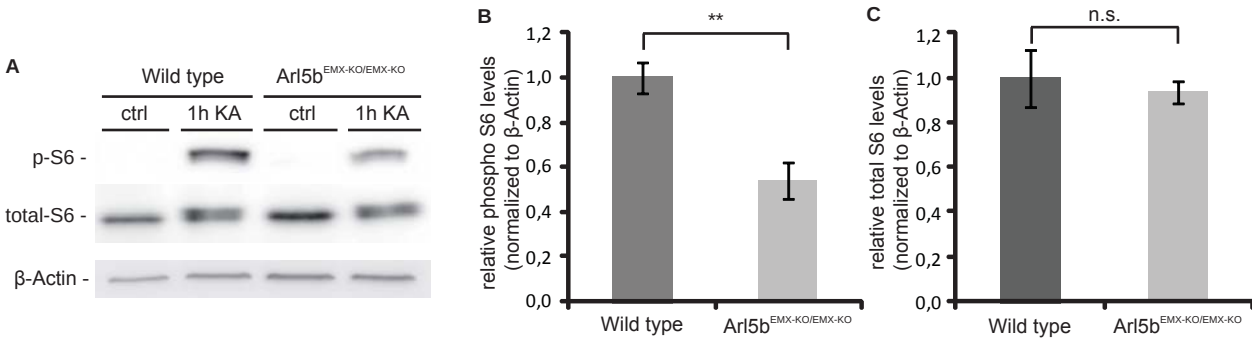

Figure 3.42. Phosphorylation of ribosomal protein S6 in the hippocampus is impaired in Arl5b knockout mice. A, Seizures were induced by injection of kainic acid in WT and Arl5b$^{EMX\text{-}KO/EMX\text{-}KO}$ mice. One hour after seizure (1 h KA) Animals were sacrificed and hippocampal lysate was prepared. Control mice were not injected. 20 µg per sample were used for western blot analysis with antibodies against phospho- and total-S6 and beta-Actin. **B,** Quantification of phospho S6 levels in WT and Arl5b$^{EMX\text{-}KO/EMX\text{-}KO}$ hippocampi 1 h after seizure normalized to beta-Actin. Phosphorylation of S6 is strongly reduced in Arl5b$^{EMX\text{-}KO/EMX\text{-}KO}$ hippocampi compared to WT mice. Statistical significance was determined by Student's t test, ** $p < 0.01$, $n = 4$. **C,** Ratio of total S6 levels in WT and Arl5b$^{EMX\text{-}KO/EMX\text{-}KO}$ hippocampi 1 h after seizure normalized to beta-Actin. Changes in total levels of S6 in Arl5b$^{EMX\text{-}KO/EMX\text{-}KO}$ hippocampi compared to WT situation are not significant, Student's t test: $p = 0.64$, $n = 4$.

3.3.6 Behavioral studies with Arl5b-deficient mice

A series of behavioral experiments was performed to investigate if the loss of Arl5b results in impairment in the formation or consolidation of long term memory. Each test was performed with four groups of mice. The Arl5b$^{EMX\text{-}KO/EMX\text{-}KO}$ mice (KO) were compared to three different groups of control littermates. Besides Arl5b$^{WT/WT}$ mice (WT) two other groups of wild type mice were tested. To exclude changes in behavior due to exogenous expression of the Cre recombinase one group of Arl5b$^{WT/WT}$; Cre$^{EMX/WT}$ mice (WT+) were included in the studies. The third wild type group, Arl5b$^{FL/FL}$ (FL), carried the floxed Exon 3 of Arl5b to exclude the possibility that the loxP sites in the Arl5b locus bear an influence on behavior of the mice. For all tests mice were between three and four month old. If not stated otherwise eight male mice were observed per group during all behavioral tasks.

Increased anxiety or impaired exploratory behavior of knockout mice can lead to biased results in experiments which assess the ability to form long-lasting memories. In order to avoid such biases the Arl5-deficient mice were examined first in the open field and elevated plus maze test. The open field test is a suitable behavioral task to test anxiety levels, locomotor activity and exploration of rodent animals (Denenberg, 1969). Mice were placed in an arena with walls to prevent escape. Over a period of 10 min-

utes the activity was automatically assessed. Mice of all groups spent a comparable time in the center of the arena (figure 3.43 A) suggesting no change in anxiety levels. In regard to exploration activity the mobility between mice of the four groups of mice was similar. The total distance the mice traveled during the time in the arena (figure 3.43 B) and their average velocity is not changed among the groups (figure 3.43 C).

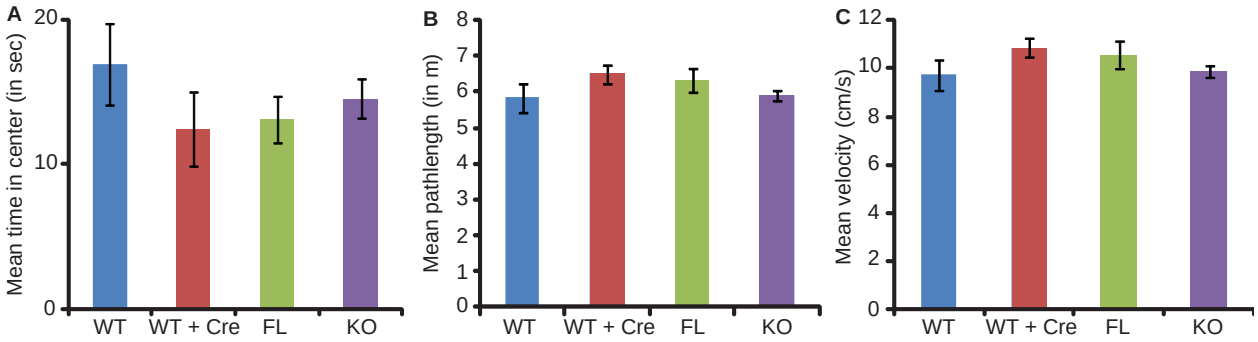

Figure 3.43. Forebrain specific knockout of Arl5b does not influence anxiety levels and exploratory behavior of mice. Mice were placed in a 50 x 50 x 50 cm measuring white box. They were allowed to explore for 10 minutes. Their behavior was recorded by a video camera and tracking was evaluated automated by Ethovision XT (Noldus Information Technology). **A,** During the open field test the duration the mice spent in the center square was measured. The total traveled distance **(B)** and the velocity **(C)** were evaluated. The mice of different genotypes did not perform differently.

The second task to test the anxiety of the mice was the elevated plus maze. For this task mice are placed on a plus-shaped apparatus which has two open and two enclosed arms which are elevated from the floor. The time the mice spend in the open arms of the apparatus is used as an indicator for the anxiety of the mice (Pellow et al., 1985). A camera was used to track the mice automated. Figure 3.44 A shows an exemplary trace (red) of one of the tested mice. Mobility of the mice of all four groups was similar. The changes of the distance traveled on average was observed (figure 3.44 B). The time the mice spent in the open arms of the elevated plus maze varied from group to group (Figure 3.44 C). However the KO mice spent approximately the same percentage of time on the open arms compared to WT and FL mice. Together the result of the open field test and the elevated plus maze conclude that the forebrain specific knockout of Arl5b has no effect on the exploratory behavior and anxiety of the mice.

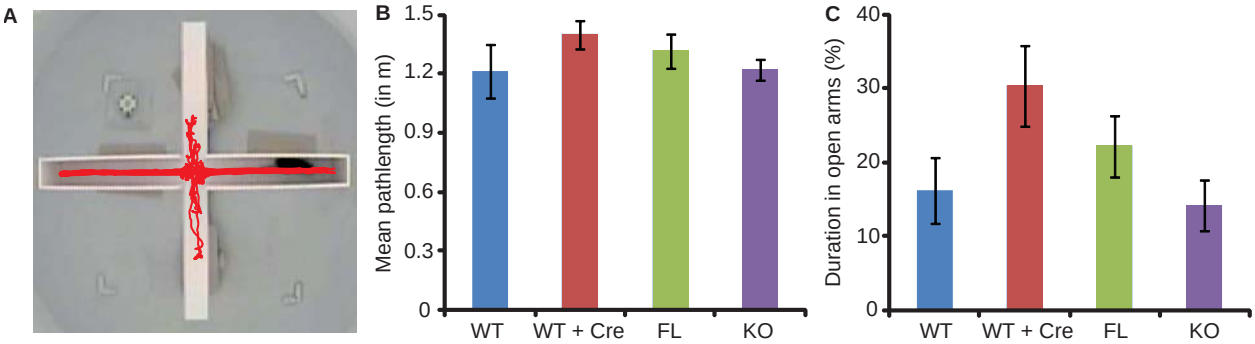

Figure 3.44. Evaluation of anxiety of Arl5b$^{EMX\text{-}KO/EMX\text{-}KO}$ mice in the elevated plus maze task. The animals were placed in the middle of the elevated plus maze and were tracked with a camera for 5 minutes. **A,** Representative video tracking image recorded during the elevated plus maze test. During the elevated plus maze test the total traveled distance **(B)** and the time spent on the open arms **(C)** were measured.

F

ear Conditioning, a classical Pavlovian conditioning, is a behavioral test in which two different kinds of memories can be tested in one experimental setup. Animals were tested for implicit (auditory cue) and explicit (context) memory. In this experiment an innocuous stimulus (conditioned stimulus, CS) is presented with a noxious stimulus (unconditioned stimulus, US), a brief electrical shock. In this case CS was presented three times with the footshock. After successful fear conditioning mice react to the CS alone with a state of fear, indicated by freezing (Orsini and Maren, 2012). Previous studies showed that the contextual CS relies on both, the hippocampus and the amygdala, whereas the auditory-cued CS depends on the amygdala (LeDoux, 2000; Maren, 2001; Maren and Quirk, 2004). Figure 3.45 A depicts the design of the fear conditioning setup and procedure.

The freezing reaction was detected automatically. Prior to conditioning none of the mice showed freezing behavior. The mean of the conditional response increased for all groups of mice during the conditioning experiment (figure 3.45 B). 24 hours later the mice were subjected again to the CS. All groups reacted with freezing to the contextual environment. The knockout group showed reduced freezing behavior (34.8% ± 8%) compared to the wild type groups (WT: 45.1% ± 6.9%; WT+Cre: 51.4% ± 4.8 %; FL: 45.3 ± 4.3 %). However, this reduction was not significant ($p > 0.05$, one-way ANOVA; figure 3.45 C). No differences were observed in the cued fear testing. The animals were allowed to explore another cage for 120 sec. In this unfamiliar environment they did not freeze. This changed during administration of the tone for 60 seconds (cued). All groups reacted with freezing behavior (figure 3.45 D).

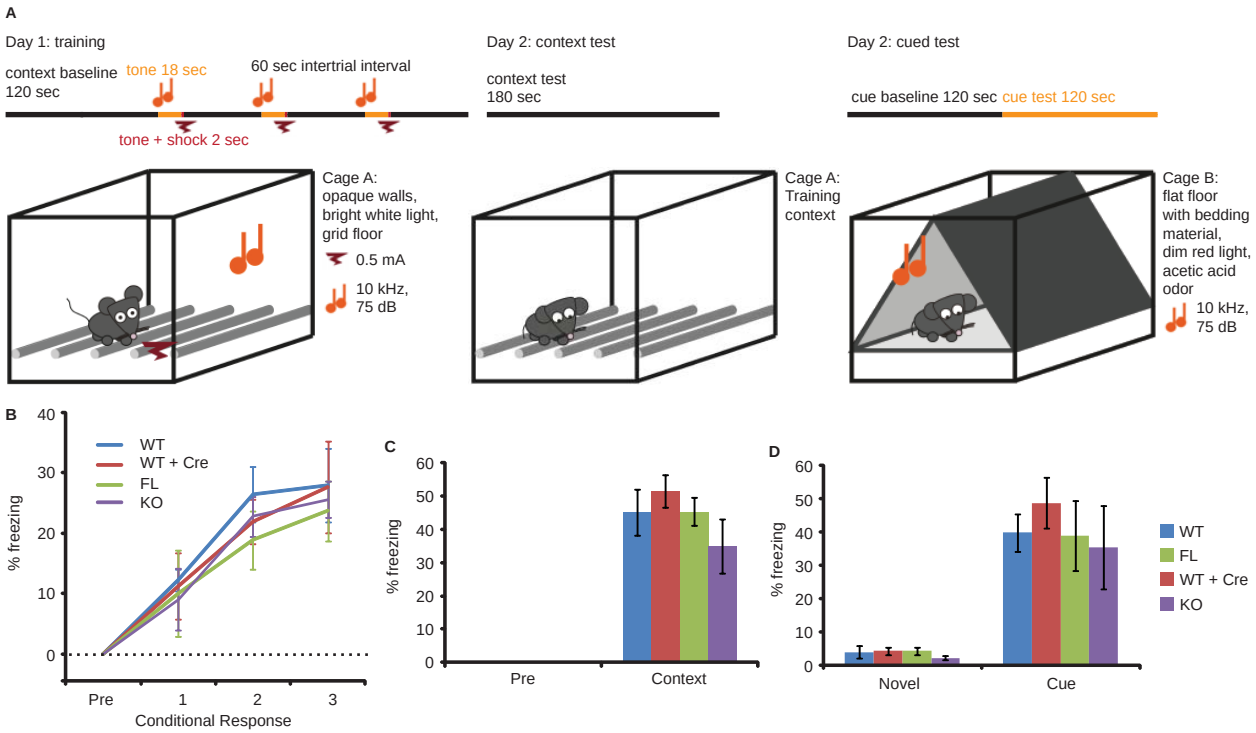

Figure 3.45. Arl5b deficient mice show a tendency for reduced fear in contextual fear conditioning. A, Schematic representation of contextual and cued fear conditioning task (adapted from Galliano et al., 2013). On the training day mice were placed in a bright square chamber with opaque walls. The floor was gridded and an Ethanol odor was present (Cage A). After a habituation time of 120 sec (pre) a tone was played for 20 sec and the last 2 sec were paired with a foot shock. The paired tone/shock presentation was repeated for three times with a 60 sec intertrial interval. On day 2 the mice were returned to Cage A for 180 sec (context test). Later the mice were placed in a dark, triangular shaped chamber with a flat floor and bedding material and acetic acid smell (Cage B). They were left free to explore for 120 sec (novel) and then exposed to a 120 sec tone (cue test). The time the animals spent freezing was assessed automated and takes as a measure of fear. **B,** Average freezing response to each CS during the acquisition phase. **C,** Time spent freezing for each mice

As the different wild type groups did not show differences during previous behavioral test we examined the spatial learning capability of Arl5b$^{EMX\text{-}KO/EMX\text{-}KO}$ mice by working with KO and FL mice. While fear conditioning is a test to assess the intactness of associative memory, the Morris water maze is used to examine another learning paradigm. By this experiment I tested the role Arl5b in the hippocampal-dependent formation of spatial memories (Morris, 1984). All mice were trained to swim in a water tank filled with opaque water. The mice were trained to find a hidden platform (escape latency) for 6 days. External visual cues were allowed the mice to orient. During this acquisition phase the escape latency was determined which reduced over the time of the acquisition phase for both groups (figure 3.46 A). 24 hours after the last training day a probe trial, without the hidden platform in the water tank, was performed. The frequency with which the wild type and knockout mice crossed the area of the platform during the probe trial was not significantly different from each other ($p > 0.05$, one-way ANOVA; Figure 3.46 B). Similarly the latency until the mice crossed the platform area for the first time during the probe trial was not significantly different between wild-type and knockout mice ($p > 0.05$, one-way ANOVA; Figure 3.46 C). The time that the wild type spent in the targeted quadrant during the probe trial was significantly increased

above chance level ($p < 0.05$, one sample Student's t-Test, hypothesized mean = 25 %), indicating their spatial learning ability to locate the position of the hidden platform. The knockout mice spent more time in the target quadrant compared to the control quadrants. Though, they did not spent not significantly more time in the quadrant compared to chance levels ($p > 0.05$, one sample Student's t-Test, hypothesized mean = 25 %).

The KO mice performed worse compared to wild type littermates in both tasks, the contextual fear conditioning and the Morris water maze. However, the KO animals did not freeze significantly less in fear conditioning. In the Morris water maze test the reduction of the time spent in the target quadrant was also not significantly reduced when compared to the wild type group ($p > 0.05$, one-way ANOVA; Figure 3.46 D). Together the results indicate at least tendency for an impaired long term memory formation induced by loss of Arl5b in excitatory pyramidal neurons.

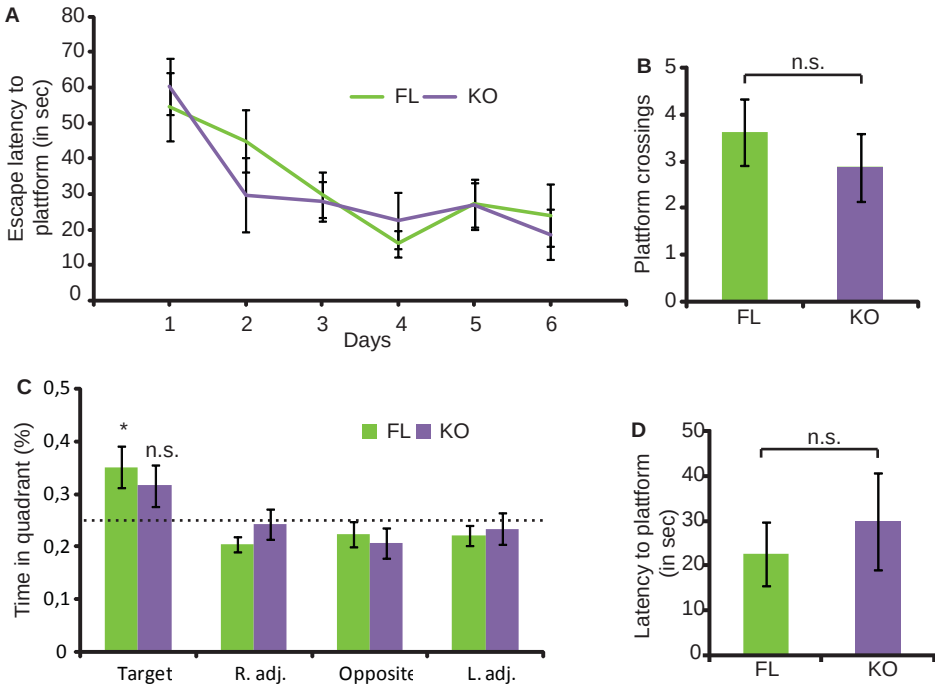

Figure 3.46. Spatial learning abilities assessed in the Morris water maze. A, Escape latency between Arl5b$^{EMX\text{-}KO/EMX\text{-}KO}$ and Arl5b$^{FL/FL}$ mice was similar during training. All mice were trained for six days 24 h after the last training the mice were placed in the water tank for 90 sec without a platform. The number of times the mice crossed the platform area **(B)** and the latency until the animals swam into the platform area **(C)** was not significantly different between KO and FL mice ($p > 0.05$, one-way ANOVA). **D,** Both groups showed a preference for the target quadrant. They spent more time in this quadrant compared to the control quadrants. The KO animals spent less time in the target quadrant compared to WT animals. The difference between both groups was not significant ($p > 0.05$, one-way ANOVA). However, the WT mice spent significantly more time in the target quadrant compared to chance levels (p-value < 0.05, one sample Student's t-Test, hypothesized mean = 25 %) while the KO did not perform above chance level (p-value = 0.137 one sample Student's t-Test, hypothesized mean = 25 %).

Finally, to study hippocampal function in a non aversive paradigm – in contrast to the fear conditioning and Morris water maze tests - the novel object recognition task was performed. This test takes advantage of the fact that mice have a tendency to approach and explore novelty. Rodents spend more time exploring a novel object than a familiar object. Discrimination of objects requires intact memory of the previously experienced object (Bevins and Besheer, 2006).

All four previously described groups of mice were subjected to the novel object recognition task, which requires BDNF (Heldt et al., 2007). As in previous tasks the three wild type control groups (Arl5b$^{WT/WT}$, Arl5b$^{WT/WT}$; Cre$^{EMX/WT}$ and Alrl5b$^{FL/FL}$) showed no differences when compared with each other and were pooled in one wild type group. The mice were allowed to explore two identical objects during the sample phase for 10 minutes. 24 h later one of the familiar objects was replaced by a novel object and the exploration behavior of the mice during the choice phase was evaluated for 3 minutes. We counter-balanced the familiar and novel objects. The mice were tracked with the Ethovision XT software. Exploration was defined as the time the nose of a mouse was at most 2.5 cm away from an object. Rearing and climbing was excluded from active exploration time. The total exploration times of both groups, wild type and knockout mice, on both days did not differ (figure 3.47 A). On the sample day the wild type and knockout groups did not show a preference for one of the identical objects (figure 3.47 B). During the choice phase the wild type mice spent significantly more time exploring the novel object ($p < 0.001$, paired two-tailed Student's t-Test). This result indicates the recognition of the familiar object by the mice. In contrast the knockout mice failed to explore the novel object significantly longer compared to the familiar object ($p > 0.05$, paired two-tailed Student's t-Test; Figure 3.47 C), indicating impaired recognition.

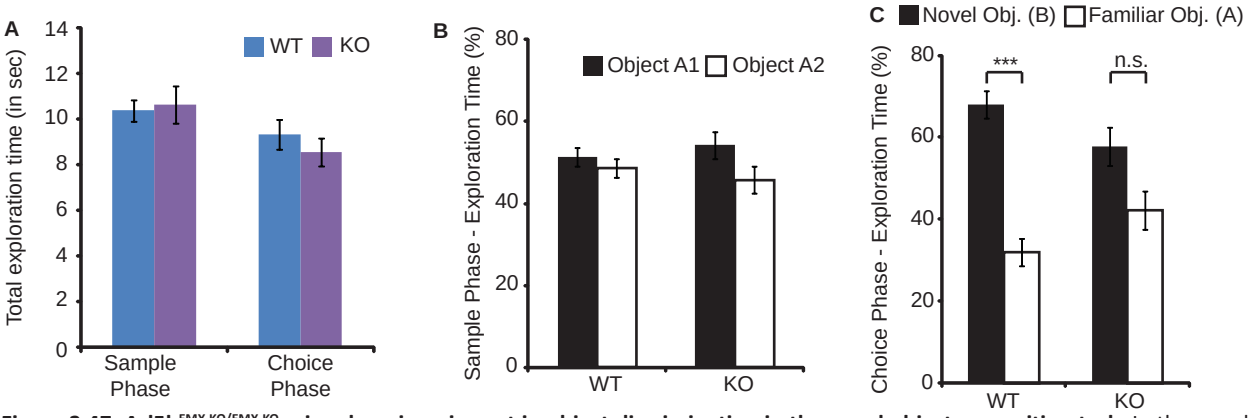

Figure 3.47. Arl5b$^{EMX-KO/EMX-KO}$ mice show impairment in object discrimination in the novel object recognition task. In the novel object recognition task mice were allowed to explore two identical objects (Object A) for 10 minutes during a sample phase. On the next day, 24 h later, they were placed in the same arena with one of the familiar objects replaced by a novel object (Object B) and were left alone to explore again (choice phase). The animals were tracked with a camera and the data was analyzed automated with Ethovision XT (Noldus information technology). Both groups explored the objects for the same time in total on both days **(A)**. **B,** The animals did not show a preference for one of the identical objects. **C,** During the Choice phase wild type but not knockout mice preferred to explore the novel object (WT: $p < 0.001$, $n = 20$; KO: $p = 0.14$, $n = 8$, paired two-tailed Student's t-Tests).

Taken together three tasks, fear conditioning, Morris water maze and novel object recognition, were used to assess the ability of the Arl5b$^{EMX-KO/EMX-KO}$ mice to form long term memories. At this stage there is no clear answer to this question. Even though the KO mice performed worse than their wild type littermates in all three tests, the observed effects were not strong. Additional investigations may verify the observed tendency of an impairment of the long-term memory formation induced by the knockout of Arl5b in excitatory neurons of the forebrain.

4. Discussion

Subject of this thesis was the small GTPase Arl5b. Initially, the knowledge about this protein was very limited. The cloning of its cDNA and a northern blot expression analysis was published in 2003 (Sebald et al. 2003). The protein was classified as a member of the Arf-like family due to its high homology to Arf proteins (Sebald et al. 2003) and unpublished results suggested a subcellular localization at the Golgi apparatus in mammalian cells (Hofmann and Munro, unpublished). Additionally, it was identified as an activity-regulated gene in our laboratory (Hermey et al., 2013). Due to its expression kinetics, sharp and fast up- and downregulation in the hippocampus after induction of neuronal activity, and a presumable role in signaling, we hypothesized that Arl5b mediates signaling in neuronal plasticity related events. The thesis followed three strategies to investigate this hypothesis. One approach focused on the examination of the cellular function of Arl5b. The identification of interaction partners of Arl5b was the second strategy. And the generation of an Arl5b knockout mouse was the third part of the thesis. The results of all three strategies contributed to gain insight the functional role of Arl5b. In the discussion I will critically summarize my results in the different areas, combine them with each other and try to put them into the larger context of synaptic plasticity.

4.1 Characterization of Arl5b as canonical Arf-like protein

To unravel the role of Arl5b in neurons I started with an analysis of the subcellular localization of Arl5b. Overexpression experiments in HeLa cells and dissociated hippocampal neurons revealed that Arl5b accumulates in the Golgi apparatus without being restricted to the cis-Golgi cisterna or the trans-Golgi network. A detailed analysis revealed the mechanism by which Arl5b is attached to the membrane and the mechanism by which this association is regulated.

In two experiments I proved that N-terminal myristoylation of Arl5b is essential for its anchorage at membranes. Membrane association by N-terminal modification is common for Arl proteins. For all Arf proteins the membrane anchorage is mediated by a myristol group covalently attached to a glycine at the N-terminus. For Arf-like proteins however, more than one mechanism is known to mediate membrane association. Besides myristoylation a second posttranslational modification, acteylation, is known. For example Arl8a and Arl8b are modified by acetylation (Hofmann and Munro, 2006).

The N-terminal sequence “MGLIFAK” of Arl5b was predicted to act as a myristoylation motif. N-terminal myristoylation is an irreversible protein modification that occurs co-translationally following enzymatic removal of the initiator methionine (Farazi et al. 2001). The following Glycine is required for myr-

istoylation of a protein since myristic acid is exclusively added to a Glycine in this position of a protein by post-translational modification (Farazi et al., 2001). I demonstrated that the mutagenesis of this Glycine at the first position of the amino acid sequence prevents incorporation of myristic acid in newly synthesized Arl5b. A second experiment supported this finding. Overexpressed in neurons and HeLa cells the mutated Arl5b failed to accumulate at the Golgi apparatus, to which the non mutated Arl5b was recruited in all cells that were analyzed. These experiments proved for the first time the predicted myristoylation of Arl5b.

The mechanism which allows Arl5b to shuttle between cytoplasm and membranes was elucidated in another set of experiments. It is established that Arf proteins remain inactive while they are in a GDP bound state and are activated after exchange of this GDP by GTP. In consequence a conformational shift exposes the myristoylated amphipathic helix mediating the attachment to membranes. I generated two additional mutants of Arl5b. One mutant was predicted to be restricted in a GTP-bound state (referred as constitutive active mutant) while the second mutant was predicted to be locked in a GDP-bound state (referred as dominant negative mutant). In HeLa cells as well as in dissociated hippocampal cells the constitutive active mutant of Arl5b accumulated to the Golgi apparatus in a comparable amount to non mutated Arl5b. However instead of being enriched in the Golgi apparatus the dominant negative variant of Arl5b was diffusely distributed in the cytoplasm of both cell types comparable to the myristoylation deficient mutant. This strongly suggests a GTP-dependent association of Arl5b to the membrane of the Golgi apparatus proven before for other proteins of the Arf family. During the course of this thesis another research group also examined this result in HeLa cells (Houghton et al., 2012). Taken together, this in depth analysis provided evidence that Arl5b associates to membranes like canonical Arf proteins.

Unfortunately, I was not able to assess endogenous Arl5b. My studies rely on the results of overexpressed tagged Arl5b, because all tested commercially available antibodies against Arl5b failed to identify Arl5b. It was not possible to detect overexpressed Arl5b with any of these antibodies neither by Western blot analysis nor by immunocytochemistry (ICC). In addition, polyclonal antibodies against Arl5b were produced during this thesis. One antibody detected exogenous Arl5b. Due to strong unspecific binding to additional proteins the antibody was not usable in assays such as Immunohistochemistry or ICC.

Therefore, all localization studies were obtained by heterologous expression of Arl5b. There are limitations in tagging Arl5b, because of its N-terminal myristoylation. Thus, results regarding the localization of Arl5b could only be confirmed by using different C-terminal tags. However, the endogenous subcellular localization of Arl5b may still differ from the localization observed by tagging and overexpressing the protein.

4.2 Arl5b regulates transport of late endosomes

I demonstrated the recruitment of Arl5b to vesicular like structures in HeLa cells and dissociated hippocampal neurons. The recruitment of Arl5b to such endosomes is mediated by the same mechanisms as its recruitment to the Golgi apparatus. Both, the dominant negative and the myristoylation-deficient mutants of Arl5b do not attach to vesicular structures. Arl5b associates to vesicles in the soma, axons and dendrites in developing and mature dissociated hippocampal neurons.

Endocytosis of growth factors is of major importance for many processes in all kind of cells and influences signal transduction (Hu et al., 2013). Receptors of growth factors are targeted to their various destinations by vesicular trafficking. Highly regulated and specialized machineries control the trafficking and sorting of such vesicles. Together with the transported cargo these proteins shape the identity of vesicles. Arf proteins are known to be a part of this machinery. They regulate vesicle identity and trafficking by recruitment of highly diverse factors effector proteins. This includes the recruitment of subunits of coat complexes, lipid modifying enzymes or regulators of other G-proteins (Donaldson and Jackson, 2011). For example Arf1 recruits the coat proteins coatomer and clathrin adaptor protein1 (Souza-Schorey and Chavier, 2006) and Arl8 couples lysosomes to kinesin-1, required for their bidirectional movement along microtubules (Rosa-Ferreira and Munro, 2011).

After detection of Arl5b positive vesicular structures I aimed at classifying these endosomes to draw conclusions to the cellular function of Arl5b. Members of the Rab family of G proteins are common regulators of vesicular trafficking. For many members of this huge group it is known to which kind of vesicles they localize. I used this fact to determine the identity of Arl5b positive vesicles. Together with colleagues I established a library of proteins with known organelle localization to identify the location of a protein of interest within a set of specific vesicles. Spinning disc live microscopy experiments revealed long-range retrograde transport of endosomes enriched with Arl5b in axons of dissociated hippocampal neurons. Previous reports provided evidence that late endosomes which undergo this kind of long-range transport are Rab7 enriched. The hypothesis that Arl5b is located to this kind of late endosomes was proven by co-localization and co-trafficking of Arl5b together with Rab7. This result was supported by further experiments which showed that Arl5b does not co-localize with markers for other endosomes, such as the early endosome marker Rab5.

Identification of the specific kind of Arl5b positive vesicles in this detailed analysis allowed me to assess a functional role of Arl5b in vesicle trafficking. Overexpression of dominant negative Rab7 negatively influences retrograde transport of late endosomes involved in BDNF signaling (Deinhardt et al., 2006). There is evidence that Arl and Rab proteins can act in concert in order to recruit effectors (Burguete et

al., 2008). Based on the hypothesis that Arl5b and Rab7 may regulate trafficking of late endosomes together I assessed the influence of dominant negative Arl5b on long-range transport of late endosomes in dissociated hippocampal neurons. The fast retrograde transport of Rab7 positive late endosomes was impaired in presence of dominant negative Arl5b. This shows for the first time a functional role of Arl5b in retrograde transport in neurons. However, it is unclear how Arl5b actually blocks the transport of Rab7 positive endosomes. The identification of effector proteins of Arl5b and their role in the fast transport of late endosomes should help to clarify how the dominant negative variant of Arl5b can impair transport.

Due to the lack of time I was not able to realize three related experiments. First, if Arl5b and Rab7 regulate trafficking of the same late endosomes, overexpression of dominant negative Rab7 should inhibit long-range retrograde transport of Arl5b in a similar way. It is known that dominant negative Rab7 can in fact impair transport of late endosomes. Long-range retrograde trafficking of vesicles enriched for TrkB and p75 receptors was completely blocked due to overexpression of dominant negative Rab7 in cultured developing motor neurons (Deinhardt et al., 2006).

Second, the presence of the Arl5b mutant did reduce but not abolish Rab7 trafficking completely. This allows speculation about a second mechanism for mediating transport of this kind of late endosomes. Arf proteins are known for redundancy, in most cases two Arf proteins act interchangeable and loss of one Arf can be compensated by its relative (Gillingham and Munro, 2007). I was able to show that a close homolog of Arl5b, Arl5a, is recruited to the same vesicles as Arl5b. It is currently not known if the dominant negative variant of Arl5a reduces trafficking of Rab7 positive vesicles.

Last, trafficking of Rab7 positive late endosomes was not examined in Arl5b-deficient cells. However, the loss of Arl5b must not have the same effect on the transport of late endosomes as expression of a dominant negative variant of Arl5b. It is possible that a redundant protein can cope with the loss of Arl5b while it may not be able to overcome the dominant negative effects exerted by the Arl5b mutant.

Beyond that it would be interesting to examine if loss of both, Arl5a and Arl5b, lead to a more severe impairment of late endosomal retrograde transport. While generation of a complete knockout of Arl5a is time consuming investigating the effect of dominant negative Arl5a overexpression in an Arl5b-deficient genomic background would be a promising strategy. However, it is currently not possible to detect EMX-Cre mediated loss of Arl5b in living dissociated hippocampal neurons with certainty. For this reason I started to crossbreed the conditional Arl5b KO line with a Cre Reporter strain. Mice from such strains carry a reporter gene. A loxP-flanked STOP cassette prevents translation of the reporter until it is excised by Cre activity, thereby expression of the reporter provides information if Cre recombination occurred in a specific cell. In this way I will be able to identify Arl5b-deficient neurons and assess the effect of dominant negative Arl5a specifically in these cells.

4.3 Arl5b mediates signaling by regulation of receptor trafficking

Signaling downstream of growth factors can require internalization and subsequent transport of receptors. For example, TrkB is transported retrogradely after activation in signaling endosomes (Bhattacharyya et al., 1997). While the PLCγ signaling cascade downstream of TrkB activation mediates Ca^{2+} signaling independently from receptor internalization, other effects rely on TrkB internalization. Due to trafficking of TrkB in signaling endosomes BDNF signaling can induce transport of PSD95 from the soma to dendrites (Yoshii and Constantine-Paton, 2007). In the past several studies addressed the identity of single molecules in signaling cascades downstream of BDNF. However, research on regulators of the transport of these signaling endosomes is still in its infancy. Deinhardt and colleagues showed that dominant negative Rab7 impairs retrograde trafficking of two receptors, TrkB and p75 (Deinhardt et al., 2007). Combining this finding with the observation that Arl5b can reduce the long-range transport of Rab7 positive vesicles the question arose if Arl5b is a regulator of TrkB trafficking. Two results suggest that Arl5b plays a role in TrkB trafficking. Here, I demonstrated that TrkB is in fact transported in Arl5b positive late endosomes. In addition, attachment of Arl5b to late endosomes can be triggered by BDNF in HeLa cells. However, additional investigations are needed to clarify if Arl5b is essential for signal transduction downstream of BDNF. Moreover, it will be important to clarify if TrkB transport is impaired by expression of dominant negative Arl5b or in the absence of Arl5a and Arl5b.

4.4 Identification of Arl5b interacting proteins

One aim of the study was to identify interaction partners of Arl5b in order to support the findings from the cell biological part of the thesis. Yeast-Two-Hybrid (Y2H) screens were performed by Hybrigenics to analyze proteins expressed in the embryonic and adult brain of mice for interaction with Arl5b. 53 different proteins were identified. Unfortunately the list did not contain known GEFs or GAPs for members of the Arf family. The majority of proteins were associated with transcription. Due to its design the Y2H assay is especially prone for false positive results in this category. For this reason I neglected putative interaction partners from this group. More interesting in the context of the results from the cellular work were 12 proteins with a predicted or described function in signaling cascades or to shaping the cytoskeleton. During my work on the thesis I verified the interaction of CK1α and Arl5b by biochemical assays *in vitro*. In a next step I showed that Arl5b and CK1α co-localize in neurons in the same vesicles. While a proven interaction *in vitro* on its own says little about the relevance of the interaction both results taken together indicates a functional *in vivo* interaction. Another hint for a physiological role of this interaction is the abnormal aggregation of Arl5b due to the overexpression of CK1α. The observation that overexpression of CK1α causes

a similar aggregation of TrkB further strengthens the relevance of the interaction between CK1α and Arl5b in regard to proposed Arl5b mediated TrkB trafficking.

Currently unknown and an issue of future research is the dependency of both proteins. Does CK1α initiate Arl5b function in endosomal trafficking by phosphorylation? Or is CK1α recruited to signaling endosomes by Arl5b where it can subsequently act within a signaling cascade? Both hypotheses are reasonable.

The Arl5b sequence contains two predicted CK1α phosphorylation sites which is in agreement with the first hypothesis. Further investigations, e.g. mutational analysis, will be needed to verify the phosphorylation of Arl5b by CK1α. The activation of Arl5b by CK1α is a possible explanation for the massive aggregation of Arl5b if CK1α abundance is raised by overexpression: CK1α triggers vesicle association of Arl5b by phosphorylation above physiological frequency. In consequence, the machinery which mediates long-range transport cannot handle the elevated number of maturing vesicles. Additionally, the aggregation of TrkB is plausible, as it seems to be one of the cargos enriched and transported in Arl5b associated vesicles.

A recent publication regarding CK1α effector proteins enhances the plausibility of the second hypothesis. It was shown that ribosomal S6 is a substrate of CK1α. Phosphorylation of ribosomal protein S6 by CK1α at S247 stabilizes the phosphorylation of ribosomal protein S6 by other kinases (p90 RSK and p70 S6K). This causes sustained activation of S6 and translation (Hutchinson et al., 2011). Recruitment of CK1α to signaling endosomes by interaction with Arl5b could specifically activate ribosomal protein s6 downstream of BDNF/TrkB. One way to prove this mechanism of action could be the artificial activation of CK1α to circumvent the reduced activation of ribosomal protein S6 in Arl5b-deficient cells.

4.5 Arl5b may play a general role for activity-dependent transport of endosomes

This thesis focused on the aspect of Arl5b mediated late endosome trafficking in regard of the BDNF/TrkB pathway. Several results indicate that the function of Arl5b may not be restricted to mediate trafficking of TrkB. By mediating late endosome trafficking in general Arl5b could be of importance for various signaling pathways, beyond of synaptic plasticity.

Even though BDNF is sufficient to mediate recruitment of Arl5b to late endosomes, this effect was not restricted to BDNF alone. Supplementation of fetal bovine serum (FCS) to serum starved HeLa cells induced translocation of Arl5b from the cytoplasm to late endosomes.

In addition, findings published during this thesis indicated that Arl5b is required for retrograde trafficking in HeLa cells. siRNA mediated knockdown of Arl5b in HeLa cells impaired retrograde trafficking of TGN38 and Shiga toxin to the Golgi apparatus after internalization (Houghton et al., 2012).

Finally, a recent publication provides information about transcriptional regulation of Arl5b in non neuronal cells. Interferon beta treatment is sufficient to upregulate Arl5b mRNA levels in peripheral blood mononuclear cells (Boppana et al, 2013). This is a hint for a role of Arl5b in another type of cells in an activity-dependent manner. However, analysis of protein trafficking was beyond the scope of this study.

4.6 Impaired activation of ribosomal protein S6 in Arl5-deficient mice

The generation of Arl5b-deficient mice was regarded as a prerequisite to properly investigate the role of Arl5b in a living organism. In a first attempt, a constitutive knockout of Arl5b turned out to be embryonic lethal. In a second approach a conditional knockout mouse line was established. Since my investigations focused on the nervous system and synaptic plasticity a strategy to delete Arl5b exclusively in the forebrain was pursued. Homozygous forebrain specific Arl5b knockout mice were vital and not distinguishable from wild type littermates. The established mouse line provided a powerful tool to investigate if the impact of Arl5b on endosome trafficking effects synaptic plasticity and long-term formation in animals.

The inhibition of TrkB phosphorylation at S^{478} impairs BDNF/TrkB signaling (Lai et al., 2012). In this study activation of the AKT/mTOR pathway was reduced in $TrkBS^{478A/S478A}$ knock-in mice and in accordance activation of ribosomal protein S6 was reduced too. As a consequence translation was disturbed in dissociated hippocampal neurons causing impairment of L-LTP in Ca3-CA1 synapses of hippocampal slices. Moreover, it was shown that inhibited phosphorylation of S^{478} of TrkB was sufficient to effect the learning ability of mice in the Morris water maze and novel object recognition (Lai et al., 2012).

I examined the role of Arl5b for activation of ribosomal protein S6 downstream of AKT/mTOR signaling by kainic acid-induced seizures *in vivo*. Indeed the phosphorylation of ribosomal protein S6 was impaired in the hippocampus upon loss of Arl5b in excitatory neurons. This result suggests a physiological function of Arl5b in signaling cascades in hippocampal neurons by mediating retrograde trafficking of late endosomes. Additional experiments are needed to specify in detail at which part of the signaling cascade Arl5b steps in. Arl5b is not recruited to Rab5 positive early endosomes but its dominant negative form impairs late endosomal transport. Therefore, Arl5b may recruit parts of the machinery that mediates long-range transport along microtubules. Loss of Arl5b would disrupt this recruitment, trap signaling endosomes after internalization of receptors and may reduce the association to their downstream effectors. In consequence transduction of the signaling cascade would be less efficient or even inhibited. One example could be ribosomal S6 kinases which can phosphorylate ribosomal protein S6. This activation would be hampered, because the transport to the effector (S6) is blocked. A possible way to examine this hypothesis

would be the analysis of members of the AKT/mTOR pathway to assess their co-localization with active translation zones (enriched in phospho-S6) in wild type and Arl5b knockout cells.

4.7 Arl5b-deficient mice in cognitive behavioral experiments

Overall the results obtained by biochemical, molecular and cell biological experiments strongly suggest that Arl5b plays a role in intracellular signaling pathways in synaptic plasticity. Finally, behavioral tests were performed to examine if the cellular functions have an impact on long-term memory formation.

Results from the open field and elevated plus maze task show that loss of Arl5b in excitatory neurons of the forebrain does not interfere with locomotor function. Additionally the mice do not show increased anxiety levels or impaired exploratory behavior.

In fear conditioning experiments the mice exhibit a conditional response curve equal to wild type mice and they can memorize the position of a hidden platform in the Morris water maze task. These findings suggest that the short-term memory of the knockout mice is intact. However, the mice show impaired long-term memory formation in the novel object recognition (NOR) task. While the wild type mice preferred to explore a novel object over a familiar object which they already explored one day before. The knockout mice did not spent significantly more time exploring the novel object apparently being unable to discriminate the novel from the familiar object. This result is in agreement with a weak but not significant reduction of freezing in the context test one day after fear conditioning. This may indicate a weaker remembrance of foot shock after confrontation with the context environment. Finally, a very weak reduction in the probe trial of the Morris water maze (MWM) task was observed. Knockout animals did spent more time in the target quadrant compared to the control quadrants, thus the percentage spent in the target quadrant was not significantly different from chance level. In contrast the wild type animals spent a higher percentage of time in the target quadrant and did perform over chance level. Comparing the performance of KO with WT mice did not reveal a significant change. The weaker performance supports impairment in spatial learning of the Arl5b KO mice.

Overall performance of Arl5b-deficient mice was slightly reduced compared to wild type mice in three learning tasks. Though, these results should be interpreted with caution. For example the mice exhibited a tendency for the novel object in NOR task and the target quadrant in the MWM. The lack of significance is possibly a result of the relatively small group (n = 8) of animals tested in this trial. In conclusion the results of the behavior experiments indicate a tendency for a weak impairment of long-term memory formation of Arl5b-deficient mice. However, the learning deficiency is clearly not as strong as observed for loss of other genes, e.g. Arg3.1/Arc. Mice which are Arg3.1/Arc-deficient do not freeze at all in the context

test after fear conditioning (Plath et al. 2006).

This mild impairment was unexpected because the reduction of ribosomal protein S6 activation is comparably strong as observed in the TrkBS$^{478A/S478A}$ mice (Lai et al., 2012). Mice carrying the S^{478}A mutation homozygously show a strong impairment in MWM and NOR. Further research is needed to figure out the reason for these unexpected results. A possible explanation focused on the abundance of ribosomal protein S6 in hippocampal neurons. It regulates local translation in dendrites (Tsokas et al., 2005) as well as in the soma (Antion et al., 2008). Activation of these alternative protein pools may play different roles in plasticity. While ribosomal protein S6 phosphorylation is impaired in both, Arl5b-deficient and TrkB$^{S478A/S478A}$ mice, it is not known if they the same pool of S6 protein is regulated. A second possible explanation for the difference in severity is the extensive crosstalk between signaling cascades activated downstream of BDNF/TrkB. It is known that the mTOR and MAPK pathways both regulate ribosomal protein S6-dependent translation. Eventually the effect of the Arl5b knockout can be compensated by changes in those signaling cascades which are not applicable for the TrkB knock-in mice.

Besides the discussed open questions the impact of Arl5b loss should be studied in a broader perspective. Due to reasons of scarcity of time I focused to assess the activation of translation as a result of BDNF signaling mediated by the AKT/mTOR pathway with phosphorylation of ribosomal protein S6 as read out. Another target of mTOR signaling, the phosphorylation of 4E-BP1, should be examined in the future. Additionally, the rapid gene induction after an activity stimulus and the role of Arl5b in retrograde transport of vesicles towards the soma suggests a function in signaling cascades which activate transcription. I ignored this possible function because a previous study demonstrated that the blockade of TrkB retrograde trafficking by dominant negative Rab7 does not interfere with activation of CREB (Deinhardt et al., 2006). Loss of CREB-mediated transcription results in impaired long-term memory and the CREB gene is a transcriptional target of BDNF-dependent signaling (Bourtchuladze et al., 1994; Kida et al., 2002;.Pittenger et al., 2002; Thomas and Huganir, 2004). Future investigations should readdress CREB activation in the context of Arl5b function.

In conclusion, I characterized Arl5b as a canonical Arf-like family member and demonstrate a functional role for Arl5b in mediating retrograde axonal endosomal trafficking. I show for the first time the interaction of Arl5b and CK1α. Although the molecular mechanisms of the interaction await detailed characterization it may be part of a signaling cascade initiated by BDNF. In accordance, the current study suggests a functional impact of Arl5b on the retrograde transport of the BDNF receptor TrkB and on activity-dependent activation of translation mediated by ribosomal protein S6 as target of BDNF-signaling. Moreover, I established a conditional knock out mouse model for Arl5b and observed a mild impairment in long-term memory formation in these mice.

5. Appendix

5.1 References

Abel, T., Nguyen, P. V, Barad, M., Deuel, T. A., Kandel, E. R., & Bourtchouladze, R. (1997). Genetic demonstration of a role for PKA in the late phase of LTP and in hippocampus-based long-term memory. Cell, 88, 615–626. doi:10.1016/S0092-8674(00)81904-2

Akama, K. T., & McEwen, B. S. (2003). Estrogen stimulates postsynaptic density-95 rapid protein synthesis via the Akt/protein kinase B pathway. The Journal of neuroscience : the official journal of the Society for Neuroscience, 23, 2333–2339.

Amaral, D. G., & Witter, M. P. (1989). The three-dimensional organization of the hippocampal formation: a review of anatomical data. Neuroscience, 31, 571–591. doi:10.1016/0306-4522(89)90424-7

Antion, M. D., Hou, L., Wong, H., Hoeffer, C. A., & Klann, E. (2008). mGluR-dependent long-term depression is associated with increased phosphorylation of S6 and synthesis of elongation factor 1A but remains expressed in S6K-deficient mice. Molecular and cellular biology, 28, 2996–3007. doi:10.1128/MCB.00201-08

Araque, A., Parpura, V., Sanzgiri, R. P., & Haydon, P. G. (1999). Tripartite synapses: glia, the unacknowledged partner. Trends in neurosciences, 22, 208–215. doi:10.1016/S0166-2236(98)01349-6

Arnold, F. J. L., Hofmann, F., Bengtson, C. P., Wittmann, M., Vanhoutte, P., & Bading, H. (2005). Microelectrode array recordings of cultured hippocampal networks reveal a simple model for transcription and protein synthesis-dependent plasticity. The Journal of physiology, 564, 3–19. doi:10.1113/jphysiol.2004.077446

Arthur, J. S. C., Fong, A. L., Dwyer, J. M., Davare, M., Reese, E., Obrietan, K., & Impey, S. (2004). Mitogen- and stress-activated protein kinase 1 mediates cAMP response element-binding protein phosphorylation and activation by neurotrophins. The Journal of neuroscience : the official journal of the Society for Neuroscience, 24, 4324–4332. doi:10.1523/JNEUROSCI.5227-03.2004

Beretta, L., Gingras, A. C., Svitkin, Y. V, Hall, M. N., & Sonenberg, N. (1996). Rapamycin blocks the phosphorylation of 4E-BP1 and inhibits cap-dependent initiation of translation. The EMBO journal, 15, 658–664.

Bevins, R. A., & Besheer, J. (2006). Object recognition in rats and mice: a one-trial non-matching-to-sample learning task to study “recognition memory”. Nature protocols, 1, 1306–1311. doi:10.1038/nprot.2006.205

Bhattacharyya, A., Watson, F. L., Bradlee, T. A., Pomeroy, S. L., Stiles, C. D., & Segal, R. A. (1997). Trk receptors function as rapid retrograde signal carriers in the adult nervous system. The Journal of neuroscience : the official journal of the Society for Neuroscience, 17, 7007–7016.

Birnboim, H. C., & Doly, J. (1979). A rapid alkaline extraction procedure for screening recombinant plasmid DNA. Nucleic acids research, 7, 1513–1523. doi:10.1093/nar/7.6.1513

Bliss, T. V. P., & Lomo, T. (1973). Long-lasting potentiation of synaptic transmission in the dentate area of the anaesthetized rabbit following stimulation of the preforant path. Journal of physiology, 232, 331–356.

Bliss, T. V, & Collingridge, G. L. (1993). A synaptic model of memory: long-term potentiation in the hippoc-

ampus. Nature, 361, 31–39. doi:10.1038/361031a0

Boppana, S., Mindur, J. E., Balashov, K. E., Dhib-Jalbut, S., & Ito, K. (n.d.). Comparison of IFN-β inducible gene expression in primary-progressive and relapsing-remitting multiple sclerosis.pdf.

Bourtchuladze, R., Frenguelli, B., Blendy, J., Cioffi, D., Schutz, G., & Silva, A. J. (1994). Deficient long-term memory in mice with a targeted mutation of the cAMP-responsive element-binding protein. Cell, 79, 59–68. doi:10.1016/0092-8674(94)90400-6

Brakeman, P. R., Lanahan, A. A., O'Brien, R., Roche, K., Barnes, C. A., Huganir, R. L., & Worley, P. F. (1997). Homer: a protein that selectively binds metabotropic glutamate receptors. Nature, 386, 284–288. doi:10.1038/386284a0

Burguete, A. S., Fenn, T. D., Brunger, A. T., & Pfeffer, S. R. (2008). Rab and Arl GTPase family members cooperate in the localization of the golgin GCC185. Cell, 132, 286–298. doi:10.1016/j.cell.2007.11.048

Burnett, P. E., Barrow, R. K., Cohen, N. A., Snyder, S. H., & Sabatini, D. M. (1998). RAFT1 phosphorylation of the translational regulators p70 S6 kinase and 4E-BP1. Proceedings of the National Academy of Sciences of the United States of America, 95, 1432–1437. doi:10.1073/pnas.95.4.1432

Carmignoto, G., Pizzorusso, T., Tia, S., & Vicini, S. (1997). Brain-derived neurotrophic factor and nerve growth factor potentiate excitatory synaptic transmission in the rat visual cortex. The Journal of physiology, 498 (Pt 1, 153–164.

Carroll, R. C., Lissin, D. V, von Zastrow, M., Nicoll, R. A., & Malenka, R. C. (1999). Rapid redistribution of glutamate receptors contributes to long-term depression in hippocampal cultures. Nature neuroscience, 2, 454–460. doi:10.1038/8123

Chang, F. L., & Greenough, W. T. (1984). Transient and enduring morphological correlates of synaptic activity and efficacy change in the rat hippocampal slice. Brain research, 309, 35–46. doi:10.1016/0006-8993(84)91008-4

Chergui, K., Svenningsson, P., & Greengard, P. (2005). Physiological role for casein kinase 1 in glutamatergic synaptic transmission. The Journal of neuroscience : the official journal of the Society for Neuroscience, 25(28), 6601–9. doi:10.1523/JNEUROSCI.1082-05.2005

Chiu, J., March, P. E., Lee, R., & Tillett, D. (2004). Site-directed, Ligase-Independent Mutagenesis (SLIM): a single-tube methodology approaching 100% efficiency in 4 h. Nucleic acids research, 32, e174. doi:10.1093/nar/gnh172

Cohen-Cory, S. (1999). BDNF modulates, but does not mediate, activity-dependent branching and remodeling of optic axon arbors *in vivo*. The Journal of neuroscience : the official journal of the Society for Neuroscience, 19, 9996–10003.

Cohen-Cory, Susana, Kidane, A. H., Shirkey, N. J., & Marshak, S. (2010). Brain-derived neurotrophic factor and the development of structural neuronal connectivity. Developmental neurobiology, 70, 271–288. doi:10.1002/dneu.20774

Cole, A. J., Saffen, D. W., Baraban, J. M., & Worley, P. F. (1989a). Rapid increase of an immediate early gene messenger RNA in hippocampal neurons by synaptic NMDA receptor activation. Nature, 340, 474–476. doi:10.1038/340474a0

Cole, A. J., Saffen, D. W., Baraban, J. M., & Worley, P. F. (1989b). Rapid increase of an immediate early gene messenger RNA in hippocampal neurons by synaptic NMDA receptor activation. Nature, 340, 474–476. doi:10.1038/340474a0

Crawley, J. N. (1985). Exploratory behavior models of anxiety in mice. Neuroscience and biobehavioral reviews, 9, 37–44.

Crowder, R. J., & Freeman, R. S. (1998). Phosphatidylinositol 3-kinase and Akt protein kinase are necessary and sufficient for the survival of nerve growth factor-dependent sympathetic neurons. The Journal of neuroscience : the official journal of the Society for Neuroscience, 18, 2933–2943.

D'Souza-Schorey, C., & Chavrier, P. (2006). ARF proteins: roles in membrane traffic and beyond. Nature reviews. Molecular cell biology, 7, 347–358. doi:10.1038/nrm1910

Deadwyler, S. A., Dunwiddie, T., & Lynch, G. (1987). A critical level of protein synthesis is required for long-term potentiation. Synapse (New York, N.Y.), 1, 90–95. doi:10.1002/syn.890010112

Deinhardt, K., Salinas, S., Verastegui, C., Watson, R., Worth, D., Hanrahan, S., … Schiavo, G. (2006). Rab5 and Rab7 control endocytic sorting along the axonal retrograde transport pathway. Neuron, 52(2), 293–305. doi:10.1016/j.neuron.2006.08.018

Denenberg, V. H. (1969). Open-field bheavior in the rat: what does it mean? Annals of the New York Academy of Science, 159, 852–859.

Dityatev, A., & Rusakov, D. A. (2011). Molecular signals of plasticity at the tetrapartite synapse. Current opinion in neurobiology, 21, 353–359. doi:10.1016/j.conb.2010.12.006

Donaldson, J. G., & Jackson, C. L. (2011). ARF family G proteins and their regulators: roles in membrane transport, development and disease. Nature reviews. Molecular cell biology, 12(6), 362–375. doi:10.1038/nrm3117

Eichenbaum, H. (2000). A cortical-hippocampal system for declarative memory. Nature reviews. Neuroscience, 1, 41–50. doi:10.1038/35036213

Farazi, T. A., Waksman, G., & Gordon, J. I. (2001). Structures of Saccharomyces cerevisiae N-myristoyltransferase with bound myristoylCoA and peptide provide insights about substrate recognition and catalysis. Biochemistry, 40, 6335–6343. doi:bi0101401 [pii]

Fields, S., & Song, O. (n.d.). A novel genetic system to detect protein-protein interactions.

Fiumelli, H., Jabaudon, D., Magistretti, P. J., & Martin, J. L. (1999). BDNF stimulates expression, activity and release of tissue-type plasminogen activator in mouse cortical neurons. The European journal of neuroscience, 11, 1639–1646.

Flavell, S. W., Kim, T.-K., Gray, J. M., Harmin, D. a, Hemberg, M., Hong, E. J., … Greenberg, M. E. (2008). Genome-wide analysis of MEF2 transcriptional program reveals synaptic target genes and neuronal activity-dependent polyadenylation site selection. Neuron, 60(6), 1022–1038. doi:10.1016/j.neuron.2008.11.029

Franke, T. F., Kaplan, D. R., & Cantley, L. C. (1997). PI3K: downstream AKTion blocks apoptosis. Cell, 88(4), 435–7. Retrieved from http://www.ncbi.nlm.nih.gov/pubmed/9038334

Frey, U., Huang, Y. Y., & Kandel, E. R. (1993). Effects of cAMP simulate a late stage of LTP in hippocampal CA1 neurons. Science (New York, N.Y.), 260, 1661–1664. doi:10.1126/science.8389057

Frey, U., Krug, M., Reymann, K. G., & Matthies, H. (1988). Anisomycin, an inhibitor of protein synthesis, blocks late phases of LTP phenomena in the hippocampal CA1 region *in vitro*. Brain research, 452, 57–65. doi:10.1016/0006-8993(88)90008-X

Frischknecht, R., & Gundelfinger, E. D. (2012). The Brain's Extracellular Matrix and Its Role in Synaptic plas-

ticity. In Synaptic plasticity (Vol. 970, pp. 153–171). doi:10.1007/978-3-7091-0932-8

Fusi, S., Drew, P. J., & Abbott, L. F. (2005). Cascade models of synaptically stored memories. Neuron, 45, 599–611. doi:10.1016/j.neuron.2005.02.001

Galliano, E., Potters, J.-W., Elgersma, Y., Wisden, W., Kushner, S. a, De Zeeuw, C. I., & Hoebeek, F. E. (2013). Synaptic transmission and plasticity at inputs to murine cerebellar Purkinje cells are largely dispensable for standard nonmotor tasks. The Journal of neuroscience : the official journal of the Society for Neuroscience, 33, 12599–618. doi:10.1523/JNEUROSCI.1642-13.2013

Garami, A., Zwartkruis, F. J. T., Nobukuni, T., Joaquin, M., Roccio, M., Stocker, H., … Thomas, G. (2003). Insulin activation of Rheb, a mediator of mTOR/S6K/4E-BP signaling, is inhibited by TSC1 and 2. Molecular cell, 11, 1457–1466. doi:10.1016/S1097-2765(03)00220-X

Gey, G. O., Coffman, W., & Kubicek, M. T. (1952). Tissue culture studies of the proliferative capacity of cervical carcinoma and normal epithelium. Cancer Research, 12, 264–265. Retrieved from http://www.ncbi.nlm.nih.gov/pubmed/14905453\nhttp://scholar.google.com/scholar?hl=en&btnG=Search&q=intitle:Tissue+culture+studies+of+the+proliferative+capacity+of+cervical+carcinoma+and+normal+epithelium.+Cancer+Res.+12:+264,+1952.

Gillingham, A. K., & Munro, S. (2007). The small G proteins of the Arf family and their regulators. Annual review of cell and developmental biology, 23, 579–611. doi:10.1146/annurev.cellbio.23.090506.123209

Graham, F. L., Graham, F. L., Smiley, J., Smiley, J., Russell, W. C., Russell, W. C., Nairn, R. (1977). Characteristics of a human cell line transformed by DNA from human adenovirus type 5. The Journal of general virology, 36, 59–74. doi:10.1099/0022-1317-36-1-59

Gundelfinger, E. D., Frischknecht, R., Choquet, D., & Heine, M. (2010). Converting juvenile into adult plasticity: a role for the brain's extracellular matrix. The European journal of neuroscience, 31, 2156–2165. doi:10.1111/j.1460-9568.2010.07253.x

Hadari, Y. R., Kouhara, H., Lax, I., & Schlessinger, J. (1998). Binding of Shp2 tyrosine phosphatase to FRS2 is essential for fibroblast growth factor-induced PC12 cell differentiation. Molecular and cellular biology, 18, 3966–3973.

Hara, K., Yonezawa, K., Kozlowski, M. T., Sugimoto, T., Andrabi, K., Weng, Q. P., … Avruch, J. (1997). Regulation of eIF-4E BP1 phosphorylation by mTOR. The Journal of biological chemistry, 272, 26457–26463. doi:10.1074/jbc.272.42.26457

Hayward, W. S., Neel, B. G., & Astrin, S. M. (1981). Activation of a cellular onc gene by promoter insertion in ALV-induced lymphoid leukosis. Nature, 290, 475–480. doi:10.1038/290475a0

Hebb, D. O. (1949). The Organization of Behavior: A Neuropsychological Theory. Science Education (Vol. 44, p. 335). doi:10.2307/1418888

Heldt, S. A., Stanek, L., Chhatwal, J. P., & Ressler, K. J. (2007). Hippocampus-specific deletion of BDNF in adult mice impairs spatial memory and extinction of aversive memories. Molecular psychiatry, 12, 656–670. doi:10.1038/sj.mp.4001957

Herculano-Houzel, S. (2012). The remarkable, yet not extraordinary, human brain as a scaled-up primate brain and its associated cost. Proceedings of the National Academy of Sciences. doi:10.1073/pnas.1201895109

Hermey, G., Mahlke, C., Gutzmann, J. J., Schreiber, J., Blüthgen, N., & Kuhl, D. (2013). Genome-wide profiling of the activity-dependent hippocampal transcriptome. PloS one, 8(10), e76903. doi:10.1371/

journal.pone.0076903

Heynen, A. J., Quinlan, E. M., Bae, D. C., & Bear, M. F. (2000). Bidirectional, activity-dependent regulation of glutamate receptors in the adult hippocampus in vivo. Neuron, 28, 527–536. doi:10.1016/S0896-6273(00)00130-6

Holgado-Madruga, M., Moscatello, D. K., Emlet, D. R., Dieterich, R., & Wong, A. J. (1997). Grb2-associated binder-1 mediates phosphatidylinositol 3-kinase activation and the promotion of cell survival by nerve growth factor. Proceedings of the National Academy of Sciences of the United States of America, 94, 12419–12424. doi:10.1073/pnas.94.23.12419

Hollmann, M., & Heinemann, S. (1994). Cloned glutamate receptors. Annual review of neuroscience, 17, 31–108. doi:10.1146/annurev.neuro.17.1.31

Houghton, F. J., Bellingham, S. a., Hill, A. F., Bourges, D., Ang, D. K. Y., Gemetzis, T., … Gleeson, P. a. (2012). Arl5b is a Golgi-localised small G protein involved in the regulation of retrograde transport. Experimental Cell Research, 318(5), 464–477. doi:10.1016/j.yexcr.2011.12.023

Hu, C.-T., Wu, J.-R., & Wu, W.-S. (2013). The role of endosomal signaling triggered by metastatic growth factors in tumor progression. Cellular signalling, 25(7), 1539–45. doi:10.1016/j.cellsig.2013.03.022

Huang, Y. Y., Li, X. C., & Kandel, E. R. (1994). cAMP contributes to mossy fiber LTP by initiating both a covalently mediated early phase and macromolecular synthesis-dependent late phase. Cell, 79, 69–79. doi:10.1016/0092-8674(94)90401-4

Huber, K. M., Roder, J. C., & Bear, M. F. (2001). Chemical induction of mGluR5- and protein synthesis--dependent long-term depression in hippocampal area CA1. Journal of neurophysiology, 86, 321–325.

Hutchinson, J. A., Shanware, N. P., Chang, H., & Tibbetts, R. S. (2011). Regulation of ribosomal protein S6 phosphorylation by casein kinase 1 and protein phosphatase 1. The Journal of biological chemistry, 286, 8688–8696. doi:10.1074/jbc.M110.141754

Hyman, S. E., & Malenka, R. C. (2001). Addiction and the brain: the neurobiology of compulsion and its persistence. Nature reviews. Neuroscience, 2, 695–703. doi:10.1038/35094560

Ingi, T., Krumins, A. M., Chidiac, P., Brothers, G. M., Chung, S., Snow, B. E., … Worley, P. F. (1998). Dynamic regulation of RGS2 suggests a novel mechanism in G-protein signaling and neuronal plasticity. The Journal of neuroscience : the official journal of the Society for Neuroscience, 18, 7178–7188.

Isaac, J. T., Nicoll, R. A., & Malenka, R. C. (1995). Evidence for silent synapses: implications for the expression of LTP. Neuron, 15, 427–434. doi:10.1016/0896-6273(95)90046-2

Iwasato, T., Datwani, A., Wolf, A. M., Nishiyama, H., Taguchi, Y., Tonegawa, S., … Itohara, S. (2000). Cortex-restricted disruption of NMDAR1 impairs neuronal patterns in the barrel cortex. Nature, 406, 726–731. doi:10.1038/35021059

Jefferies, H. B., Fumagalli, S., Dennis, P. B., Reinhard, C., Pearson, R. B., & Thomas, G. (1997). Rapamycin suppresses 5'TOP mRNA translation through inhibition of p70s6k. The EMBO journal, 16, 3693–3704. doi:10.1093/emboj/16.12.3693

Johnston, M. V. (2004). Clinical disorders of brain plasticity. Brain & development, 26, 73–80. doi:10.1016/S0387-7604(03)00102-5

Kamikubo, Y., Egashira, Y., Tanaka, T., Shinoda, Y., Tominaga-Yoshino, K., & Ogura, A. (2006). Long-lasting synaptic loss after repeated induction of LTD: independence to the means of LTD induction. The

European journal of neuroscience, 24, 1606–1616. doi:10.1111/j.1460-9568.2006.05032.x

Kang, H., & Schuman, E. M. (1995). Long-lasting neurotrophin-induced enhancement of synaptic transmission in the adult hippocampus. Science (New York, N.Y.), 267, 1658–1662. doi:10.1126/science.7886457

Kang, J., Jiang, L., Goldman, S. A., & Nedergaard, M. (1998). Astrocyte-mediated potentiation of inhibitory synaptic transmission. Nature neuroscience, 1, 683–692. doi:10.1038/3684

Kaplan, D. R., & Miller, F. D. (2000). Neurotrophin signal transduction in the nervous system. Current opinion in neurobiology, 10, 381–391. doi:10.1016/S0959-4388(00)00092-1

Karachot, L., Shirai, Y., Vigot, R., Yamamori, T., & Ito, M. (2001). Induction of long-term depression in cerebellar Purkinje cells requires a rapidly turned over protein. Journal of neurophysiology, 86, 280–289.

Káradóttir, R., Hamilton, N. B., Bakiri, Y., & Attwell, D. (2008). Spiking and nonspiking classes of oligodendrocyte precursor glia in CNS white matter. Nature neuroscience, 11(4), 450–456. doi:10.1038/nn2060

Kaufman, M. H., & Bard, J. (1999). The Anatomical Basis of mouse development (p. 291). Academic Press.

Kauselmann, G., Weiler, M., Wulff, P., Jessberger, S., Konietzko, U., Scafidi, J., … Kuhl, D. (1999). The polo-like protein kinases Fnk and Snk associate with a Ca(2+)- and integrin-binding protein and are regulated dynamically with synaptic plasticity. The EMBO journal, 18, 5528–5539. doi:10.1093/emboj/18.20.5528

Kelleher, R. J., Govindarajan, A., & Tonegawa, S. (2004). Translational regulatory mechanisms in persistent forms of synaptic plasticity. Neuron, 44, 59–73. doi:10.1016/j.neuron.2004.09.013

Kelly, K., Cochran, B. H., Stiles, C. D., & Leder, P. (1983). Cell-specific regulation of the c-myc gene by lymphocyte mitogens and platelet-derived growth factor. Cell, 35, 603–610. doi:10.1016/0092-8674(83)90092-2

Kida, S., Josselyn, S. A., Peña de Ortiz, S., Kogan, J. H., Chevere, I., Masushige, S., & Silva, A. J. (2002). CREB required for the stability of new and reactivated fear memories. Nature neuroscience, 5, 348–355. doi:10.1038/nn819

Korte, M., Carroll, P., Wolf, E., Brem, G., Thoenen, H., & Bonhoeffer, T. (1995). Hippocampal long-term potentiation is impaired in mice lacking brain-derived neurotrophic factor. Proceedings of the National Academy of Sciences of the United States of America, 92, 8856–8860. doi:10.1073/pnas.92.19.8856

Kouhara, H., Hadari, Y. R., Spivak-Kroizman, T., Schilling, J., Bar-Sagi, D., Lax, I., & Schlessinger, J. (1997). A lipid-anchored Grb2-binding protein that links FGF-receptor activation to the Ras/MAPK signaling pathway. Cell, 89, 693–702. doi:10.1016/S0092-8674(00)80252-4

Krug, M., Lössner, B., & Ott, T. (1984). Anisomycin blocks the late phase of long-term potentiation in the dentate gyrus of freely moving rats. Brain research bulletin, 13, 39–42. doi:10.1016/0361-9230(84)90005-4

Lai, K.-O., Wong, A. S. L., Cheung, M.-C., Xu, P., Liang, Z., Lok, K.-C., … Ip, N. Y. (2012). TrkB phosphorylation by Cdk5 is required for activity-dependent structural plasticity and spatial memory. Nature Neuroscience, 15(11), 1506–1515. doi:10.1038/nn.3237

LeDoux, J. E. (2000). Emotion circuits in the brain. Annual review of neuroscience, 23, 155–184. doi:10.1146/annurev.neuro.23.1.155

Lee, C.-C., Huang, C.-C., Wu, M.-Y., & Hsu, K.-S. (2005). Insulin stimulates postsynaptic density-95 protein

translation via the phosphoinositide 3-kinase-Akt-mammalian target of rapamycin signaling pathway. The Journal of biological chemistry, 280, 18543–18550. doi:10.1074/jbc.M414112200

Lee, K. S., Schottler, F., Oliver, M., & Lynch, G. (1980). Brief bursts of high-frequency stimulation produce two types of structural change in rat hippocampus. Journal of neurophysiology, 44(2), 247–58. Retrieved from http://www.ncbi.nlm.nih.gov/pubmed/7411185

Lentze, N., & Auerbach, D. (2008). The yeast two-hybrid system, 505–516.

Leslie, J. H., & Nedivi, E. (2012). Activity-Regulated Genes as Mediators of Neural Circuit Plasticity, 94(3), 223–237. doi:10.1016/j.pneurobio.2011.05.002.Activity-Regulated

Levy, W. B., & Steward, O. (1979). Synapses as associative memory elements in the hippocampal formation. Brain research, 175, 233–245. doi:10.1016/0006-8993(79)91003-5

Liao, D., Hessler, N. A., & Malinow, R. (1995). Activation of postsynaptically silent synapses during pairing-induced LTP in CA1 region of hippocampal slice. Nature, 375, 400–404. doi:10.1038/375400a0

Lin, Y., Bloodgood, B. L., Hauser, J. L., Lapan, A. D., Koon, A. C., Kim, T.-K., … Greenberg, M. E. (2008). Activity-dependent regulation of inhibitory synapse development by Npas4. Nature, 455, 1198–1204. doi:10.1038/nature07319

Link, W., Konietzko, U., Kauselmann, G., Krug, M., Schwanke, B., Frey, U., & Kuhl, D. (1995). Somatodendritic expression of an immediate early gene is regulated by synaptic activity. Proceedings of the National Academy of Sciences of the United States of America, 92, 5734–5738.

Liu, Y., & Rohrschneider, L. R. (2002). The gift of Gab. FEBS letters, 515, 1–7. doi:10.1016/S0014-5793(02)02425-0

Lois, C., Hong, E. J., Pease, S., Brown, E. J., & Baltimore, D. (2002). Germline transmission and tissue-specific expression of transgenes delivered by lentiviral vectors. Science (New York, N.Y.), 295, 868–872. doi:10.1126/science.1067081

Lyford, G. L., Yamagata, K., Kaufmann, W. E., Barnes, C. A., Sanders, L. K., Copeland, N. G., … Worley, P. F. (1995). Arc, a growth factor and activity-regulated gene, encodes a novel cytoskeleton-associated protein that is enriched in neuronal dendrites. Neuron, 14, 433–445. doi:10.1016/0896-6273(95)90299-6

Lynch, G., Larson, J., Kelso, S., Barrionuevo, G., & Schottler, F. (1983). Intracellular injections of EGTA block induction of hippocampal long-term potentiation. Nature, 305, 719–21.

Malenka, R C, Lancaster, B., & Zucker, R. S. (1992). Temporal limits on the rise in postsynaptic calcium required for the induction of long-term potentiation. Neuron, 9, 121–128. doi:10.1016/0896-6273(92)90227-5

Malenka, Robert C, & Bear, M. F. (2004). LTP and LTD: an embarrassment of riches. Neuron, 44, 5–21. doi:10.1016/j.neuron.2004.09.012

Malinow, R, Schulman, H., & Tsien, R. W. (1989). Inhibition of postsynaptic PKC or CaMKII blocks induction but not expression of LTP. Science (New York, N.Y.), 245, 862–866. doi:10.1126/science.2549638

Malinow, Roberto, & Malenka, R. C. (2002). AMPA receptor trafficking and synaptic plasticity. Annual review of neuroscience, 25, 103–126. doi:10.1146/annurev.neuro.25.112701.142758

Manning, B. D., Tee, A. R., Logsdon, M. N., Blenis, J., & Cantley, L. C. (2002). Identification of the tuberous sclerosis complex-2 tumor suppressor gene product tuberin as a target of the phosphoinositide

3-kinase/akt pathway. Molecular cell, 10, 151–162. doi:10.1016/S1097-2765(02)00568-3

Maren, S. (2001). Neurobiology of Pavlovian fear conditioning. Annual review of neuroscience, 24, 897–931. doi:10.1146/annurev.neuro.24.1.897

Maren, Stephen, & Quirk, G. J. (2004). Neuronal signalling of fear memory. Nature reviews. Neuroscience, 5, 844–852. doi:10.1038/nrn1535

Mayer, M. L., Westbrook, G. L., & Guthrie P.B. (1984). Voltage dependent block by Mg2+ of NMDA responses in spinal cord neurons. Nature, 309, 261–263.

Mayford, M., Siegelbaum, S. A., & Kandel, E. R. (2012). Synapses and Memory Storage. Cold Spring Harbor Perspectives in Biology. doi:10.1101/cshperspect.a005751

McAllister, A. K., Lo, D. C., & Katz, L. C. (1995). Neurotrophins regulate dendritic growth in developing visual cortex. Neuron, 15, 791–803. doi:10.1016/0896-6273(95)90171-X

McKinsey, T. A., Zhang, C. L., & Olson, E. N. (2002). MEF2: a calcium-dependent regulator of cell division, differentiation and death. Trends in biochemical sciences, 27, 40–47. doi:10.1016/S0968-0004(01)02031-X

Meyuhas, O. (2000). Synthesis of the translational apparatus is regulated at the translational level. European journal of biochemistry / FEBS, 267, 6321–6330. doi:10.1046/j.1432-1327.2000.01719.x

Minichiello, L. (2009). TrkB signalling pathways in LTP and learning. Nature reviews. Neuroscience, 10, 850–860. doi:10.1038/nrn2738

Morgan, J. I., Cohen, D. R., Hempstead, J. L., & Curran, T. (1987). Mapping patterns of c-fos expression in the central nervous system after seizure. Science (New York, N.Y.), 237, 192–197. doi:10.1126/science.3037702

Morris, R. (1984). Developments of a water-maze procedure for studying spatial learning in the rat. Journal of neuroscience methods, 11, 47–60. doi:10.1016/0165-0270(84)90007-4

Nedivi, E., Hevroni, D., Naot, D., Israeli, D., & Citri, Y. (1993). Numerous candidate plasticity-related genes revealed by differential cDNA cloning. Nature, 363, 718–722. doi:10.1038/363718a0

Neves, G., Cooke, S. F., & Bliss, T. V. P. (2008). Synaptic plasticity, memory and the hippocampus: a neural network approach to causality. Nature reviews. Neuroscience, 9, 65–75. doi:10.1038/nrn2303

Newman, E. A. (2003). New roles for astrocytes: regulation of synaptic transmission. Trends in neurosciences, 26, 536–542. doi:10.1016/S0166-2236(03)00237-6

Ng, E. L., & Tang, B. L. (2008). Rab GTPases and their roles in brain neurons and glia. Brain research reviews, 58(1), 236–246. doi:10.1016/j.brainresrev.2008.04.006

Nowak, L., Bregestovski, P., Ascher, P., Herbet, A., & Prochiantz, A. (1984). Magnesium gates glutamate-activated channels in mouse central neurones. Nature, 307, 462–465.

Orsini, C. A., & Maren, S. (2012). Neural and cellular mechanisms of fear and extinction memory formation. Neuroscience & Biobehavioral Reviews. doi:10.1016/j.neubiorev.2011.12.014

Panja, D., & Bramham, C. R. (2014). BDNF mechanisms in late LTP formation: A synthesis and breakdown. Neuropharmacology, 76 Pt C, 664–76. doi:10.1016/j.neuropharm.2013.06.024

Patterson, S. L., Grover, L. M., Schwartzkroin, P. A., & Bothwell, M. (1992). Neurotrophin expression in rat hippocampal slices: a stimulus paradigm inducing LTP in CA1 evokes increases in BDNF and NT-3

mRNAs. Neuron, 9, 1081–1088. doi:10.1016/0896-6273(92)90067-N

Pear, W. S., Nolan, G. P., Scott, M. L., & Baltimore, D. (1993). Production of high-titer helper-free retroviruses by transient transfection. Proceedings of the National Academy of Sciences of the United States of America, 90, 8392–8396. doi:10.1073/pnas.90.18.8392

Pellow, S., Chopin, P., File, S. E., & Briley, M. (1985). Validation of open:closed arm entries in an elevated plus-maze as a measure of anxiety in the rat. Journal of neuroscience methods, 14, 149–167. doi:10.1016/0165-0270(85)90031-7

Pittenger, C., Huang, Y. Y., Paletzki, R. F., Bourtchouladze, R., Scanlin, H., Vronskaya, S., & Kandel, E. R. (2002). Reversible inhibition of CREB/ATF transcription factors in region CA1 of the dorsal hippocampus disrupts hippocampus-dependent spatial memory. Neuron, 34, 447–462. doi:10.1016/S0896-6273(02)00684-0

Plath, N., Ohana, O., Dammermann, B., Errington, M. L., Schmitz, D., Gross, C., … Kuhl, D. (2006). Arc/Arg3.1 is essential for the consolidation of synaptic plasticity and memories. Neuron, 52(3), 437–444. doi:10.1016/j.neuron.2006.08.024

Qian, Z., Gilbert, M. E., Colicos, M. A., Kandel, E. R., & Kuhl, D. (1993). Tissue-plasminogen activator is induced as an immediate-early gene during seizure, kindling and long-term potentiation. Nature, 361, 453–457. doi:10.1038/361453a0

Reichardt, L. F. (2006). Neurotrophin-regulated signalling pathways. Philosophical transactions of the Royal Society of London. Series B, Biological sciences, 361, 1545–1564. doi:10.1098/rstb.2006.1894

Rosa-Ferreira, C., & Munro, S. (2011). Arl8 and SKIP Act Together to Link Lysosomes to Kinesin-1. Developmental Cell. doi:10.1016/j.devcel.2011.10.007

Rutherford, L. C., Nelson, S. B., & Turrigiano, G. G. (1998). BDNF has opposite effects on the quantal amplitude of pyramidal neuron and interneuron excitatory synapses. Neuron, 21, 521–530. doi:10.1016/S0896-6273(00)80563-2

Sanger, F., Nicklen, S., & Coulson, A. R. (1977). DNA sequencing with chain-terminating inhibitors. Proceedings of the National Academy of Sciences of the United States of America, 74, 5463–5467. doi:10.1073/pnas.74.12.5463

Schratt, G. M., Nigh, E. A., Chen, W. G., Hu, L., & Greenberg, M. E. (2004). BDNF regulates the translation of a select group of mRNAs by a mammalian target of rapamycin-phosphatidylinositol 3-kinase-dependent pathway during neuronal development. The Journal of neuroscience : the official journal of the Society for Neuroscience, 24, 7366–7377. doi:10.1523/JNEUROSCI.1739-04.2004

Schratt, G. M., Tuebing, F., Nigh, E. A., Kane, C. G., Sabatini, M. E., Kiebler, M., & Greenberg, M. E. (2006). A brain-specific microRNA regulates dendritic spine development. Nature, 439, 283–289. doi:10.1038/nature04909

Sebald, E., Krueger, R., King, L. M., Cohn, D. H., & Krakow, D. (2003). Isolation of a new member of the ADP-ribosylation like factor gene family, ARL8, from a cartilage cDNA library. Gene, 311, 147–151. doi:10.1016/S0378-1119(03)00584-5

Sheng, M., & Greenberg, M. E. (1990). The regulation and function of c-fos and other immediate early genes in the nervous system. Neuron, 4, 477–485. doi:10.1016/0896-6273(90)90106-P

Sheng, M., Thompson, M. A., & Greenberg, M. E. (1991). CREB: a Ca(2+)-regulated transcription factor phosphorylated by calmodulin-dependent kinases. Science (New York, N.Y.), 252, 1427–1430.

doi:10.1126/science.1646483

Shinoda, Y., Kamikubo, Y., Egashira, Y., Tominaga-Yoshino, K., & Ogura, A. (2005). Repetition of mGluR-dependent LTD causes slowly developing persistent reduction in synaptic strength accompanied by synapse elimination. Brain research, 1042, 99–107. doi:10.1016/j.brainres.2005.02.028

Squire, L R, & Barondes, S. H. (1972). Variable decay of memory and its recovery in cycloheximide-treated mice. Proceedings of the National Academy of Sciences of the United States of America, 69, 1416–1420. doi:10.1073/pnas.69.6.1416

Squire, Larry R, & Davis, H. P. (1981). The Pharmacology of Memory: A Neurobiological Perspective. Annual Review of Pharmacology and Toxicology, 21, 323–356.

Stanton, P. K., & Sarvey, J. M. (1984). Blockade of long-term potentiation in rat hippocampal CA1 region by inhibitors of protein synthesis. The Journal of neuroscience : the official journal of the Society for Neuroscience, 4, 3080–3088.

Stent, G. S. (1973). A physiological mechanism for Hebb's postulate of learning. Proceedings of the National Academy of Sciences of the United States of America, 70, 997–1001. doi:10.1073/pnas.70.4.997

Tee, A. R., Manning, B. D., Roux, P. P., Cantley, L. C., & Blenis, J. (2003). Tuberous sclerosis complex gene products, Tuberin and Hamartin, control mTOR signaling by acting as a GTPase-activating protein complex toward Rheb. Current biology : CB, 13, 1259–1268. doi:10.1016/S0960-9822(03)00506-2

Thomas, G. M., & Huganir, R. L. (2004). MAPK cascade signalling and synaptic plasticity. Nature reviews. Neuroscience, 5, 173–183. doi:10.1038/nrn1346

Treisman, R. (1987). Identification and purification of a polypeptide that binds to the c-fos serum response element. The EMBO journal, 6, 2711–2717.

Tsokas, P., Grace, E. A., Chan, P., Ma, T., Sealfon, S. C., Iyengar, R., … Blitzer, R. D. (2005). Local protein synthesis mediates a rapid increase in dendritic elongation factor 1A after induction of late long-term potentiation. The Journal of neuroscience : the official journal of the Society for Neuroscience, 25, 5833–5843. doi:10.1523/JNEUROSCI.0599-05.2005

Tsui, C. C., Copeland, N. G., Gilbert, D. J., Jenkins, N. A., Barnes, C., & Worley, P. F. (1996). Narp, a novel member of the pentraxin family, promotes neurite outgrowth and is dynamically regulated by neuronal activity. The Journal of neuroscience : the official journal of the Society for Neuroscience, 16, 2463–2478.

Van Strien, N. M., Cappaert, N. L. M., & Witter, M. P. (2009). The anatomy of memory: an interactive overview of the parahippocampal-hippocampal network. Nature reviews. Neuroscience, 10, 272–282. doi:10.1038/nrn2614

Waltereit, R., Dammermann, B., Wulff, P., Scafidi, J., Staubli, U., Kauselmann, G., … Kuhl, D. (2001). Arg3.1/Arc mRNA induction by Ca2+ and cAMP requires protein kinase A and mitogen-activated protein kinase/extracellular regulated kinase activation. The Journal of neuroscience : the official journal of the Society for Neuroscience, 21, 5484–5493. doi:21/15/5484 [pii]

Whitlock, J. R., Heynen, A. J., Shuler, M. G., & Bear, M. F. (2006). Learning induces long-term potentiation in the hippocampus. Science (New York, N.Y.), 313, 1093–1097. doi:10.1126/science.1128134

Wibrand, K., Messaoudi, E., Håvik, B., Steenslid, V., Løvlie, R., Steen, V. M., & Bramham, C. R. (2006). Identification of genes co-upregulated with Arc during BDNF-induced long-term potentiation in adult rat dentate gyrus in vivo. The European journal of neuroscience, 23, 1501–1511. doi:10.1111/j.1460-

9568.2006.04687.x

Wiegert, J. S., & Oertner, T. G. (2013). Long-term depression triggers the selective elimination of weakly integrated synapses. Proceedings of the National Academy of Sciences of the United States of America, 2013, 1–10. doi:10.1073/pnas.1315926110

Wisden, W., Errington, M. L., Williams, S., Dunnett, S. B., Waters, C., Hitchcock, D., … Hunt, S. P. (1990). Differential expression of immediate early genes in the hippocampus and spinal cord. Neuron, 4, 603–614. doi:2108708

Wisden, W., & Seeburg, P. H. (1993). Mammalian ionotropic glutamate receptors. Current opinion in neurobiology, 3, 291–298.

Wright, J. H., Drueckes, P., Bartoe, J., Zhao, Z., Shen, S. H., & Krebs, E. G. (1997). A role for the SHP-2 tyrosine phosphatase in nerve growth-induced PC12 cell differentiation. Molecular biology of the cell, 8, 1575–1585.

Yamada, M., Ohnishi, H., Sano, S. i, Nakatani, A., Ikeuchi, T., & Hatanaka, H. (1997). Insulin receptor substrate (IRS)-1 and IRS-2 are tyrosine-phosphorylated and associated with phosphatidylinositol 3-kinase in response to brain-derived neurotrophic factor in cultured cerebral cortical neurons. The Journal of biological chemistry, 272, 30334–30339. doi:10.1074/jbc.272.48.30334

Yamagata, K., Andreasson, K. I., Sugiura, H., Maru, E., Dominique, M., Irie, Y., … Worley, P. F. (1999). Arcadlin is a neural activity-regulated cadherin involved in long term potentiation. The Journal of biological chemistry, 274, 19473–11979. doi:10.1074/jbc.274.27.19473

Yamagata, K., Sanders, L. K., Kaufmann, W. E., Yee, W., Barnes, C. A., Nathans, D., & Worley, P. F. (1994). rheb, a growth factor- and synaptic activity-regulated gene, encodes a novel Ras-related protein. The Journal of biological chemistry, 269, 16333–16339.

Yeckel, M. F., & Berger, T. W. (1990). Feedforward excitation of the hippocampus by afferents from the entorhinal cortex: redefinition of the role of the trisynaptic pathway. Proceedings of the National Academy of Sciences of the United States of America, 87, 5832–5836. doi:10.1073/pnas.87.15.5832

Yoshii, A., & Constantine-Paton, M. (2007). BDNF induces transport of PSD-95 to dendrites through PI3K-AKT signaling after NMDA receptor activation. Nature neuroscience, 10, 702–711. doi:10.1038/nn1903

Zafra, F., Hengerer, B., Leibrock, J., Thoenen, H., & Lindholm, D. (1990). Activity dependent regulation of BDNF and NGF mRNAs in the rat hippocampus is mediated by non-NMDA glutamate receptors. The EMBO journal, 9, 3545–3550.

Zhang, S.-J., Steijaert, M. N., Lau, D., Schütz, G., Delucinge-Vivier, C., Descombes, P., & Bading, H. (2007). Decoding NMDA receptor signaling: identification of genomic programs specifying neuronal survival and death. Neuron, 53(4), 549–562. doi:10.1016/j.neuron.2007.01.025

5.2 Statement of contribution

Animal breeding and caring was provided by Eva Kronenberg and Hiltrud Voss. Cultivation and injection of embryonic stem cells was performed by Irm Hermans-Borgmeyer and Sarah Homann. All competent bacteria used for molecular cloning were kindly provided by Ute Süsens. Kainic acid injection for seizure induction were performed either by or under the supervision of PD Dr. Guido Hermey. Perfusions were carried out under the supervision of either PD Dr. Guido Hermey. Fear conditioning experiments were performed together with Mario Sergio Castro-Gomez. Technical assistance was provided by Barbara Merz, Andrea Zeisser and Ute Süsens for this work. Specifically molecular cloning (A.Z.), Southern Blot analysis (U.S.), *in situ* hybridizations and Nissl-staining (B.M.).

Eidesstattliche Versicherung

Hiermit erkläre ich an Eides statt, dass ich die vorliegende Dissertationsschrift selbst verfasst und keine anderen als die angegebenen Quellen und Hilfsmittel benutzt habe.

Hamburg, den 30. Januar 2014

Ort, Datum Unterschrift

Eidesstattliche Erklärung

Ich erkläre hiermit, dass ich mich bisher keiner weiteren Doktorprüfung unterzogen habe. Ich habe die Dissertation in der gegenwärtigen oder einer anderen Fassung an keiner anderen Fakultät eingereicht.

Hamburg, den 30. Januar 2014

Ort, Datum Unterschrift